

CARBON STARS IN THE LARGE MAGELLANIC CLOUD

by

Dennis Richard Crabtree

B.Sc. University of British Columbia, 1974

A THESIS SUBMITTED IN PARTIAL FULFILLMENT OF
THE REQUIREMENTS FOR THE DEGREE OF
MASTER OF SCIENCE

in the Department
of
GEOPHYSICS and ASTRONOMY

We accept this thesis as conforming to the
required standard.

The University of British Columbia

August, 1976

© Dennis Richard Crabtree 1976

In presenting this thesis in partial fulfilment of the requirements for an advanced degree at the University of British Columbia, I agree that the Library shall make it freely available for reference and study.

I further agree that permission for extensive copying of this thesis for scholarly purposes may be granted by the Head of my Department or by his representatives. It is understood that copying or publication of this thesis for financial gain shall not be allowed without my written permission.

Department of Geophysics / Astronomy

The University of British Columbia
2075 Wesbrook Place
Vancouver, Canada
V6T 1W5

Date Sept 30 / 76

Abstract

A catalogue of cool carbon stars in the Large Magellanic Cloud is presented along with photometric and spectroscopic observations of some of the members. Image tube spectra at a dispersion of 117 Å/mm were obtained for seven of the stars in order to investigate some of the grosser features of the spectrum. In addition photometric observations on the VRI system of forty stars have been made.

The spectra indicate that three of the carbon stars observed show enhancement of spectral features involving the ^{13}C isotope. Using the photometric observations to place the stars in a theoretical Hertzsprung-Russell diagram, it is concluded that (1) all forty stars are in the double-shell source phase of evolution and, (2) the helium shell flashes are responsible for the formation of the majority of cool N-type carbon stars.

Table of Contents

	page
I Introduction	1
II Catalogue of Carbon Stars	5
III Photometric Observations	66
IV Spectroscopic Observations	76
V Carbon Stars in the H-R Diagram	87
VI Summary	98
Bibliography	101

List of Tables

	page
I. Plate Centres	8
II. Carbon Star Coordinates	9
III. Carbon Star Photometry	67
IV. Spectroscopic Observations	79
V. Properties of the Seven Carbon Stars	81
VI. Classification of Carbon Stars	82

List of Figures

	page
1. Finding Charts	27
2. V versus R-I	70
3. V versus V-I	71
4. V versus V-R	72
5. Mbol versus V-R	74
6a. Carbon Star Spectra, region 1	77
6b. Carbon Star Spectra, region 2	78
7. Bolometric Corrections	88
8. Colour Temperature versus R-I	92
9. Theoretical Hertzsprung-Russell Diagram	93

Acknowledgements

I would like to thank my supervisor Harvey Richer for his patience and enthusiastic support during the course of this work. I thank B.I. Olson for supplying many of the computer programs used in this study. I also thank B.E. Westerlund for kindly supplying the original charts on which he had marked the suspected program stars. I thank the University of British Columbia for support from a postgraduate fellowship. Finally I would like to thank the graduate students of the department for making the department such an enjoyable place to work.

I Introduction

Among the stars classified as red giants there are many groups which show anomalous abundances of certain elements. One of these groups is the carbon stars. These stars show an enhancement of absorption bands of CH, CN, and C_2 including, in some cases, bands of molecules involving the ^{13}C isotope.

In the Henry Draper Catalogue these stars were originally classified as type R or N; N being reserved for the redder members. Shane(1928) reclassified these into subdivisions but it was discovered later that this system was not a true temperature sequence as was the rest of the Henry Draper system. Subsequently Keenan and Morgan(1941) proposed the C-classification for carbon stars based on temperature and carbon abundance. However this system of classification has by no means solved the classification problem. Any classification system that is to be successful must be able to sort out the many differing abundances as well as the temperature sequence in these stars. Yamashita(1967) has devised a system in which he estimates the intensities of eleven spectral features as well as classifying each star on the C classification system. One deficiency of the C system is that the sequence from C5-C9 probably does not represent a true temperature sequence (Richer 1971;Scalo 1973).

Much of the theoretical work on carbon stars has been hampered by the lack of good absolute visual magnitudes for

individual objects. Some results do exist(Gordon 1968; Richer 1972, 1975; Olson and Richer 1975) but the number of stars involved is not large enough to cover all the spectral subtypes and peculiarities observed in these objects. This follows from the fact that these objects are relatively rare in our Galaxy. Attempts to measure the absolute magnitudes of individual objects run into the usual sort of problems encountered in this endeavor; no object is close enough to have a reliable trigonometric parallax, carbon stars are rarely members of clusters, few are members of binary systems, the Wilson-Bappu effect is difficult to use for the R stars and impossible to use for the N stars, etc.

The absolute magnitude problem is closely related to the problems of the effective temperature and radii of carbon stars. Only two carbon stars have had their angular diameters measured by the method of lunar occultation, 19 Psc and X Cnc. A direct measurement of the radius is difficult since no carbon star is a member of an eclipsing binary nor has a measurable parallax. The temperature classes of the later stars in the C classification do not correlate well with the colour temperatures that have been obtained by Mendoza and Johnson (1965); Richer (1971) or Wing (1967) from extensive photometric observations. Colour-colour relations have shown that the cool carbon stars radiate more like black-bodies than do M giants (Bahng 1966; Scalo 1973). Therefore any attempt to use a calibration between colour and effective temperature that is based on normal M giants should be treated with caution.

Wallerstein(1973) gives a good review of the physical properties of carbon stars as well as one possible evolutionary sequence. The carbon stars are believed to be well evolved stars that are exhibiting the products of nucleosynthesis in their outer atmosphere.

The first part of this thesis contains a catalogue of carbon stars in the Large Magellanic Cloud. A catalogue of these stars should be a very useful document now that several large telescopes are becoming operational in the southern hemisphere. If one obtains accurate absolute magnitudes and good medium dispersion spectra of carbon stars in the Large Magellanic Cloud it should be possible to better locate these stars in current evolutionary models. Along with the catalogue, photometric observations on the VRI system of forty stars are presented together with image tube spectra of seven of the brighter members. Using the best available data for bolometric corrections and the relation between photometric colour and effective temperature, these stars are placed in a theoretical Hertzsprung-Russell diagram. The results are compared with current models of the cool carbon stars.

The medium dispersion spectra of the seven brighter members indicate that three of the seven show enhancement of molecular bands containing the ^{13}C isotope. A detailed discussion of the spectra is presented in section IV of this thesis. The catalogue itself is presented in section II while the

photometric observations are discussed in section III. Section V contains a discussion of the Hertzsprung-Russell diagram with respect to the carbon stars while section VI contains a summary of the results.

II Catalogue of Carbon Stars

The most efficient way to discover and classify a large number of objects is to use an objective prism survey. This method is particularly useful in the search for objects whose spectra are easily separable from most other astronomical spectra. Such objects include emission line stars, planetary nebulae and carbon stars.

The stars discussed below were identified by Dr. B.E. Westerlund who has kindly supplied charts of the Large Magellanic Cloud marking suspected carbon stars on them. Dr. Westerlund identified these stars from 2100 Å/mm I-N objective prism plates obtained with the 20/26 inch Schmidt telescope at the Uppsala Southern Station on Mount Stromlo. Carbon stars are much brighter in the I band than either the B or V bands, thus the reason for using I-N plates. This also reduces the overlap of spectra on the plate since most other stars are much fainter (absolutely) in this region of the spectrum. The plates obtained reached to about I=14 magnitude and the carbon stars were identified using the criteria established by Nassau (cf. Mavridis 1967). The main indicators used to identify these stars were the CN bands at $\lambda 7945$ Å, $\lambda 8125$ Å and $\lambda 8320$ Å. Other CN bands shortward of the atmospheric A-band ($\lambda 7600$ Å) appear only when the spectrum is heavily overexposed.

Westerlund (1964) has given a preliminary discussion of this plate material emphasizing the distribution of the carbon stars

within the Large Magellanic Cloud. He found that the carbon stars tend to avoid the central regions as well as the regions rich in nebulosity and in blue stars. He also noted that they appear to form clusterings, possibly in the shape of arms, and that the position of these clusterings agreed well with the structural features noted by de Vaucouleurs (1955) on heavily exposed photographs. Westerlund also estimated that the mean apparent visual magnitude was 15.7 ± 0.5 .

The chart material consisted of two separate sections. The first section was at a scale of about $11.8''$ arc/mm while the second section, which also included all the first section, was at a scale of $27''$ arc/mm. The first set was measured in May 1974 while the second set was measured in August 1975. The method used to get from the X,Y position to right ascension and declination on the sky is that described by Smart (1971). Briefly, it consists of considering the tangent plane and a star's projected position on this plane if the telescope is not pointed directly at this star (as in a photograph). The point at which the tangent plane contacts the celestial sphere (the point at which the telescope is aimed) is taken to be the origin. If we take the meridian of this point, it projects into a straight line on the tangent plane. This line forms one axis for an orthogonal coordinate system on the sky. The other axis is taken to be a line drawn perpendicular to the first axis. The standard coordinates of the image of the star on the photographic plate are found with reference to rectangular axes drawn through the centre of the plate and drawn parallel to the

orthogonal axes on the sky. By using three standard reference stars, the plate constants relating the measured X-Y positions to the standard coordinate system can be calculated. Once the plate constants have been evaluated it is an easy matter to go from X-Y values to standard coordinates to equatorial coordinates.

The first set of charts were measured on a standard drafting table using a drafting square and a millimeter ruler. To check the accuracy of the measurements each chart was measured twice and the resulting coordinates averaged together. The second set of charts were measured on the X-Y digitizer of the Department of Mechanical Engineering at UBC. In order to check the accuracy of the transformations the X-Y positions of three bright reference stars were measured at the same time the positions of the suspected carbon stars were measured. After the transformation to right ascension and declination had been completed the computed coordinates of the reference stars were compared to those tabulated in the SAO catalogue. In both sets of charts the coordinates are good to about 10" arc. This accuracy was confirmed, as all the stars were found quite easily at the telescope. Table I contains the approximate plate centres of each of the fields as well as the number of stars measured and the number of stars for which photometry was obtained.

Table II contains a list of the coordinates for the epoch 1975.0 of all the suspected carbon stars. Finding charts for

Table I Plate Centres

Field	R.A.	Dec.	# of Carbon stars found	# of Stars Photometry
1.	4 50	-60°	29	13
2.	4 45	-69°	14	-
3.	4 40	-72°	18	-
4.	5 20	-66°	33	7
5.	5 20	-69°	24	-
6.	5 20	-72°	76	20
7.	5 50	-66°	3	-
8.	5 55	-69°	14	-
9.	6 00	-72°	36	-
20.	6 05	-75°	4	-
23.	6 30	-69°	51	-
24.	6 40	-72°	3	-

these stars are presented in Fig. 1. The field of these finding charts is approximately 11' arc by 16' arc with north to the top and east to the left.

L.M.C. Field #1

<u>Star</u>	<u>Right Ascension (1975)</u>	<u>Declination (1975)</u>
1	4 ^h 52 ^m 28 ^s	-66° 28'.0
2	4 ^h 53 ^m 2 ^s	-66° 27'.0
3	4 ^h 58 ^m 36 ^s	-66° 52'.4
4	5 ^h 0 ^m 12 ^s	-66° 28'.2
5	5 ^h 1 ^m 19 ^s	-66° 52'.9
6	5 ^h 2 ^m 9 ^s	-67° 18'.1
7	5 ^h 2 ^m 17 ^s	-66° 57'.0
8	5 ^h 2 ^m 28 ^s	-67° 12'.5
9	4 ^h 59 ^m 00 ^s	-65° 57'.7
10	5 ^h 1 ^m 41 ^s	-65° 51'.9
11	5 ^h 2 ^m 53 ^s	-65° 58'.9
12	5 ^h 3 ^m 11 ^s	-66° 2'.9
13	5 ^h 2 ^m 47 ^s	-66° 26'.5
14	5 ^h 3 ^m 25 ^s	-66° 55'.9
15	5 ^h 4 ^m 50 ^s	-67° 13'.1
16	5 ^h 5 ^m 50 ^s	-66° 15'.3
17	4 ^h 58 ^m 43 ^s	-65° 26'.6
18	4 ^h 58 ^m 32 ^s	-65° 22'.2
19	4 ^h 59 ^m 13 ^s	-64° 59'.0
20	5 ^h 0 ^m 26 ^s	-65° 2'.5
21	5 ^h 2 ^m 22 ^s	-65° 9'.3
22	5 ^h 2 ^m 43 ^s	-65° 11'.1
23	4 ^h 53 ^m 23 ^s	-64° 37'.9
24	4 ^h 50 ^m 32 ^s	-67° 0'.7

Table II cont'd

L.M.C. Field #1

<u>Star</u>	<u>Right Ascension (1975)</u>	<u>Declination (1975)</u>
25	4 ^h 49 ^m 28 ^s	-67°16'.3
26	4 ^h 50 ^m 34 ^s	-67°10'.6
27	4 ^h 52 ^m 30 ^s	-67°11'.1
28	4 ^h 57 ^m 56 ^s	-67°19'.4
29	5 ^h 0 ^m 3 ^s	-67°14'.5

Table II cont'd

L.M.C. Field #2

<u>Star</u>	<u>Right Ascension (1975)</u>	<u>Declination (1975)</u>
1	4 ^h 33 ^m 51 ^s	-70° 15'.6
2	4 ^h 39 ^m 5 ^s	-70° 10'.0
3	4 ^h 40 ^m 12 ^s	-70° 13'.1
4	4 ^h 49 ^m 48 ^s	-69° 58'.8
5	4 ^h 52 ^m 54 ^s	-69° 57'.4
6	4 ^h 53 ^m 44 ^s	-67° 41'.4
7	4 ^h 55 ^m 25 ^s	-68° 54'.2
8	4 ^h 54 ^m 39 ^s	-70° 2'.3
9	4 ^h 55 ^m 11 ^s	-70° 2'.8
10	4 ^h 55 ^m 43 ^s	-70° 1'.9
11	4 ^h 55 ^m 35 ^s	-70° 9'.7
12	4 ^h 58 ^m 39 ^s	-70° 11'.3
13	4 ^h 59 ^m 19 ^s	-70° 10'.3
14	5 ^h 0 ^m 23 ^s	-70° 15'.7

Table II cont'd

L.M.C. Field #3

<u>Star</u>	<u>Right Ascension (1975)</u>	<u>Declination (1975)</u>
1	4 ^h 41 ^m 46 ^s	-70°52'.5
2	4 ^h 42 ^m 34 ^s	-70°39'.4
3	4 ^h 44 ^m 56 ^s	-70°31'.3
4	4 ^h 48 ^m 43 ^s	-72°28'.0
5	4 ^h 51 ^m 9 ^s	-72°45'.1
6	4 ^h 53 ^m 0 ^s	-73°18'.5
7	4 ^h 50 ^m 15 ^s	-71° 3'.0
8	4 ^h 50 ^m 35 ^s	-70°25'.6
9	4 ^h 53 ^m 24 ^s	-70°38'.3
10	4 ^h 53 ^m 1 ^s	-71°15'.2
11	4 ^h 57 ^m 2 ^s	-73°14'.5
12	4 ^h 55 ^m 28 ^s	-70°21'.9
13	4 ^h 56 ^m 14 ^s	-70°20'.0
14	4 ^h 58 ^m 3 ^s	-70°50'.4
15	4 ^h 57 ^m 50 ^s	-71°21'.8
16	4 ^h 58 ^m 41 ^s	-71°58'.5
17	5 ^h 1 ^m 52 ^s	-72°56'.6
18	5 ^h 0 ^m 36 ^s	-71°14'.5

Table II cont'd

L.M.C. Field #4

<u>Star</u>	<u>Right Ascension (1975)</u>	<u>Declination (1975)</u>
1	5 ^h 7 ^m 8 ^s	-64°27'.2
2	5 ^h 8 ^m 44 ^s	-64°42'.3
3	5 ^h 11 ^m 31 ^s	-64°11'.9
4	5 ^h 12 ^m 31 ^s	-64°14'.1
5	5 ^h 11 ^m 50 ^s	-65° 9'.8
6	5 ^h 11 ^m 42 ^s	-65°16'.1
7	5 ^h 15 ^m 17 ^s	-65° 9'.6
8	5 ^h 16 ^m 9 ^s	-64°52'.1
9	5 ^h 17 ^m 10 ^s	-64°48'.5
10	5 ^h 19 ^m 45 ^s	-65° 4'.2
11	5 ^h 23 ^m 2 ^s	-64°54'.7
12	5 ^h 4 ^m 55 ^s	-64°30'.7
13	5 ^h 9 ^m 21 ^s	-64°28'.2
14	5 ^h 16 ^m 34 ^s	-64°21'.1
15	5 ^h 8 ^m 54 ^s	-65°43'.7
16	5 ^h 10 ^m 44 ^s	-65°42'.1
17	5 ^h 12 ^m 6 ^s	-65°47'.6
18	5 ^h 12 ^m 55 ^s	-65°43'.3
19	5 ^h 15 ^m 33 ^s	-65°47'.5
20	5 ^h 5 ^m 59 ^s	-65°58'.8
21	5 ^h 7 ^m 46 ^s	-66° 5'.5
22	5 ^h 3 ^m 32 ^s	-66°23'.2
23	5 ^h 6 ^m 13 ^s	-66°26'.4
24	5 ^h 8 ^m 24 ^s	-66°26'.8

Table II cont'd

L.M.C. Field #4

<u>Star</u>	<u>Right Ascension (1975)</u>	<u>Declination (1975)</u>
25	5 ^h 11 ^m 44 ^s	-66° 52'.7
26	5 ^h 6 ^m 44 ^s	-67° 4'.9
27	5 ^h 10 ^m 50 ^s	-67° 27'.2
28	5 ^h 15 ^m 19 ^s	-67° 15'.9
29	5 ^h 16 ^m 28 ^s	-67° 19'.6
30	5 ^h 19 ^m 39 ^s	-67° 36'.6
31	5 ^h 20 ^m 44 ^s	-67° 37'.4
32	5 ^h 15 ^m 4 ^s	-64° 48'.4
33	5 ^h 14 ^m 15 ^s	-65° 3'.5

Table II cont'd

L.M.C. Field #5

<u>Star</u>	<u>Right Ascension (1975)</u>	<u>Declination (1975)</u>
1	4 ^h 59 ^m 57 ^s	-67° 14'.1
2	5 ^h 0 ^m 47 ^s	-69° 9'.0
3	5 ^h 2 ^m 10 ^s	-68° 55'.6
4	5 ^h 2 ^m 7 ^s	-68° 46'.1
5	5 ^h 3 ^m 38 ^s	-68° 35'.5
6	5 ^h 3 ^m 35 ^s	-68° 19'.7
7	5 ^h 3 ^m 43 ^s	-67° 39'.2
8	5 ^h 8 ^m 54 ^s	-67° 26'.2
9	5 ^h 4 ^m 18 ^s	-69° 15'.6
10	5 ^h 7 ^m 5 ^s	-69° 58'.2
11	5 ^h 9 ^m 11 ^s	-69° 28'.4
12	5 ^h 9 ^m 24 ^s	-69° 13'.2
13	5 ^h 10 ^m 25 ^s	-70° 24'.2
14	5 ^h 16 ^m 14 ^s	-69° 57'.1
15	5 ^h 18 ^m 49 ^s	-70° 1'.9
16	5 ^h 21 ^m 59 ^s	-69° 56'.6
17	5 ^h 24 ^m 43 ^s	-69° 21'.7
18	5 ^h 28 ^m 20 ^s	-70° 21'.6
19	5 ^h 27 ^m 40 ^s	-69° 6'.8
20	5 ^h 27 ^m 20 ^s	-67° 23'.6
21	5 ^h 29 ^m 46 ^s	-68° 4'.6
22	5 ^h 30 ^m 28 ^s	-68° 57'.7
23	5 ^h 32 ^m 57 ^s	-70° 12'.8
24	5 ^h 33 ^m 34 ^s	-68° 51'.4

Table II cont'd

L.M.C. Field #6

<u>Star</u>	<u>Right Ascension (1975)</u>	<u>Declination (1975)</u>
1	5 ^h 0 ^m 24 ^s	-70° 15'.8
2	5 ^h 0 ^m 46 ^s	-70° 39'.4
3	5 ^h 1 ^m 28 ^s	-70° 38'.2
4	5 ^h 2 ^m 4 ^s	-70° 53'.3
5	5 ^h 5 ^m 4 ^s	-70° 30'.9
6	5 ^h 5 ^m 6 ^s	-70° 27'.6
7	5 ^h 6 ^m 14 ^s	-70° 19'.4
8	5 ^h 8 ^m 16 ^s	-71° 7'.8
9	5 ^h 13 ^m 10 ^s	-71° 1'.6
10	5 ^h 11 ^m 27 ^s	-70° 46'.1
11	5 ^h 15 ^m 8 ^s	-73° 17'.8
12	5 ^h 16 ^m 8 ^s	-73° 18'.2
13	5 ^h 26 ^m 4 ^s	-73° 19'.8
14	5 ^h 26 ^m 41 ^s	-73° 2'.8
15	5 ^h 28 ^m 45 ^s	-73° 4'.6
16	5 ^h 24 ^m 44 ^s	-72° 9'.7
17	5 ^h 27 ^m 20 ^s	-72° 12'.7
18	5 ^h 32 ^m 40 ^s	-70° 53'.1
19	5 ^h 33 ^m 54 ^s	-70° 53'.4
20	5 ^h 35 ^m 10 ^s	-71° 1'.4
21	5 ^h 37 ^m 12 ^s	-70° 58'.6
22	5 ^h 38 ^m 0 ^s	-70° 49'.1
23	5 ^h 38 ^m 14 ^s	-72° 9'.3
24	5 ^h 38 ^m 58 ^s	-72° 2'.4
25	5 ^h 39 ^m 19 ^s	-72° 10'.4
26	5 ^h 39 ^m 16 ^s	-72° 5'.0

Table II cont'd

L.M.C. Field #6

<u>Star</u>	<u>Right Ascension (1975)</u>	<u>Declination (1975)</u>
27	5 ^h 41 ^m 14 ^s	-72° 30'.7
28	5 ^h 38 ^m 35 ^s	-71° 36'.0
29	4 ^h 59 ^m 57 ^s	-71° 1'.6
30	5 ^h 2 ^m 29 ^s	-71° 3'.9
31	5 ^h 4 ⁹ 9 ^s	-72° 19'.4
32	5 ^h 7 ^m 11 ^s	-73° 9'.4
33	5 ^h 8 ^m 6 ^s	-72° 49'.2
34	5 ^h 8 ^m 52 ^s	-72° 47'.3
35	5 ^h 10 ^m 7 ^s	-72° 17'.8
36	5 ^h 10 ^m 32 ^s	-71° 47'.6
37	5 ^h 13 ^m 36 ^s	-70° 52'.5
37a	5 ^h 12 ^m 29 ^s	-70° 50'.3
38	5 ^h 12 ^m 49 ^s	-71° 47'.7
39	5 ^h 13 ^m 50 ^s	-72° 55'.1
40	5 ^h 15 ^m 55 ^s	-72° 33'.2
41	5 ^h 14 ^m 44 ^s	-71° 44'.7
42	5 ^h 16 ^m 15 ^s	-71° 52'.4
43	5 ^h 16 ^m 35 ^s	-72° 14'.2
44	5 ^h 18 ^m 32 ^s	-71° 53'.4
45	5 ^h 17 ^m 38 ^s	-71° 4'.4
46	5 ^h 18 ^m 33 ^s	-70° 57'.7
47	5 ^h 20 ^m 21 ^s	-72° 43'.3
48	5 ^h 22 ^m 20 ^s	-72° 30'.5
49	5 ^h 22 ^m 13 ^s	-72° 5'.3
50	5 ^h 23 ^m 26 ^s	-71° 59'.0

Table II cont'd

L.M.C. Field #6

<u>Star</u>	<u>Right Ascension (1975)</u>	<u>Declination (1975)</u>
51	5 ^h 23 ^m 11 ^s	-71° 44'.5
52	5 ^h 24 ^m 4 ^s	-71° 47'.2
53	5 ^h 21 ^m 34 ^s	-71° 29'.8
54	5 ^h 23 ^m 5 ^s	-71° 25'.6
55	5 ^h 23 ^m 44 ^s	-71° 34'.3
56	5 ^h 23 ^m 59 ^s	-71° 27'.9
57	5 ^h 24 ^m 50 ^s	-71° 26'.0
58	5 ^h 23 ^m 44 ^s	-70° 45'.3
59	5 ^h 24 ^m 56 ^s	-71° 5'.4
60	5 ^h 24 ^m 53 ^s	-70° 59'.8
61	5 ^h 27 ^m 34 ^s	-70° 58'.3
62	5 ^h 28 ^m 8 ^s	-70° 55'.4
63	5 ^h 26 ^m 56 ^s	-70° 40'.3
64	5 ^h 27 ^m 33 ^s	-70° 40'.5
65	5 ^h 26 ^m 26 ^s	-72° 13'.5
66	5 ^h 30 ^m 47 ^s	-72° 4'.9
67	5 ^h 31 ^m 58 ^s	-71° 44'.5
68	5 ^h 32 ^m 16 ^s	-71° 11'.9
69	5 ^h 33 ^m 2 ^s	-71° 32'.7
70	5 ^h 33 ^m 28 ^s	-71° 34'.9
71	5 ^h 33 ^m 6 ^s	-71° 27'.8
72	5 ^h 34 ^m 6 ^s	-71° 23'.0
73	5 ^h 33 ^m 53 ^s	-72° 4'.9
74	5 ^h 34 ^m 37 ^s	-71° 59'.1
75	5 ^h 35 ^m 27 ^s	-72° 5'.7
76	5 ^h 38 ^m 4 ^s	-70° 55'.9

L.M.C. Field #7

<u>Star</u>	<u>Right Ascension (1975)</u>	<u>Declination (1975)</u>
1	5 ^h 31 ^m 11 ^s	-65°33'.2
2	5 ^h 34 ^m 24 ^s	-67°29'.5
3	5 ^h 35 ^m 41 ^s	-66°21'.8

Table II cont'd

L.M.C. Field #8

<u>Star</u>	<u>Right Ascension (1975)</u>	<u>Declination (1975)</u>
1	5 ^h 44 ^m 33 ^s	-69° 8'.6
2	5 ^h 48 ^m 21 ^s	-67° 14'.5
3	5 ^h 48 ^m 3 ^s	-69° 22'.1
4	5 ^h 52 ^m 42 ^s	-67° 54'.5
5	5 ^h 53 ^m 25 ^s	-68° 46'.1
6	6 ^h 5 ^m 56 ^s	-69° 27'.2
7	6 ^h 7 ^m 41 ^s	-70° 31'.0
8	6 ^h 7 ^m 33 ^s	-69° 26'.2
9	6 ^h 8 ^m 43 ^s	-69° 58'.4
10	6 ^h 7 ^m 23 ^s	-67° 52'.4
11	6 ^h 7 ^m 41 ^s	-67° 52'.0
12	6 ^h 8 ^m 47 ^s	-68° 15'.9
13	6 ^h 9 ^m 10 ^s	-67° 12'.3
14	6 ^h 10 ^m 50 ^s	-67° 16'.5

L.M.C. Field #9

<u>Star</u>	<u>Right Ascension (1975)</u>	<u>Declination (1975)</u>
1	5 ^h 45 ^m 19 ^s	-71°35'.2
2	5 ^h 45 ^m 24 ^s	-70°38'.2
3	5 ^h 47 ^m 23 ^s	-70°33'.5
4	5 ^h 46 ^m 49 ^s	-71°13'.8
5	5 ^h 48 ^m 12 ^s	-71°13'.0
6	5 ^h 48 ^m 6 ^s	-70°58'.4
7	5 ^h 48 ^m 54 ^s	-71°42'.8
8	5 ^h 49 ^m 37 ^s	-71°39'.2
9	5 ^h 49 ^m 1 ^s	-70°46'.0
10	5 ^h 49 ^m 13 ^s	-70°44'.8
11	5 ^h 49 ^m 55 ^s	-70°52'.6
12	5 ^h 50 ^m 7 ^s	-70°59'.5
13	5 ^h 50 ^m 31 ^s	-70°45'.2
14	5 ^h 51 ^m 45 ^s	-72°30'.7
15	5 ^h 52 ^m 25 ^s	-72°21'.3
16	5 ^h 52 ^m 30 ^s	-70°36'.5
17	5 ^h 52 ^m 41 ^s	-71°26'.5
18	5 ^h 53 ^m 4 ^s	-71°35'.1
19	5 ^h 53 ^m 22 ^s	-71°37'.1
20	5 ^h 54 ^m 4 ^s	-70°25'.5
21	5 ^h 54 ^m 23 ^s	-70°33'.3
22	5 ^h 54 ^m 18 ^s	-71° 0'.5
23	5 ^h 56 ^m 21 ^s	-70°48'.0
24	6 ^h 0 ^m 18 ^s	-71°11'.7
25	6 ^h 7 ^m 9 ^s	-73°28'.2

Table II cont'd

L.M.C. Field #9

<u>Star</u>	<u>Right Ascension (1975)</u>	<u>Declination (1975)</u>
26	6 ^h 5 ^m 40 ^s	-71°21'.9
27	6 ^h 6 ^m 31 ^s	-70°44'.9
28	6 ^h 11 ^m 11 ^s	-71°10'.9
29	6 ^h 12 ^m 48 ^s	-72° 3'.4
30	6 ^h 13 ^m 10 ^s	-72°10'.4
31	6 ^h 16 ^m 9 ^s	-71°44'.2
32	6 ^h 17 ^m 50 ^s	-71°36'.1
33	6 ^h 20 ^m 2 ^s	-72°28'.6
34	6 ^h 19 ^m 19 ^s	-71°16'.8
35	6 ^h 19 ^m 46 ^s	-71° 9'.6
36	6 ^h 22 ^m 43 ^s	-72°37'.0

L.M.C. Field #20

<u>Star</u>	<u>Right Ascension (1975)</u>	<u>Declination (1975)</u>
1	5 ^h 57 ^m 24 ^s	-73° 52'.4
2	6 ^h 9 ^m 14 ^s	-73° 50'.1
3	6 ^h 14 ^m 22 ^s	-73° 53'.1
4	6 ^h 18 ^m 0 ^s	-74° 1'.3

Table II cont'd

L.M.C. Field #23

<u>Star</u>	<u>Right Ascension (1975)</u>	<u>Declination (1975)</u>
1	6 ^h 10 ^m 27 ^s	-68° 27'.6
2	6 ^h 11 ^m 38 ^s	-68° 5'.3
3	6 ^h 11 ^m 56 ^s	-68° 3'.7
4	6 ^h 12 ^m 45 ^s	-67° 34'.0
5	6 ^h 13 ^m 8 ^s	-67° 56'.3
6	6 ^h 13 ^m 21 ^s	-67° 49'.9
7	6 ^h 13 ^m 44 ^s	-67° 28'.4
8	6 ^h 15 ^m 39 ^s	-67° 28'.9
9	6 ^h 16 ^m 18 ^s	-67° 25'.0
10	6 ^h 16 ^m 55 ^s	-67° 29'.7
11	6 ^h 17 ^m 38 ^s	-67° 26'.4
12	6 ^h 16 ^m 52 ^s	-67° 53'.0
13	6 ^h 16 ^m 10 ^s	-68° 0'.5
14	6 ^h 16 ^m 31 ^s	-68° 3'.5
15	6 ^h 16 ^m 19 ^s	-68° 9'.1
16	6 ^h 16 ^m 35 ^s	-68° 9'.4
17	6 ^h 17 ^m 7 ^s	-68° 13'.2
18	6 ^h 18 ^m 14 ^s	-67° 47'.8
19	6 ^h 19 ^m 21 ^s	-67° 49'.8
20	6 ^h 19 ^m 26 ^s	-67° 49'.8
21	6 ^h 19 ^m 24 ^s	-68° 22'.2
22	6 ^h 20 ^m 15 ^s	-68° 27'.8
23	6 ^h 21 ^m 20 ^s	-68° 20'.7
24	6 ^h 22 ^m 0 ^s	-68° 0'.6

Table II cont'd

L.M.C. Field #23

<u>Star</u>	<u>Right Ascension (1975)</u>	<u>Declination (1975)</u>
25	6 ^h 22 ^m 10 ^s	-67° 59'.4
26	6 ^h 22 ^m 26 ^s	-67° 52'.3
27	6 ^h 23 ^m 31 ^s	-68° 35'.9
28	6 ^h 23 ^m 48 ^s	-68° 57'.0
29	6 ^h 25 ^m 55 ^s	-68° 10'.8
30	6 ^h 26 ^m 21 ^s	-68° 46'.8
31	6 ^h 26 ^m 42 ^s	-68° 49'.2
32	6 ^h 27 ^m 16 ^s	-68° 52'.0
33	6 ^h 28 ^m 56 ^s	-68° 54'.6
34	6 ^h 31 ^m 21 ^s	-69° 11'.1
35	6 ^h 14 ^m 16 ^s	-68° 48'.8
36	6 ^h 11 ^m 37 ^s	-68° 52'.8
37	6 ^h 11 ^m 57 ^s	-68° 58'.7
38	6 ^h 13 ^m 55 ^s	-68° 58'.7
39	6 ^h 11 ^m 54 ^s	-69° 15'.1
40	6 ^h 13 ^m 24 ^s	-69° 14'.4
41	6 ^h 12 ^m 21 ^s	-69° 44'.6
42	6 ^h 11 ^m 50 ^s	-70° 1'.3
43	6 ^h 13 ^m 46 ^s	-70° 13'.0
44	6 ^h 15 ^m 6 ^s	-70° 0'.2
45	6 ^h 15 ^m 15 ^s	-70° 29'.3
46	6 ^h 24 ^m 47 ^s	-70° 13'.6
47	6 ^h 24 ^m 39 ^s	-69° 53'.2
48	6 ^h 24 ^m 40 ^s	-69° 44'.1
49	6 ^h 25 ^m 5 ^s	-69° 44'.0
50	6 ^h 29 ^m 3 ^s	-70° 20'.4
51	6 ^h 13 ^m 38 ^s	-69° 28'.3

Table II cont'd

L.M.C. Field #24

<u>Star</u>	<u>Right Ascension (1975)</u>	<u>Declination (1975)</u>
1	6 ^h 26 ^m 47 ^s	-71°41'.8
2	6 ^h 29 ^m 34 ^s	-70°55'.5
3	6 ^h 30 ^m 42 ^s	-71° 0'.6

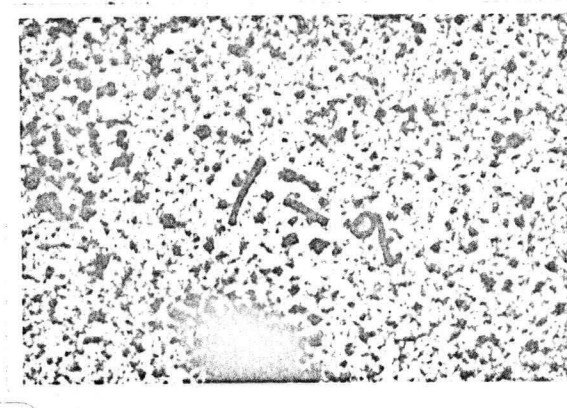
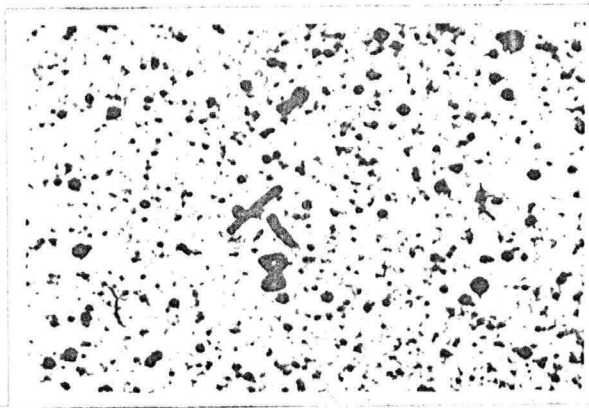
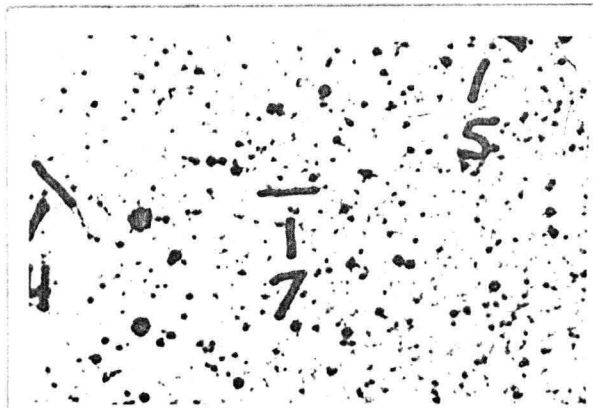
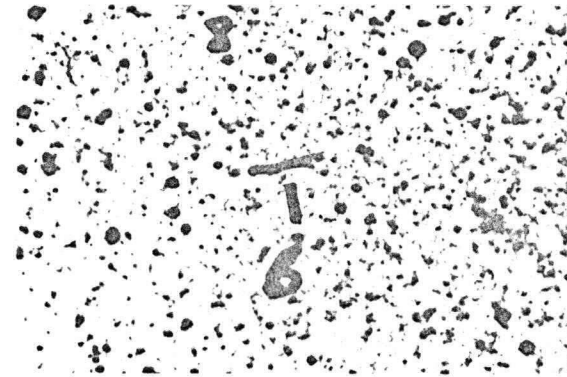
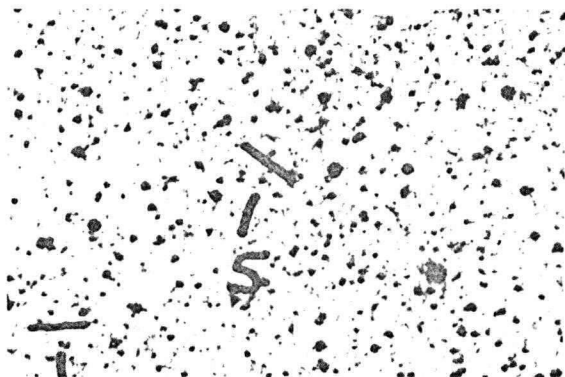
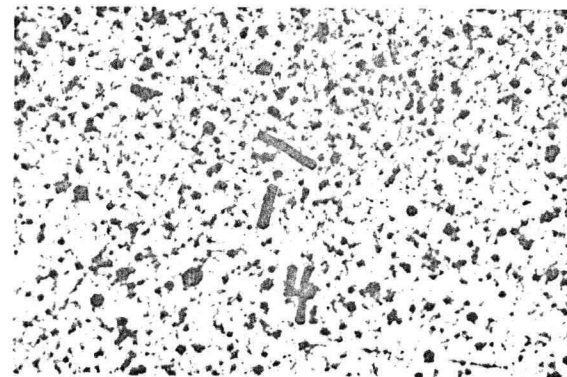
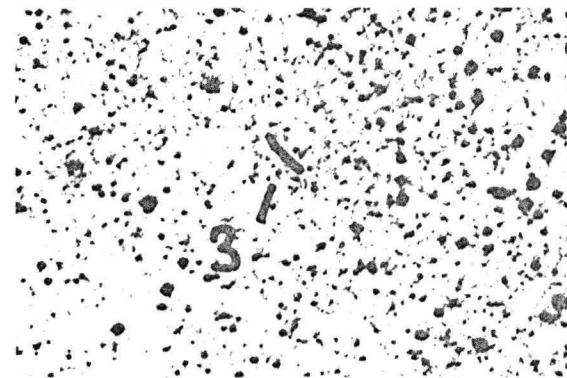
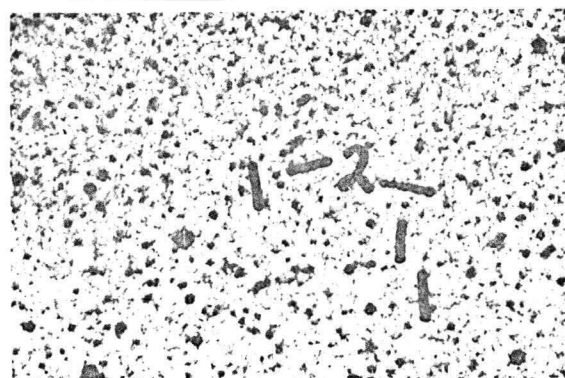
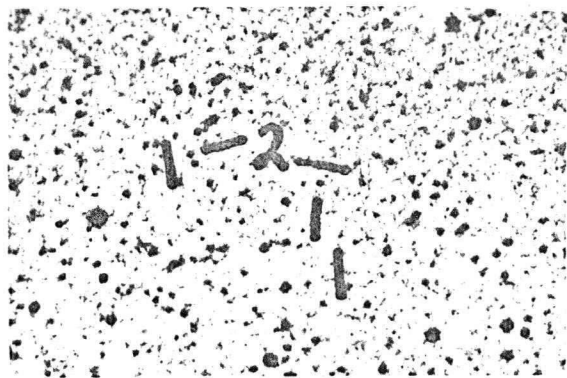


Fig. 1 Finding Charts LMC Field #1

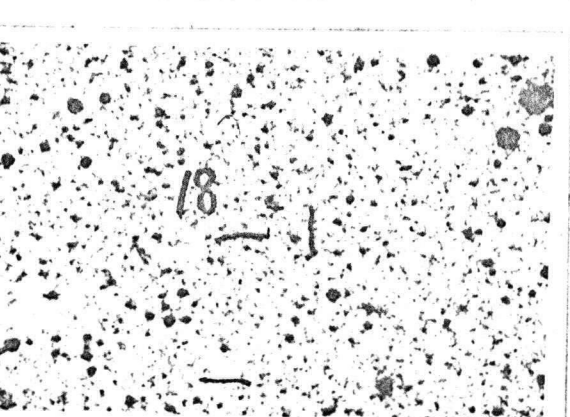
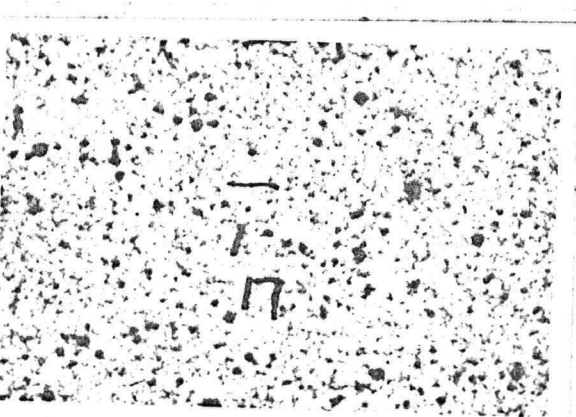
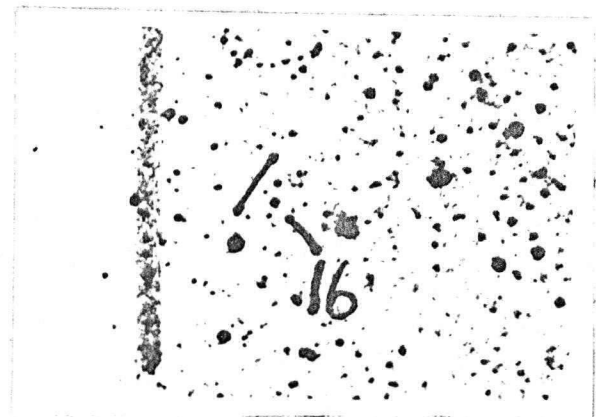
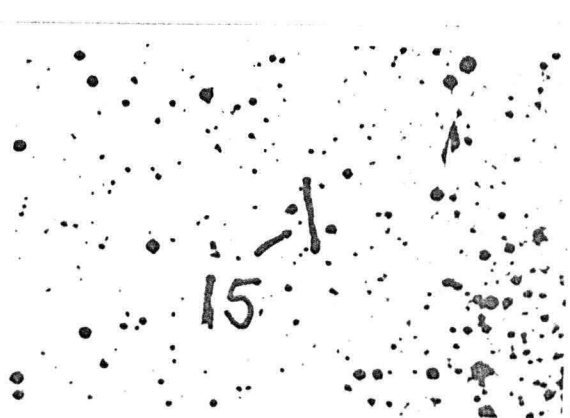
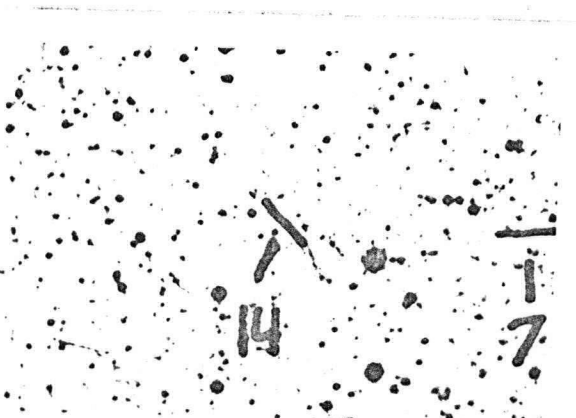
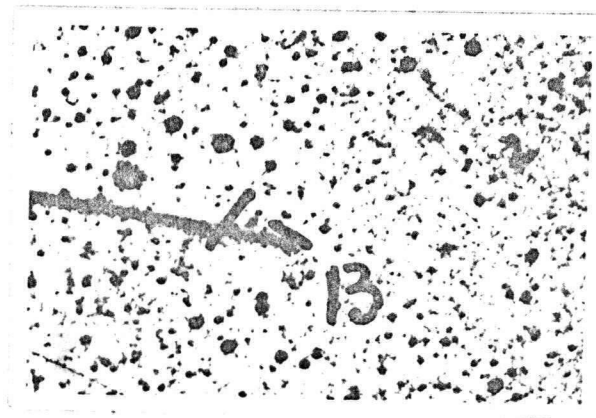
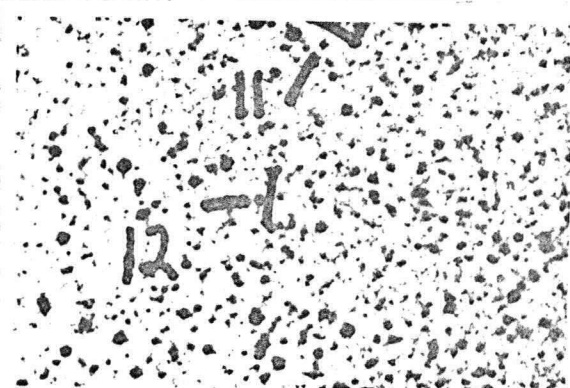
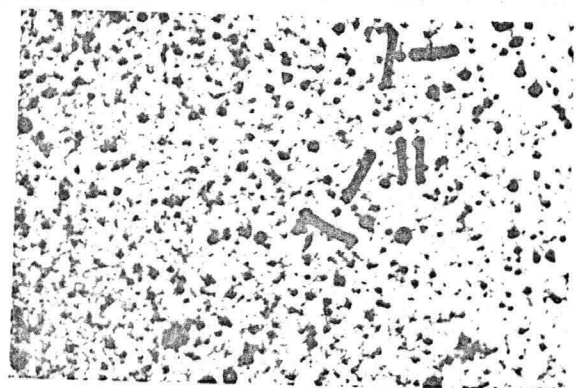
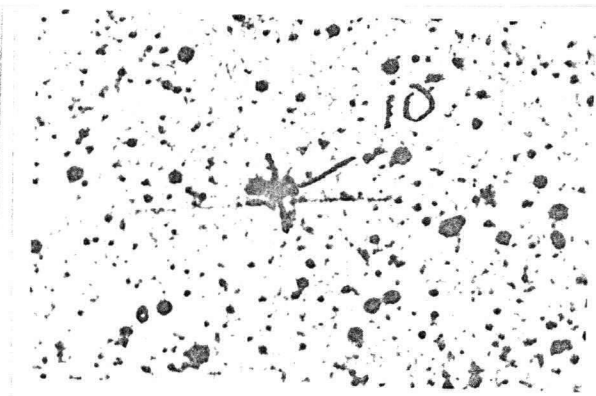


Fig. 1 cont. LMC Field #1

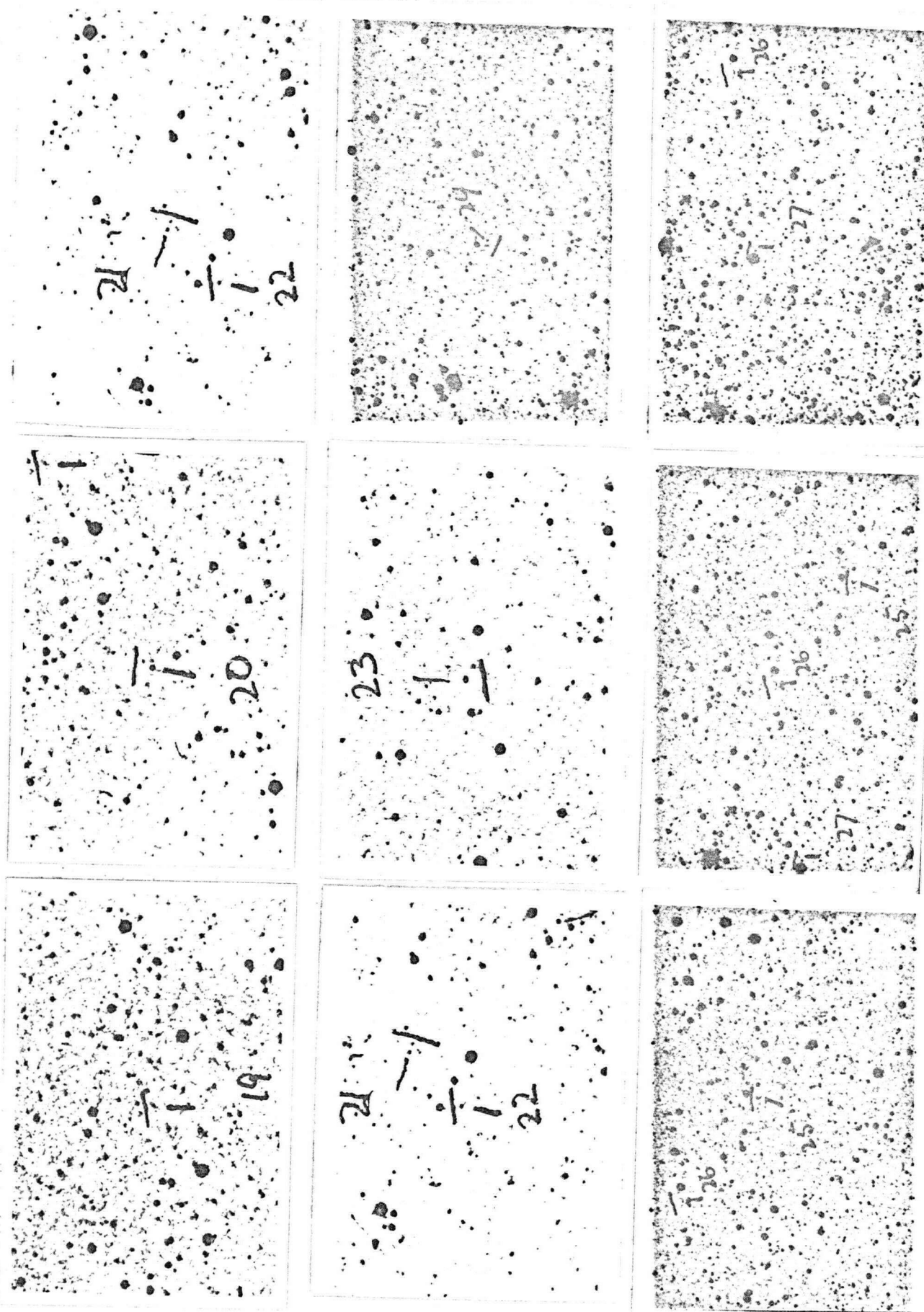


Fig. 1 cont. LMC Field #1

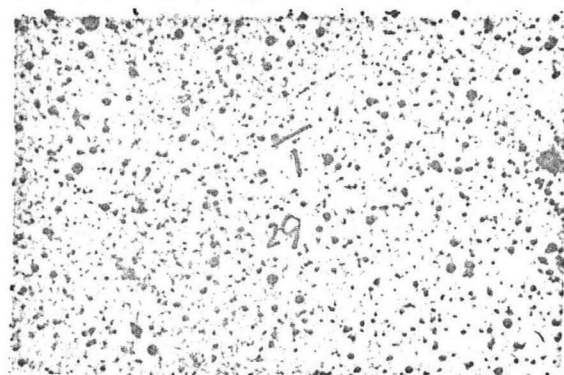
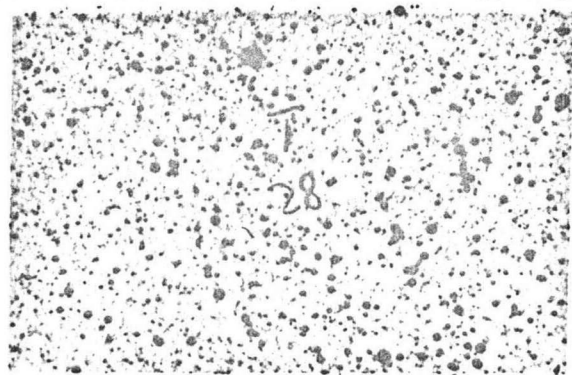


Fig. 1 cont. LMC Field #1

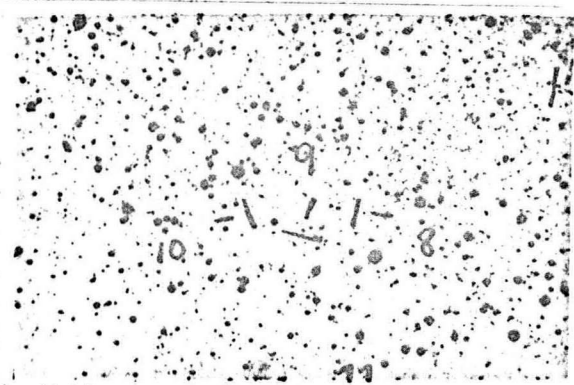
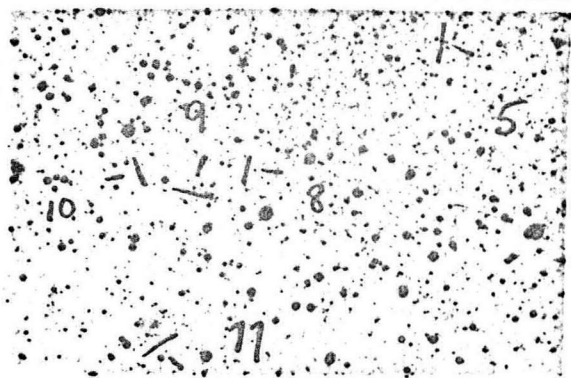
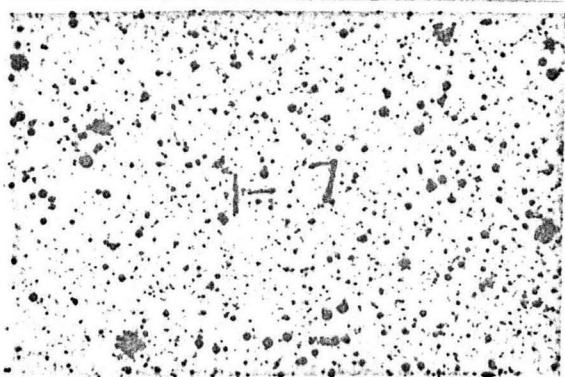
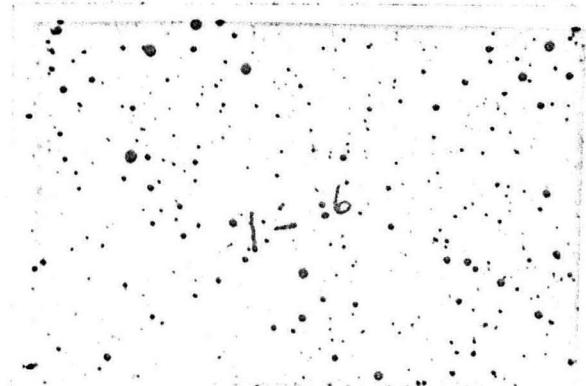
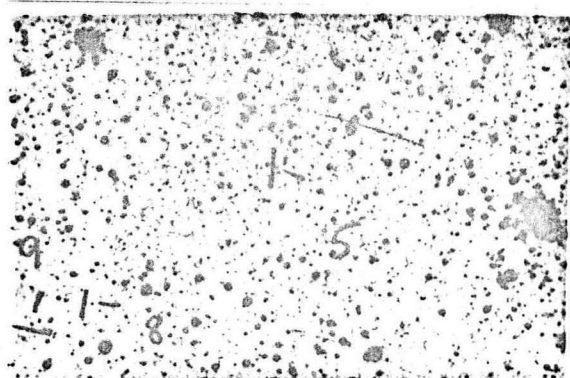
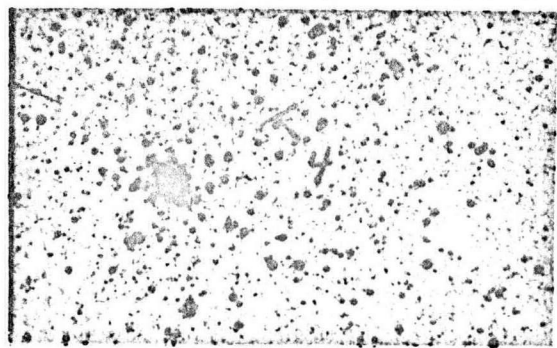
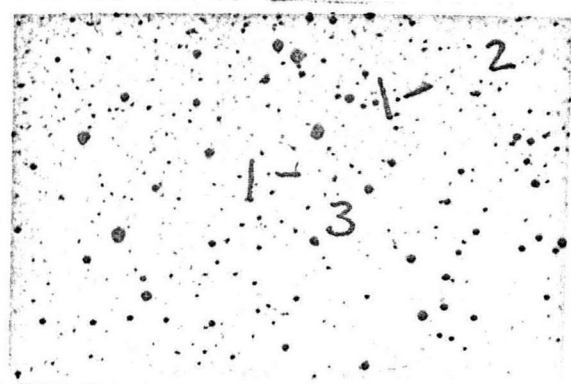
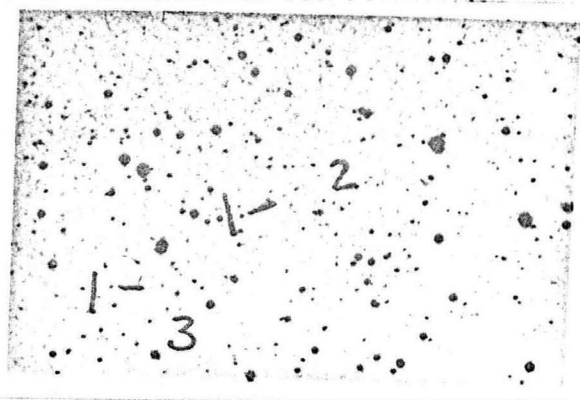
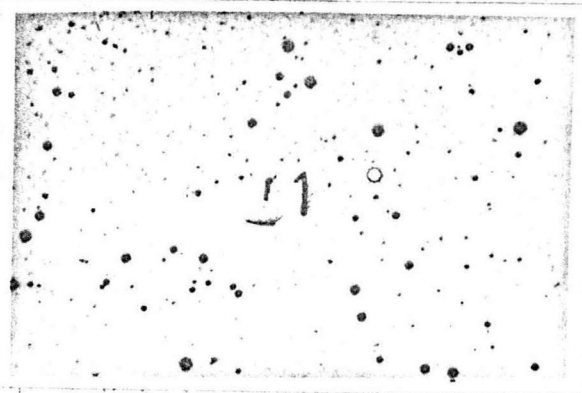


Fig. 1 cont. LMC Field #2

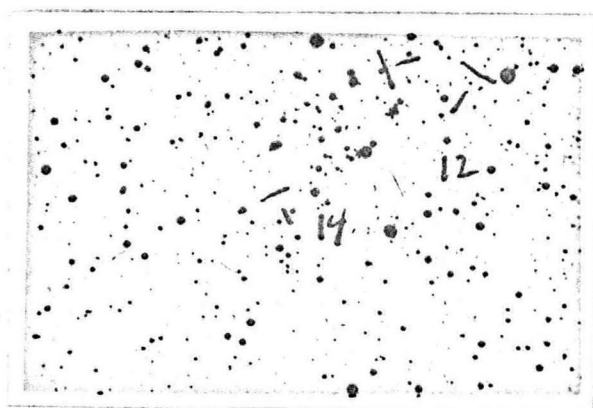
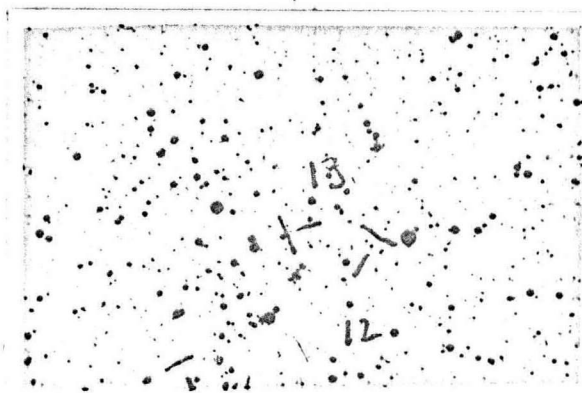
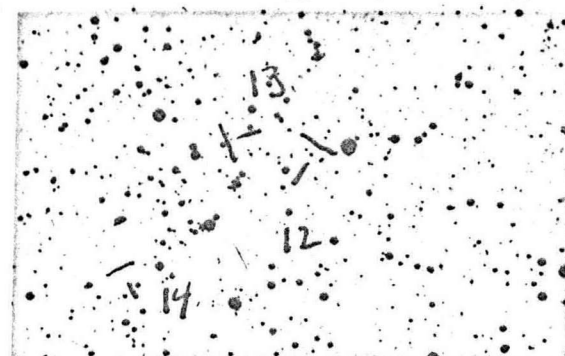
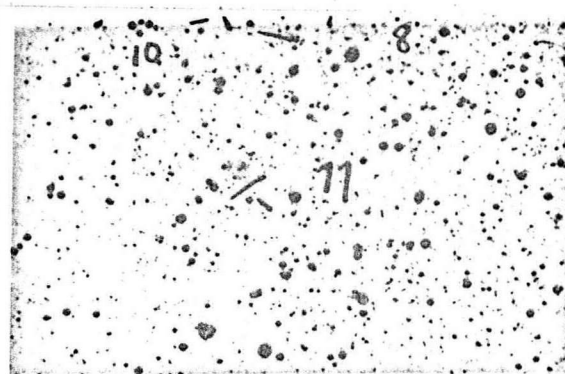
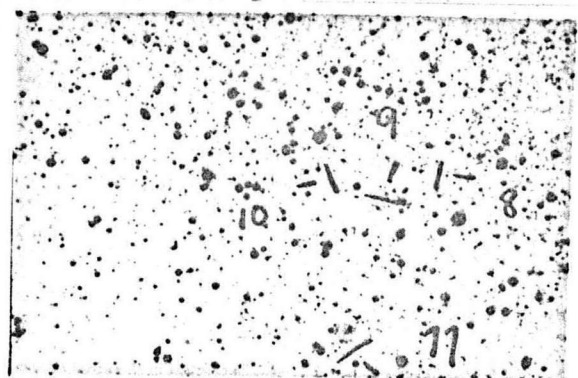


Fig. 1 cont. LMC Field #2

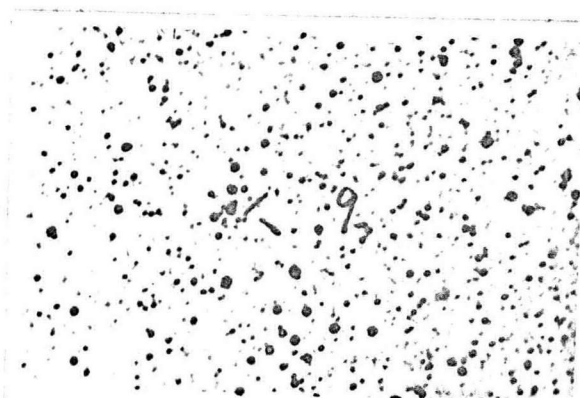
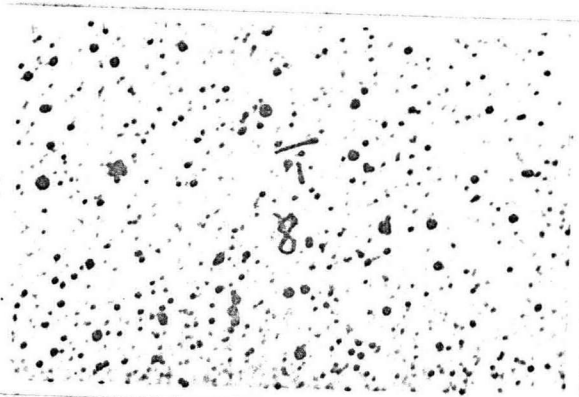
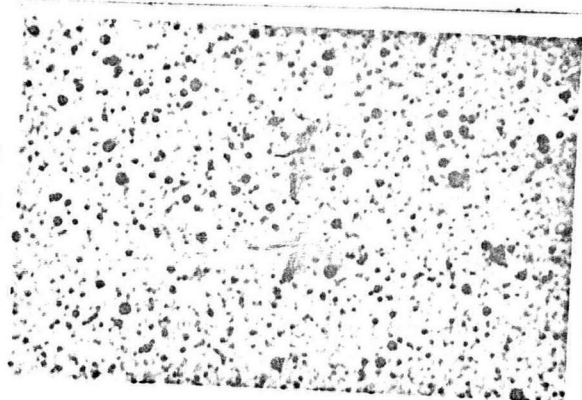
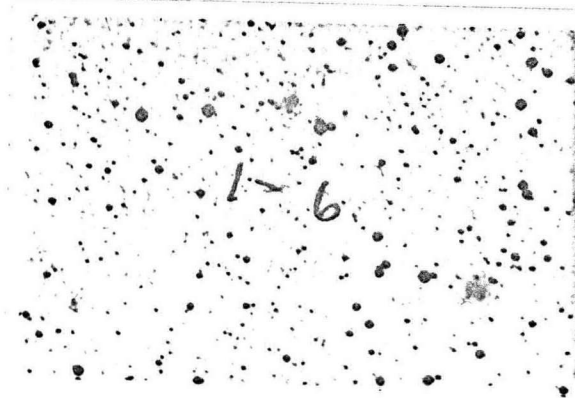
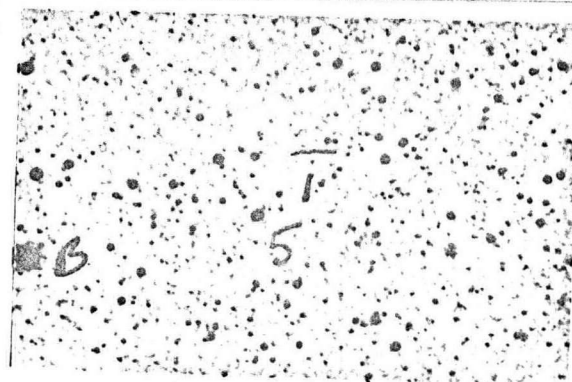
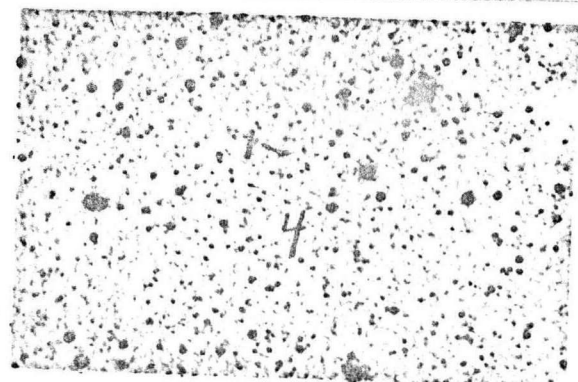
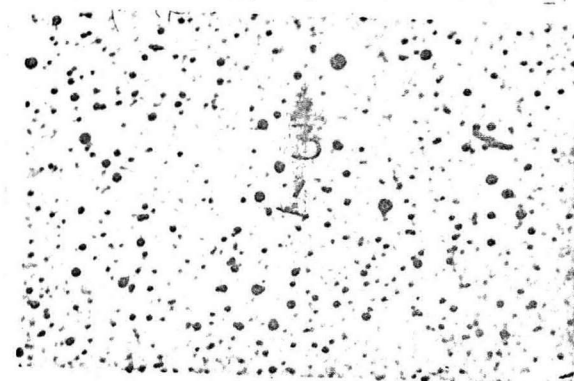
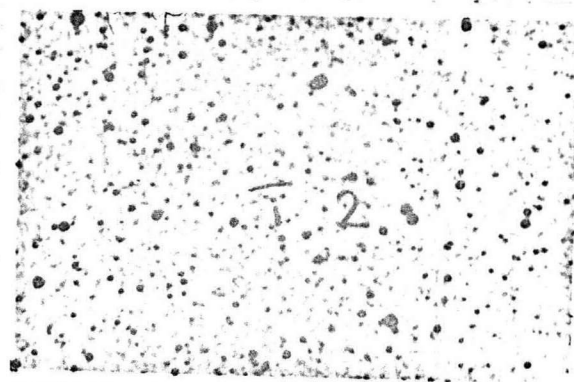
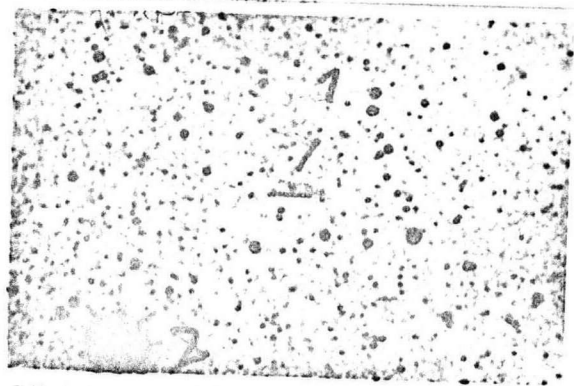


Fig. 1 cont. LMC Field #3

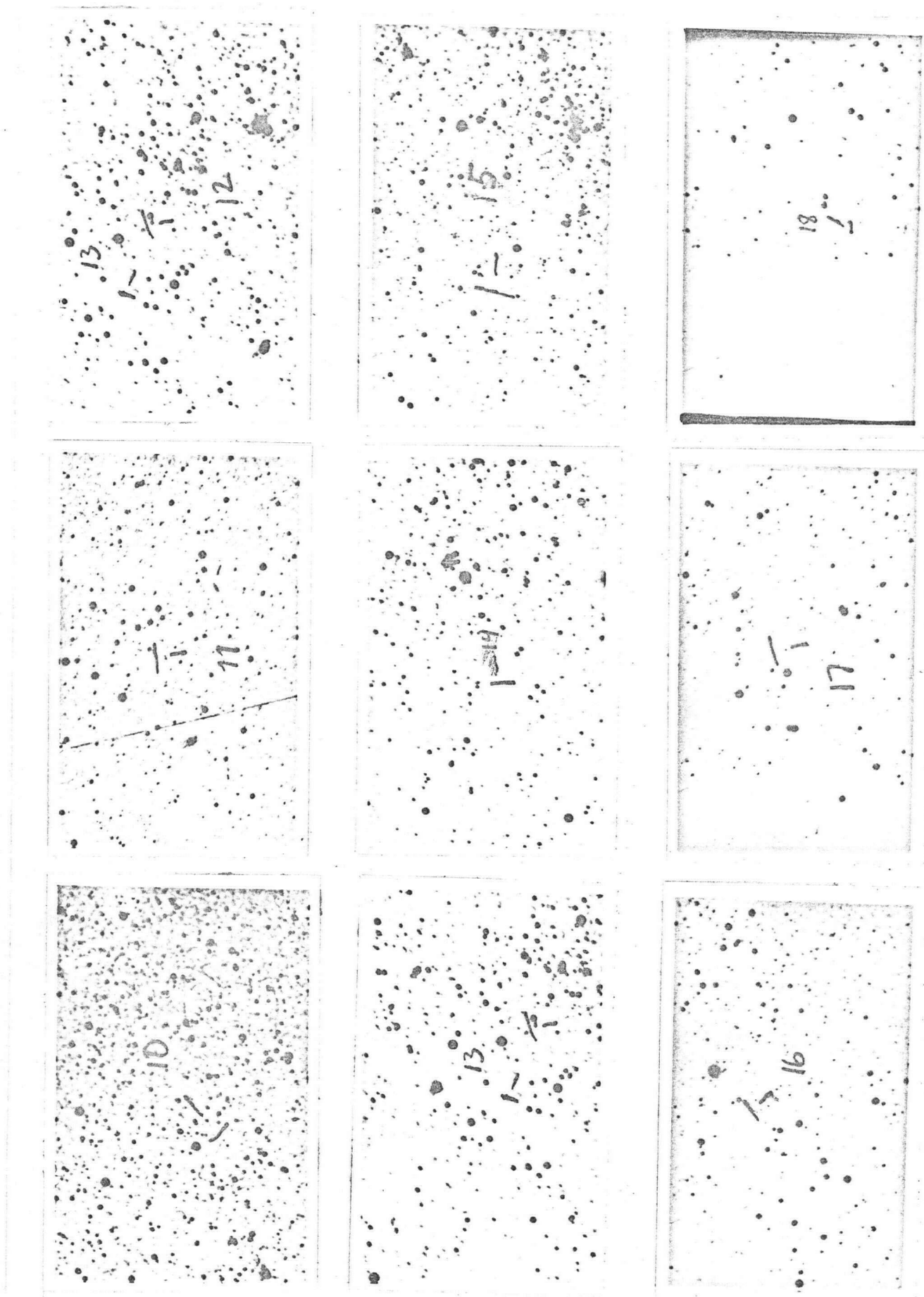


Fig. 1 cont. LMC Field #3

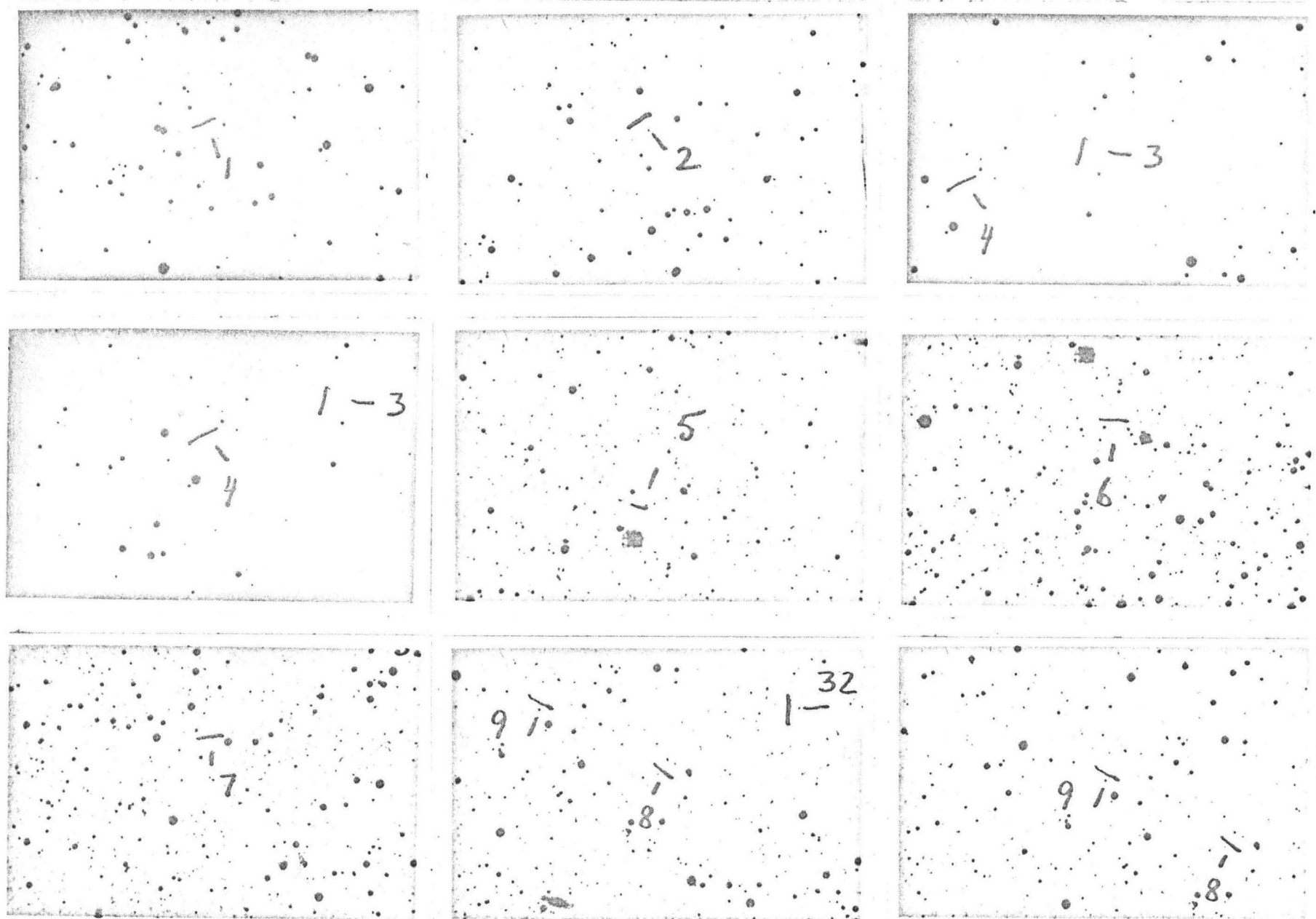


Fig. 1 cont. LMC Field #4

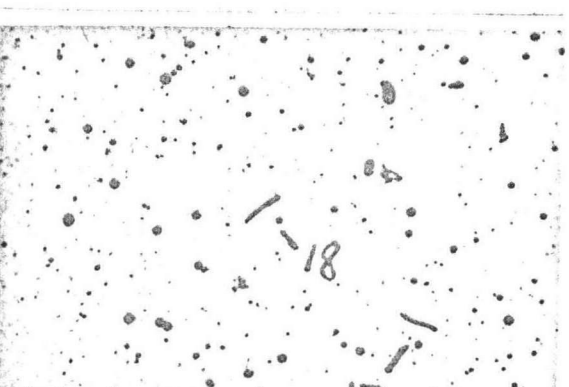
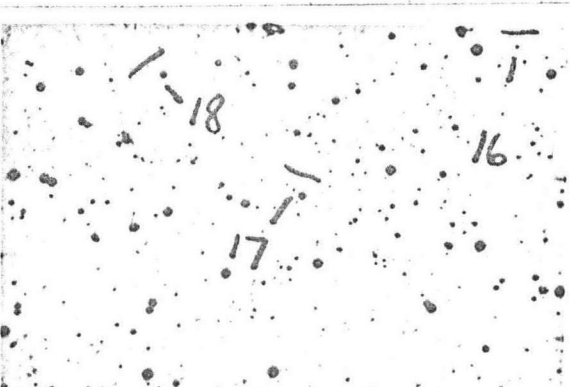
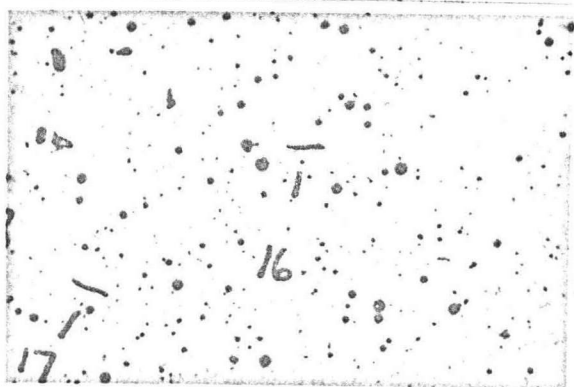
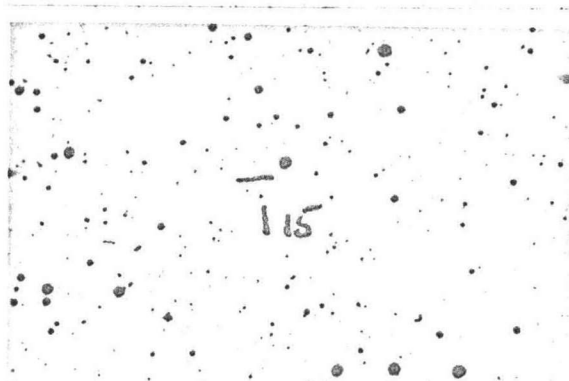
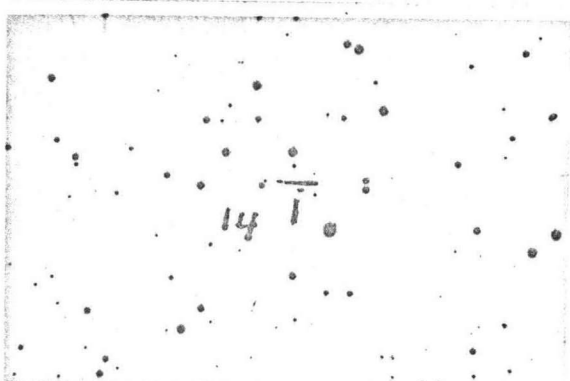
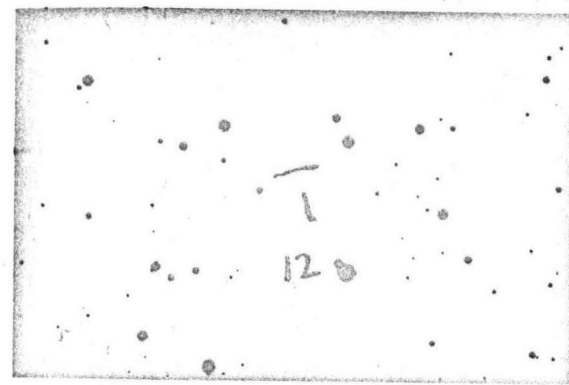
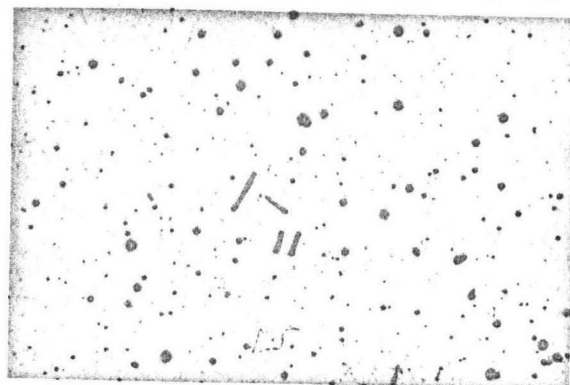


Fig. 1 cont. LMC Field #4

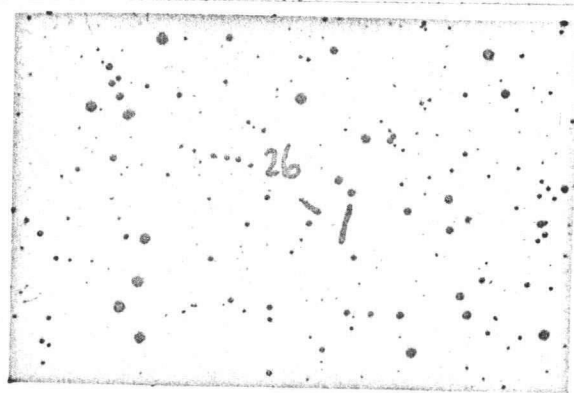
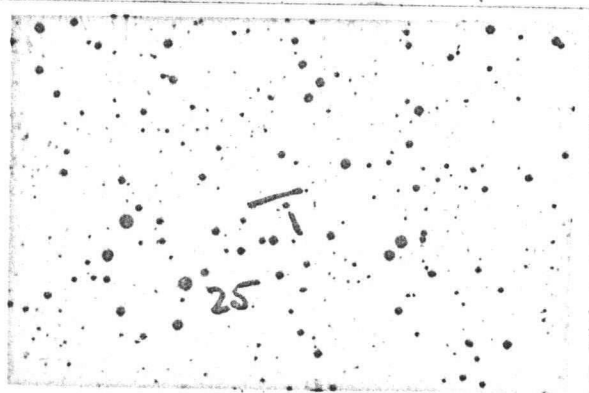
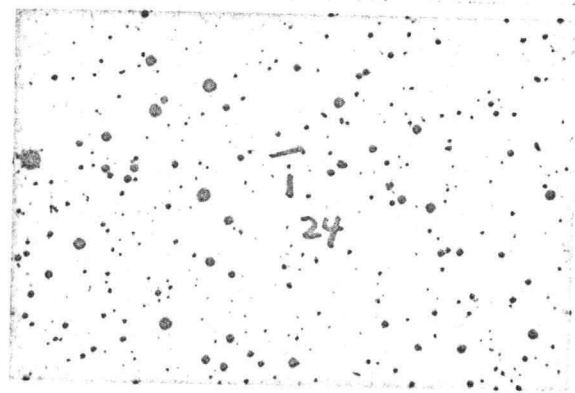
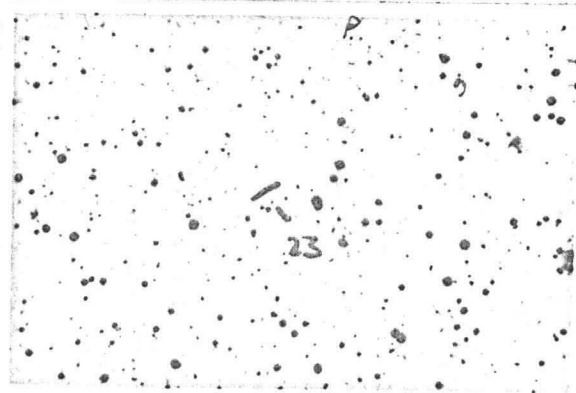
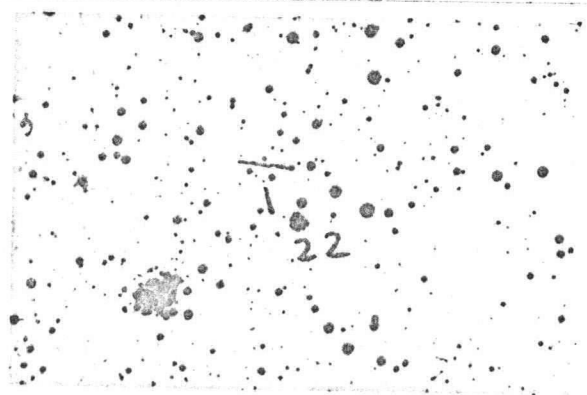
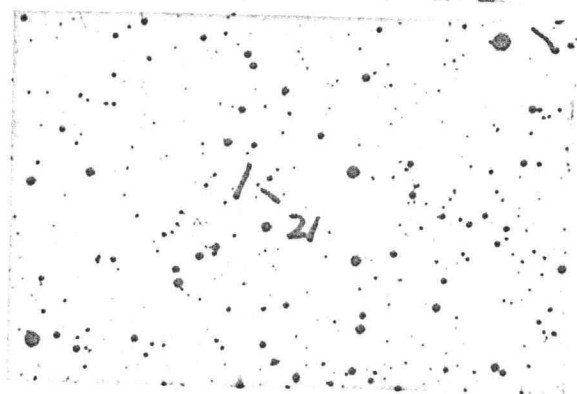
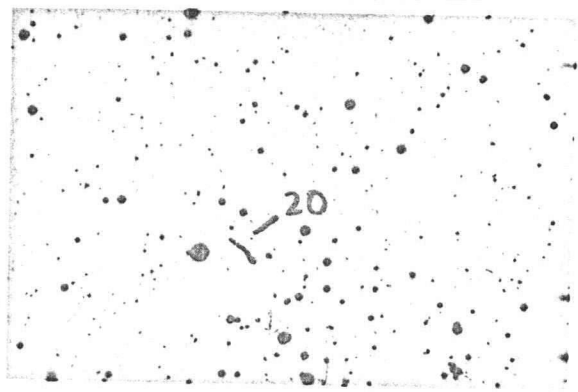
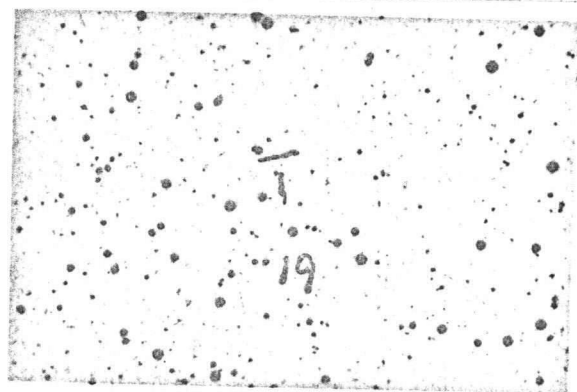


Fig. 1 cont. LMC Field #4

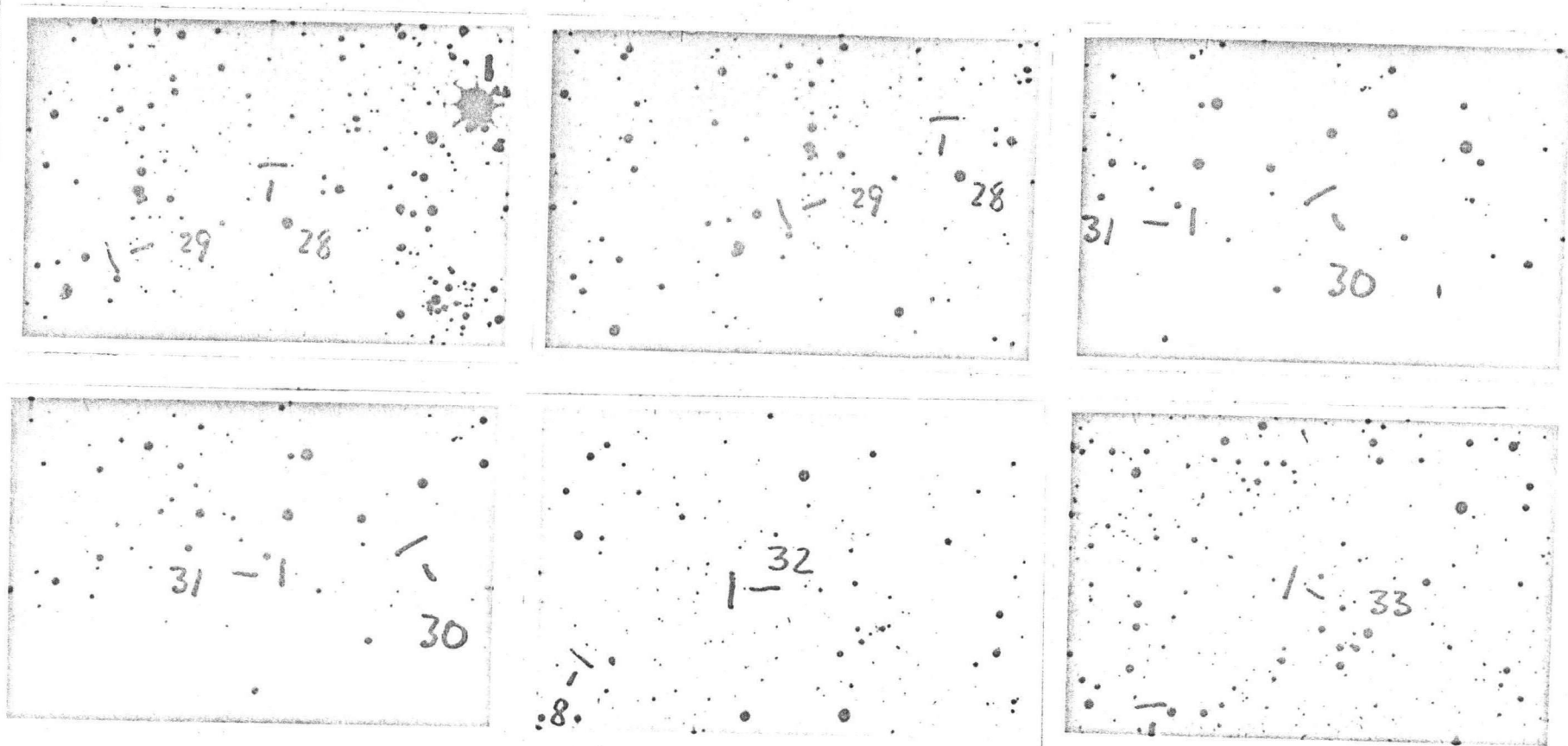


Fig. 1 cont. LMC Field #4

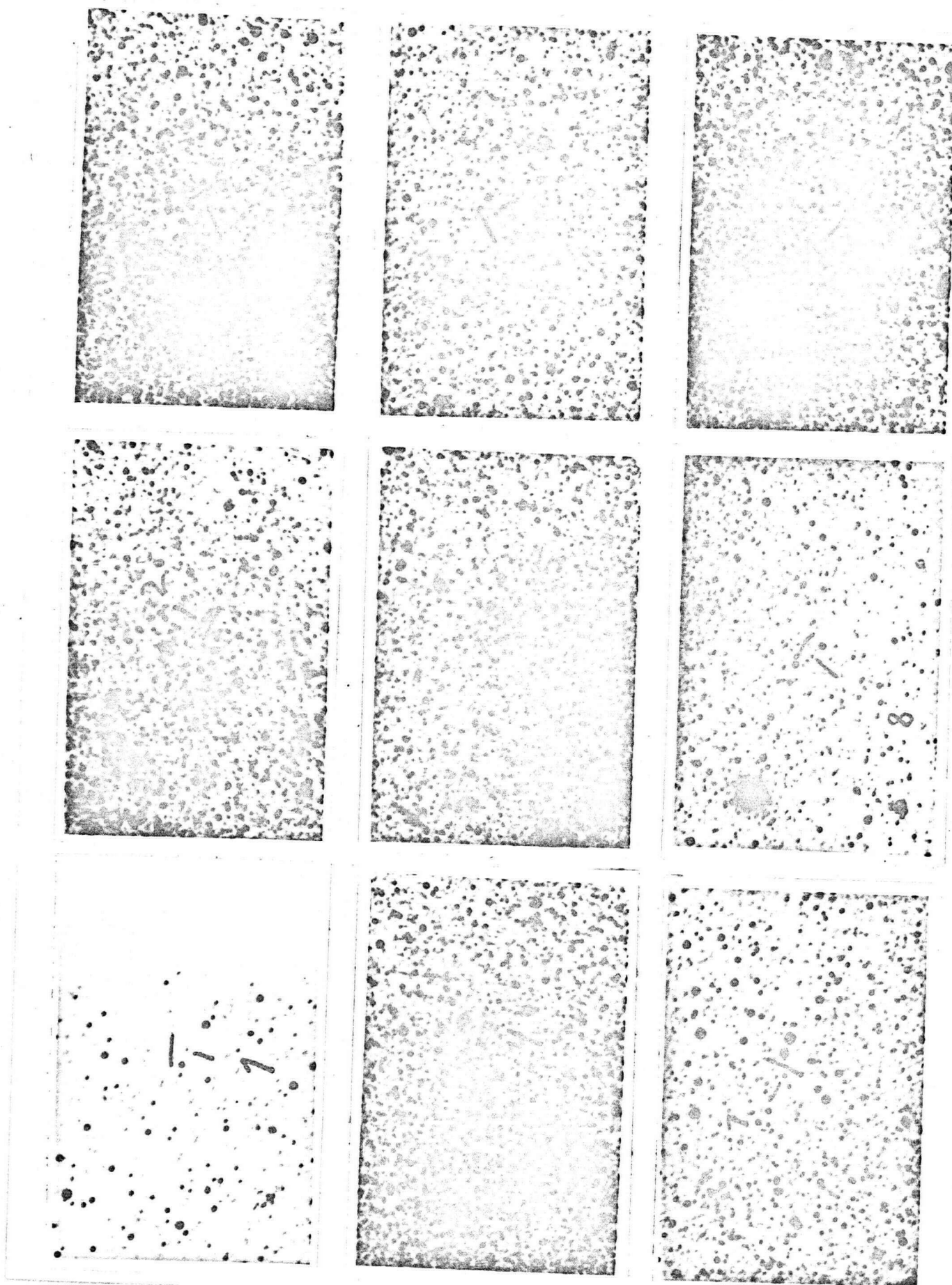


Fig. 1 cont. LMC Field #5

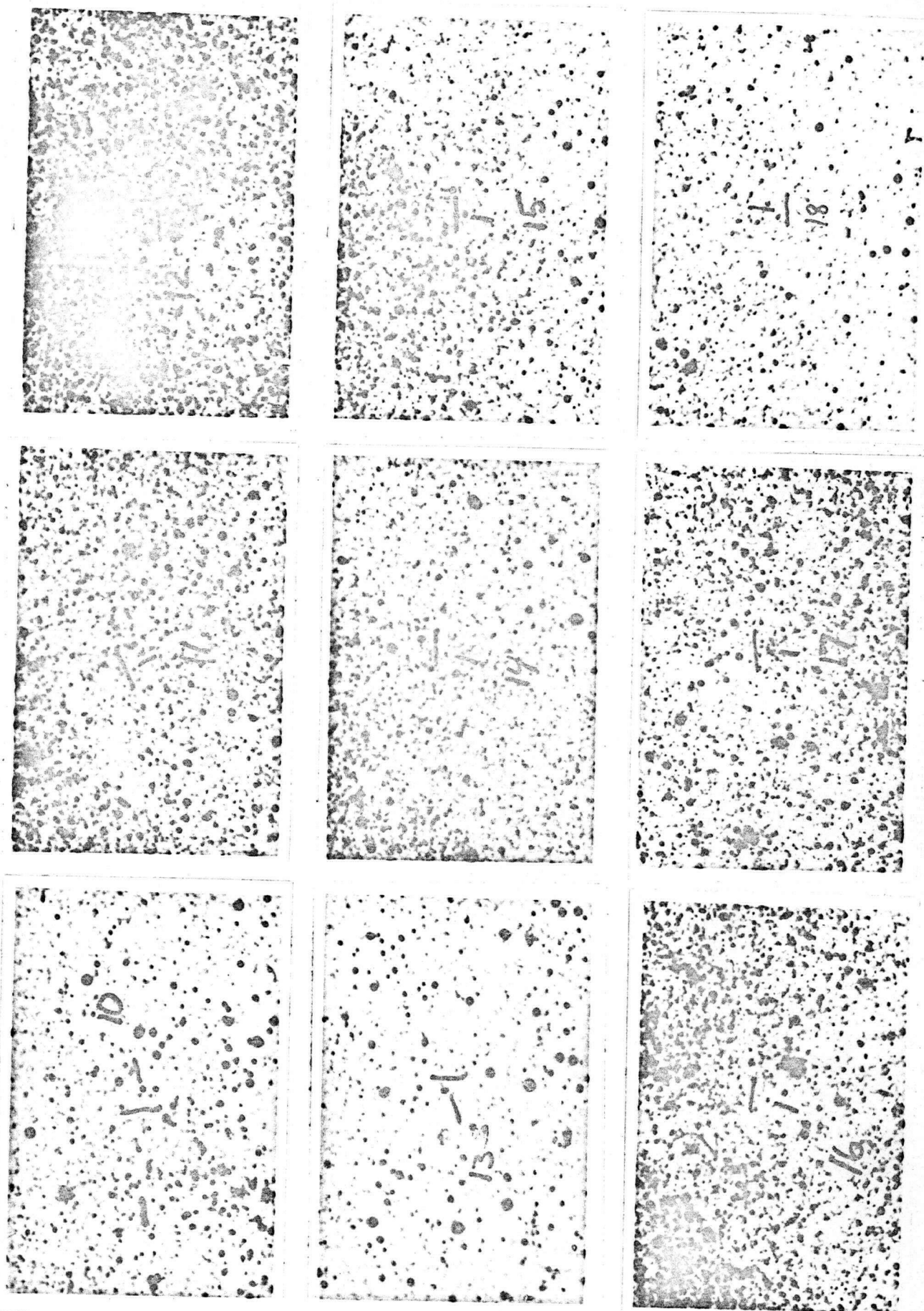
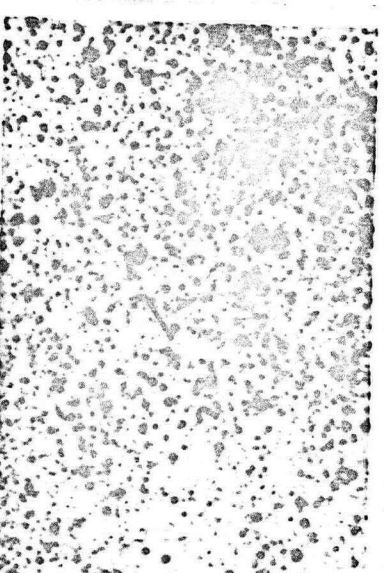
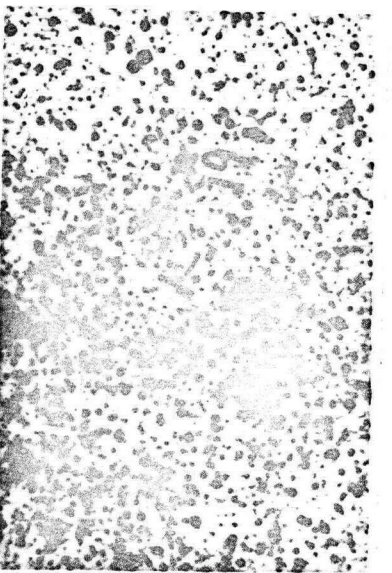
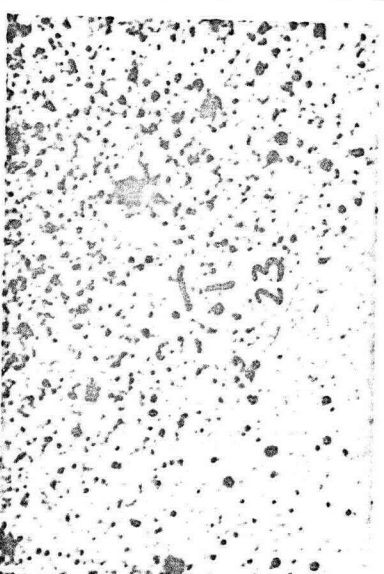
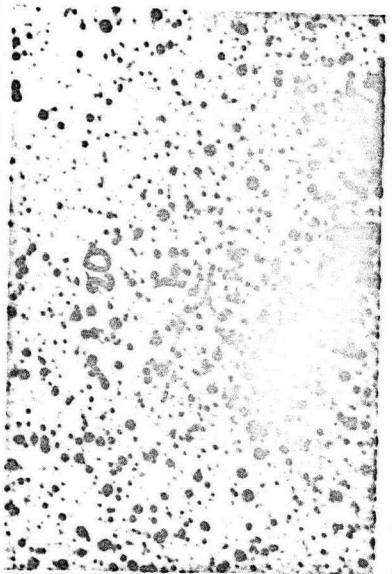
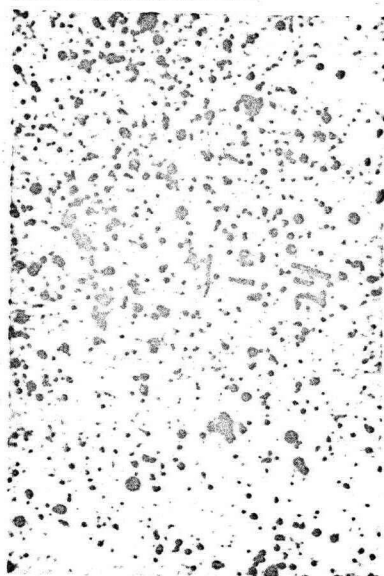
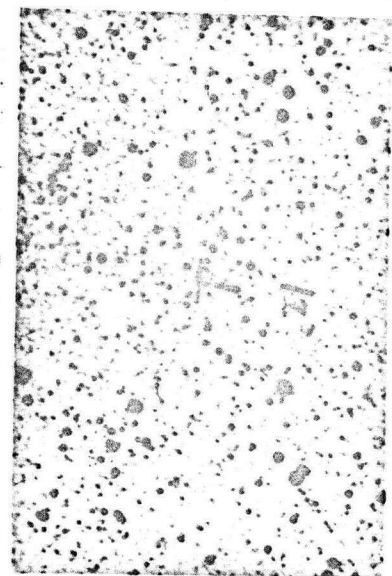


Fig. 1 cont. LMC Field #5



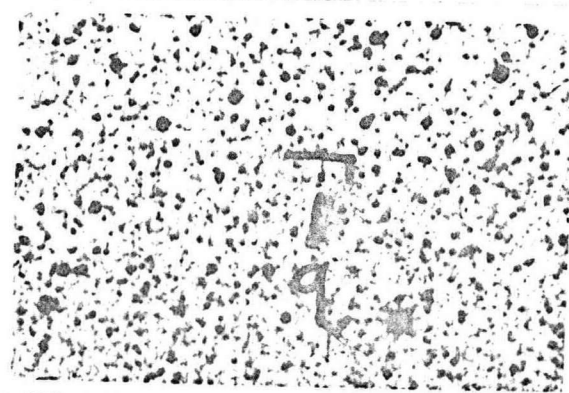
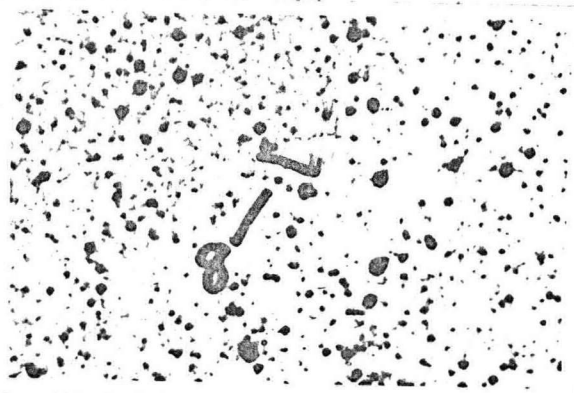
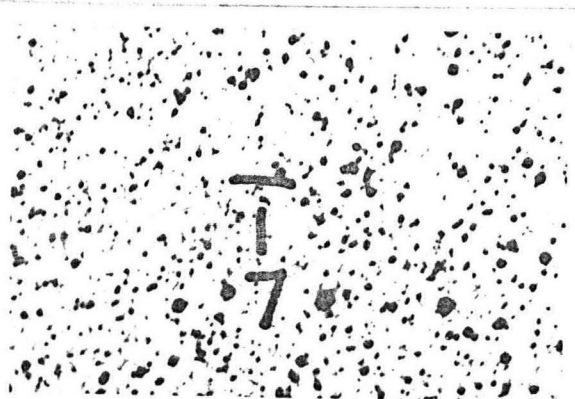
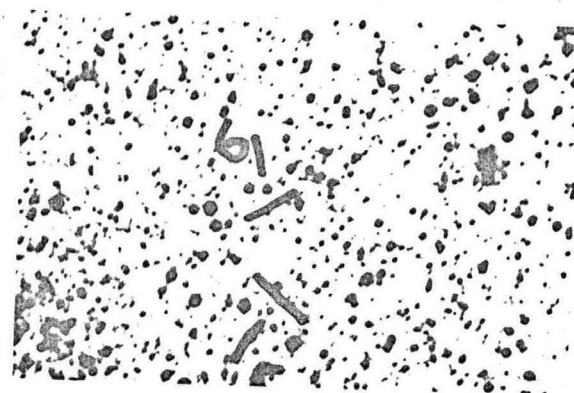
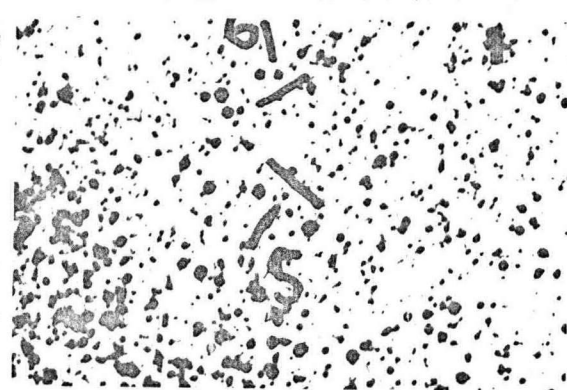
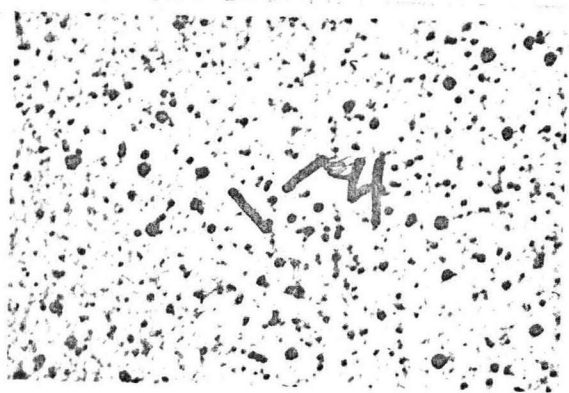
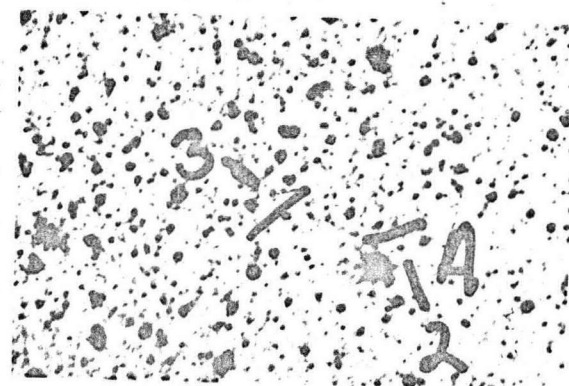
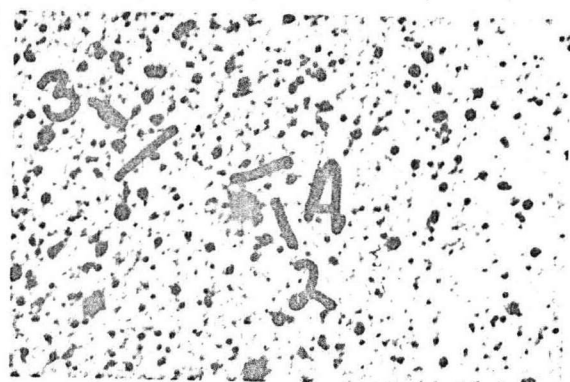
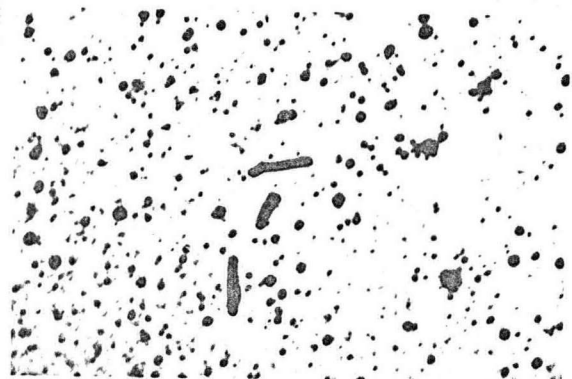


Fig. 1 cont. LMC Field #6

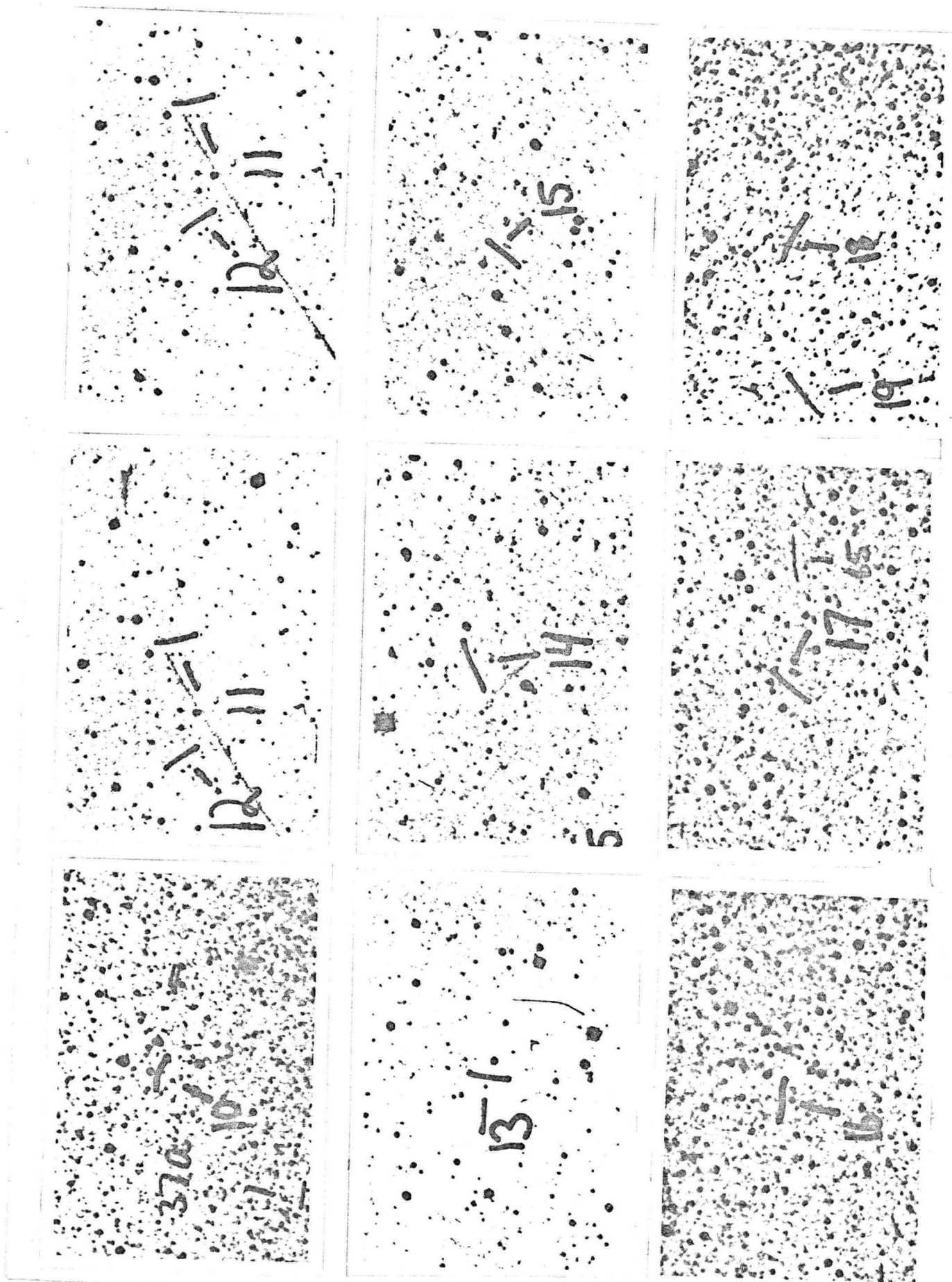


Fig. 1 cont. LMC Field #6

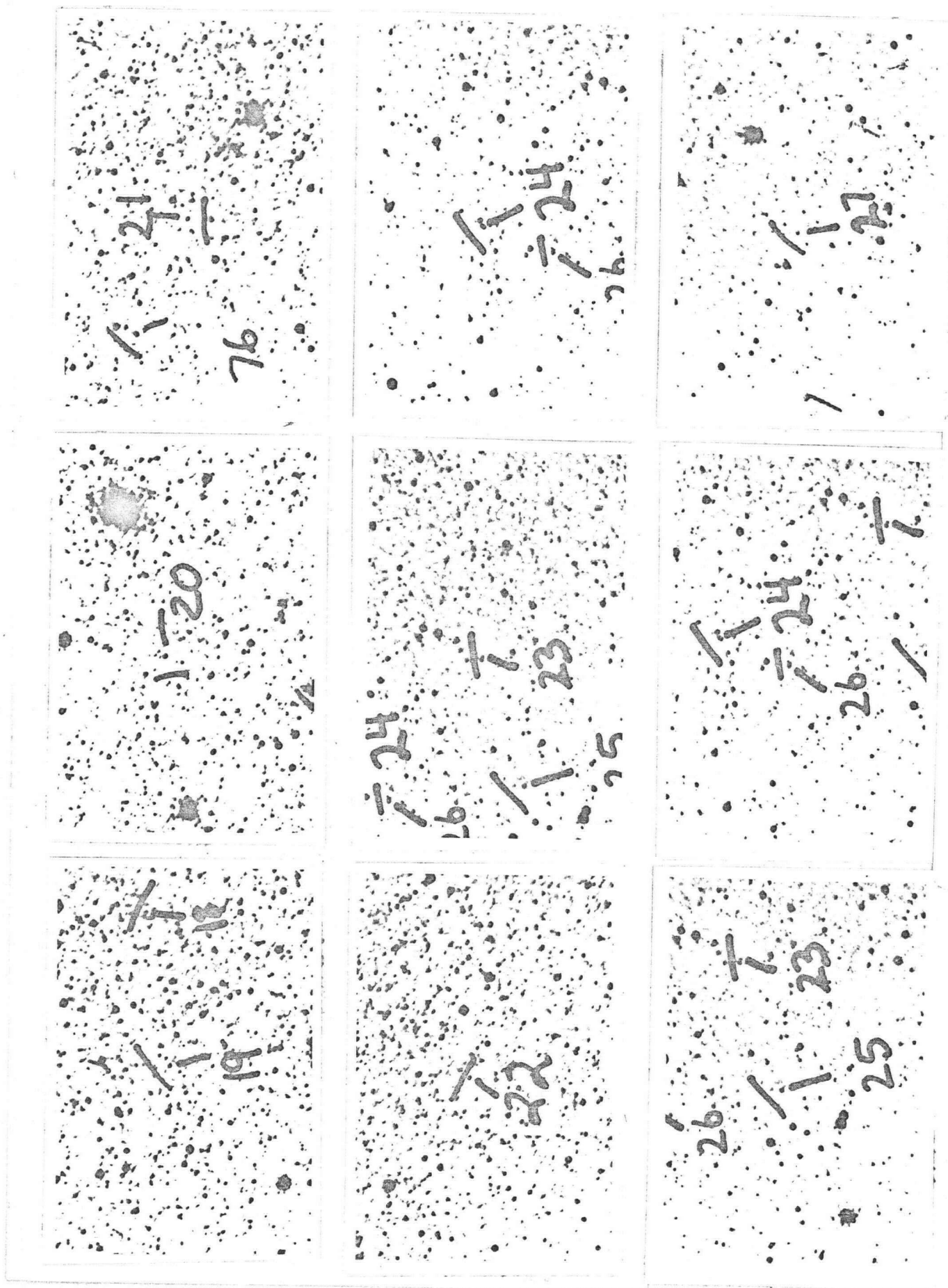


Fig. 1 cont. LMC Field #6

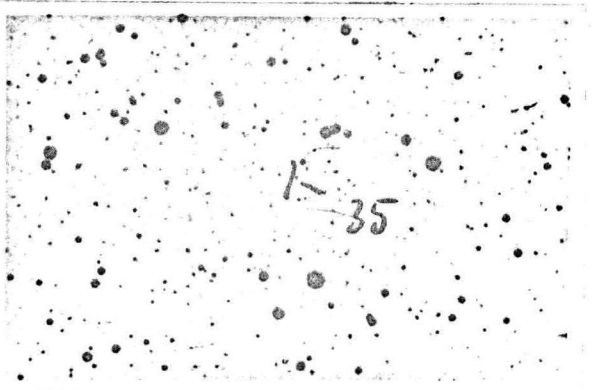
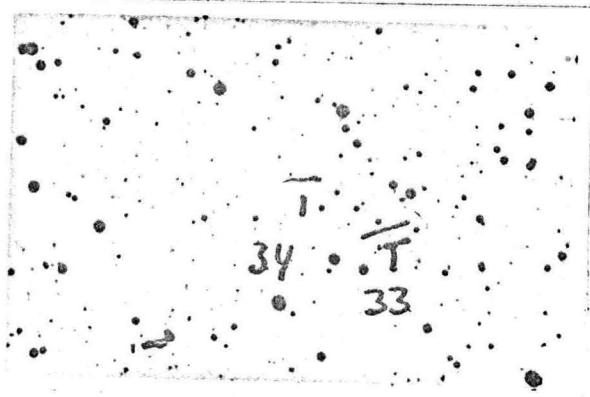
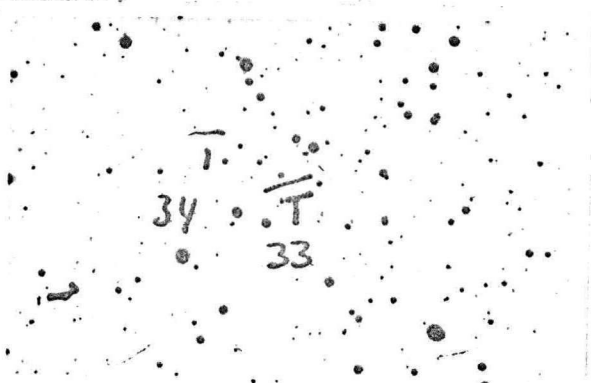
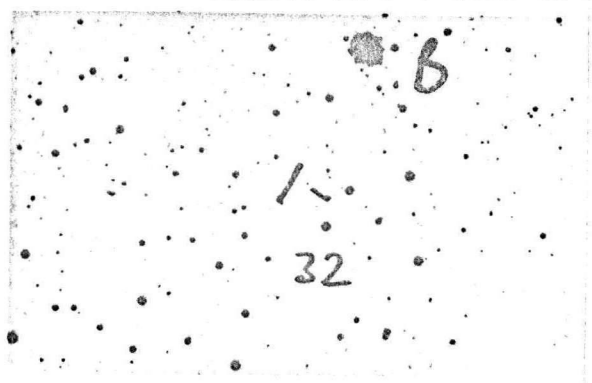
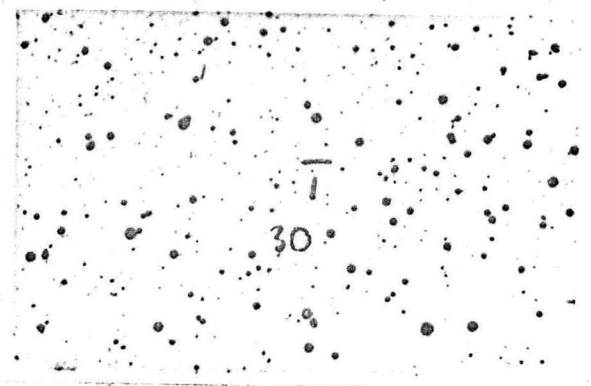
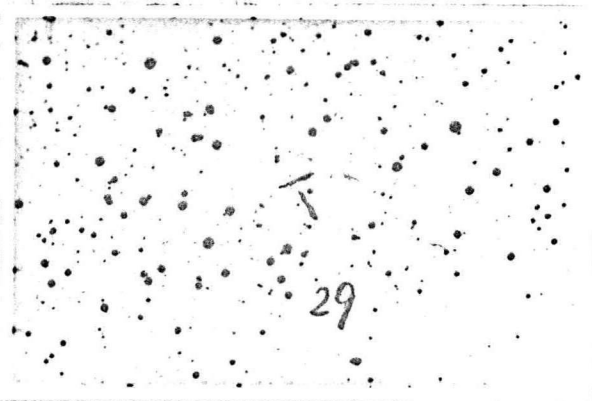


Fig. 1 cont. LMC Field #6

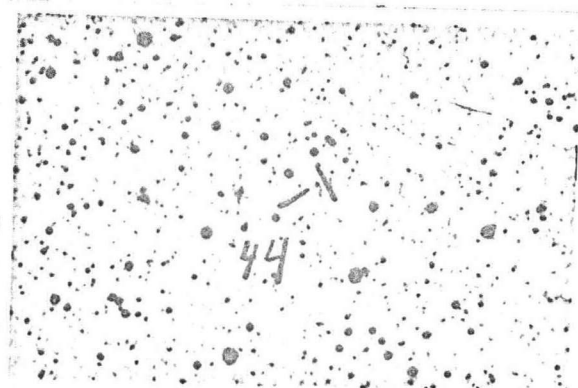
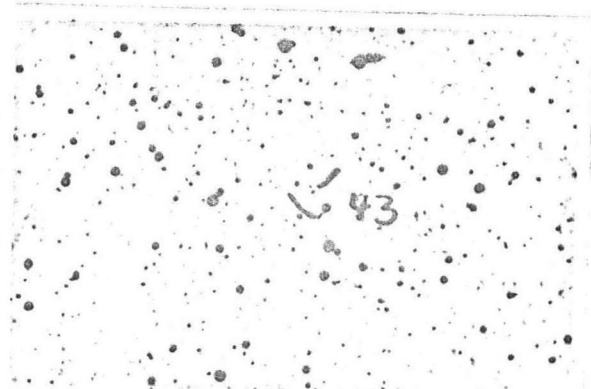
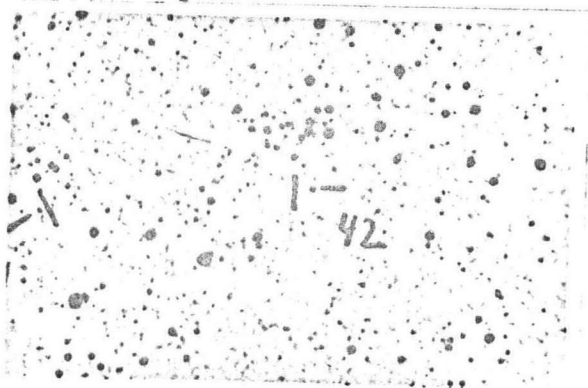
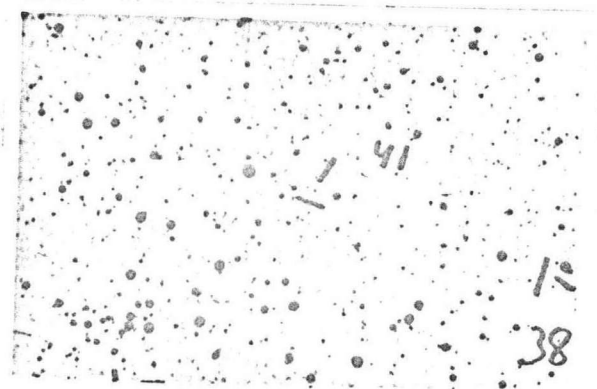
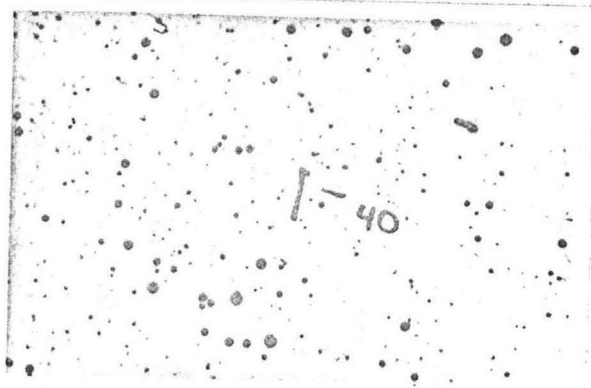
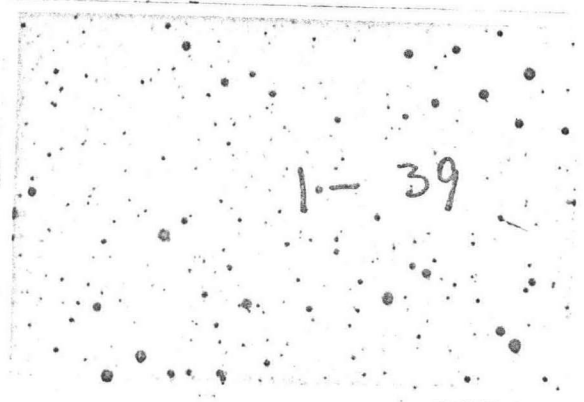
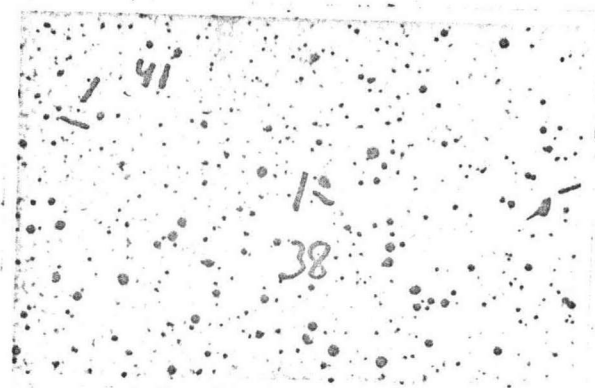
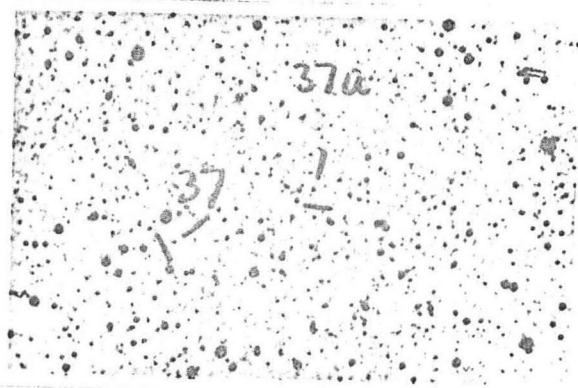
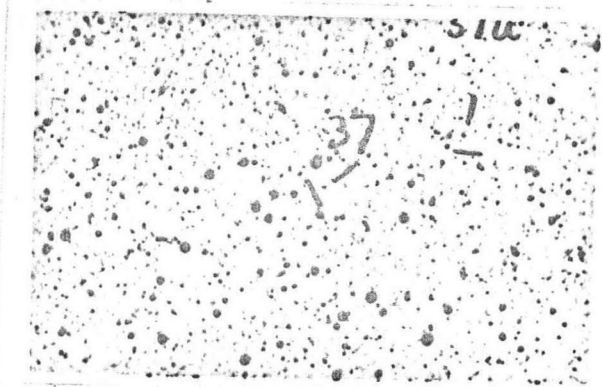


Fig. 1 cont. LMC Field #6

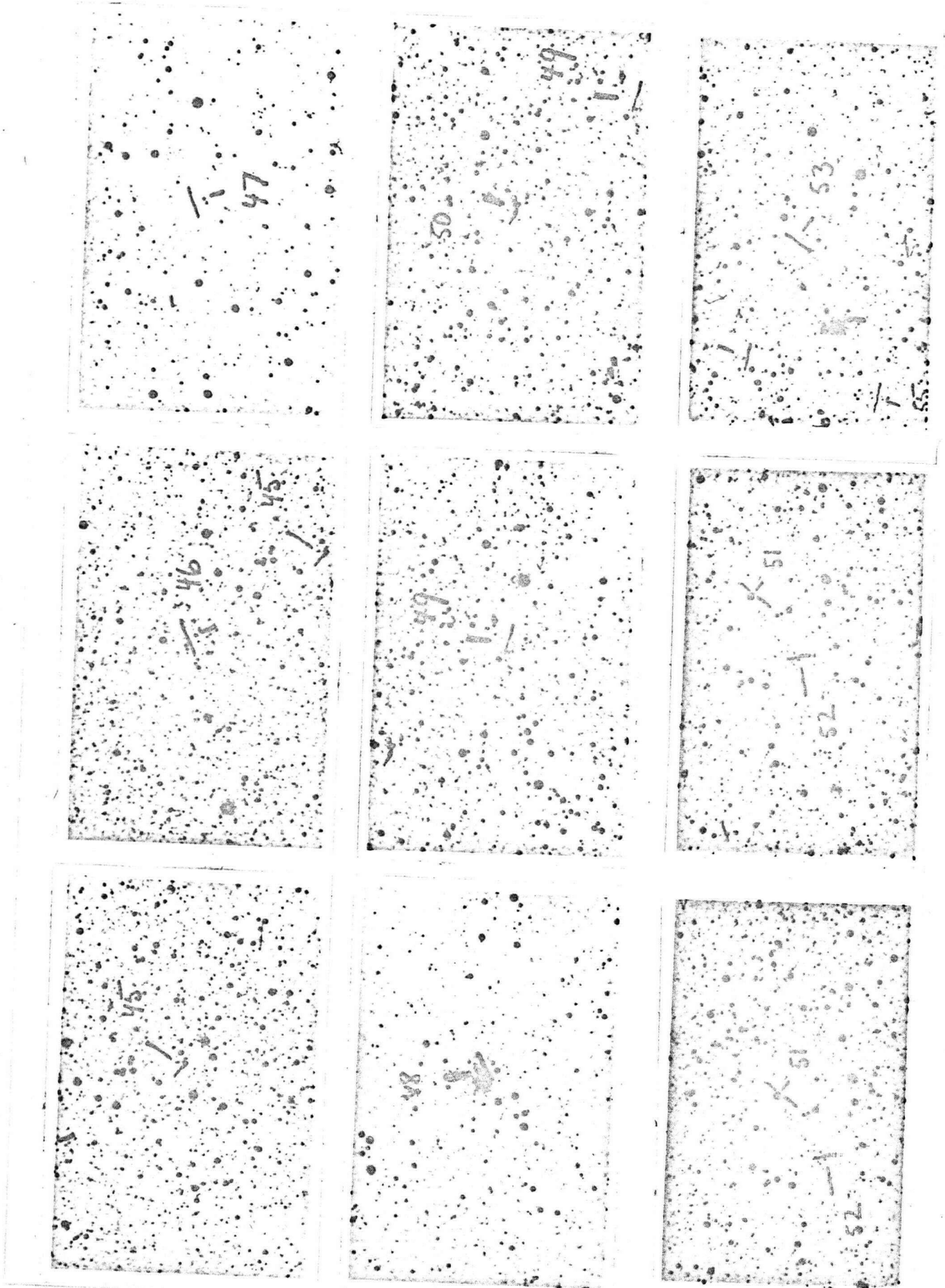


Fig. 1 cont. LMC Field #6

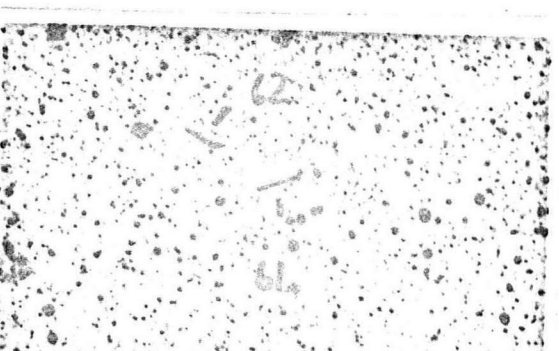
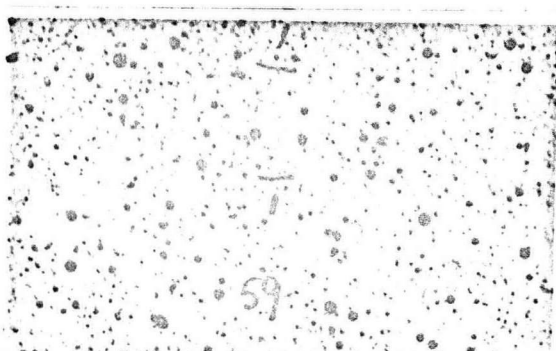
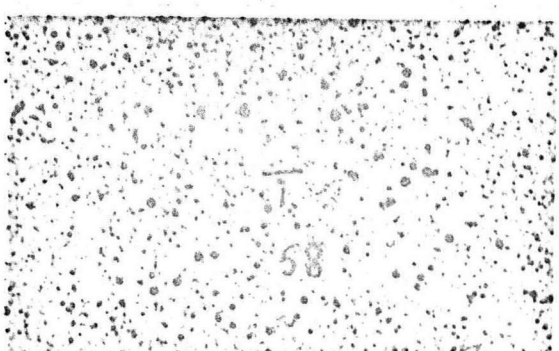
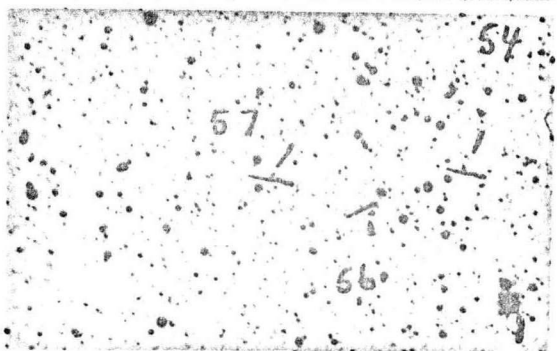
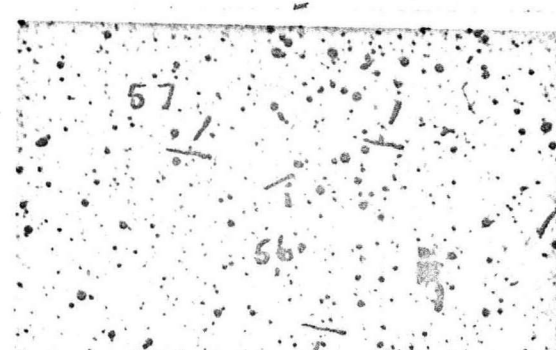
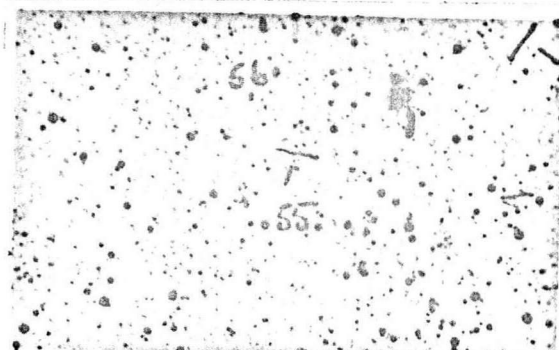
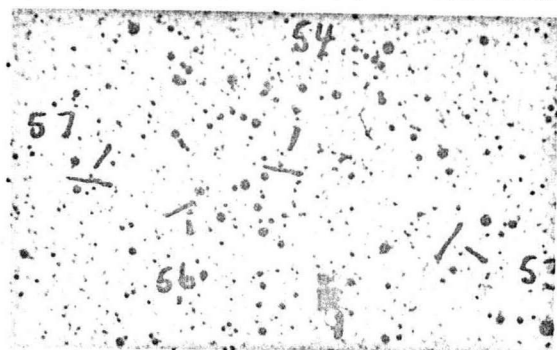


Fig. 1 cont. LMC Field #6

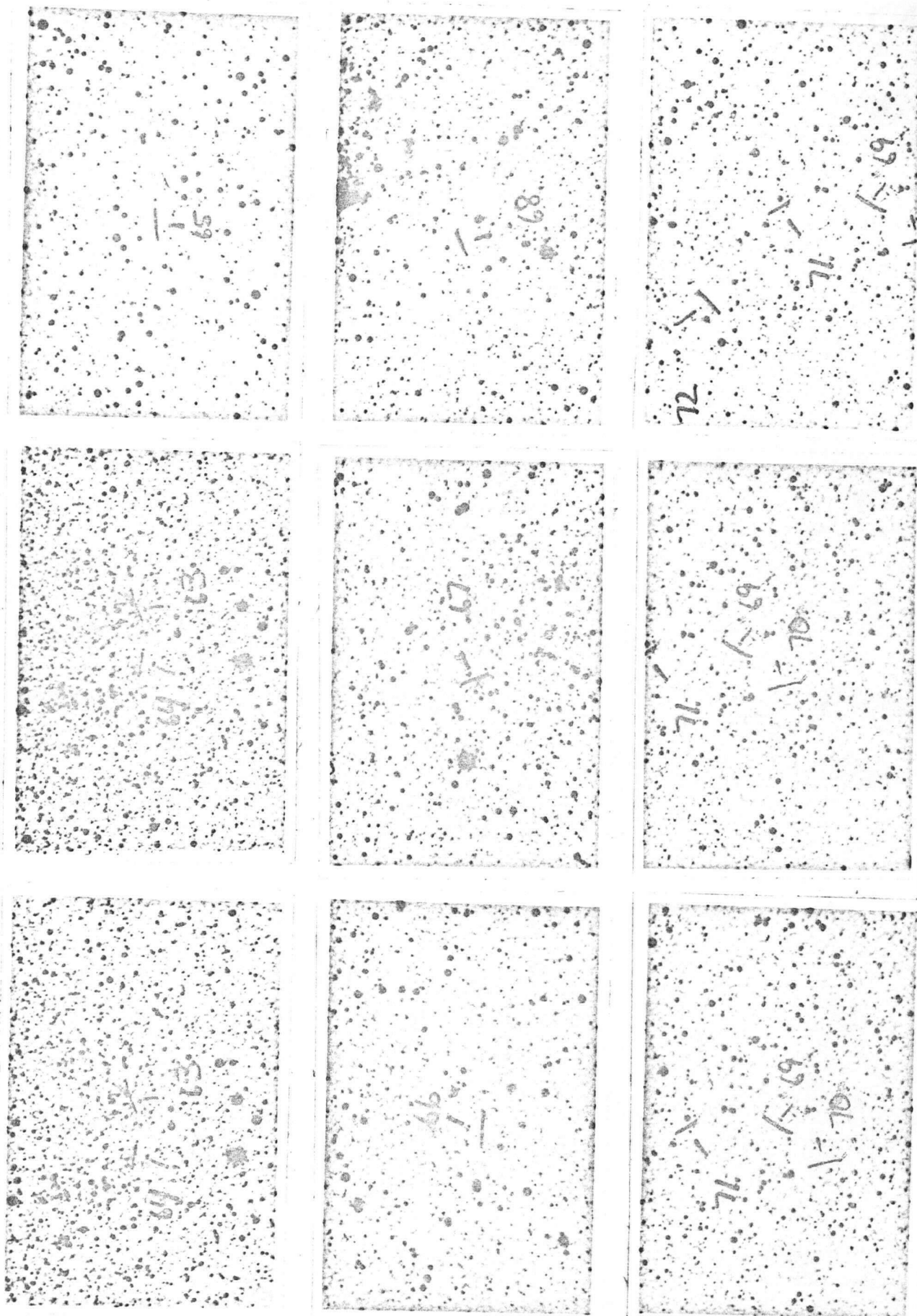


Fig. 1 cont. IMC Field #6

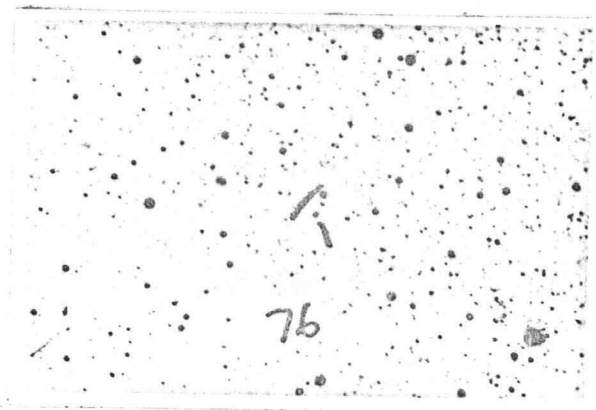
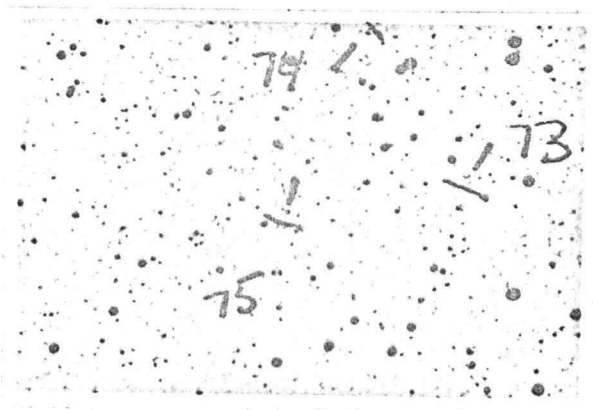
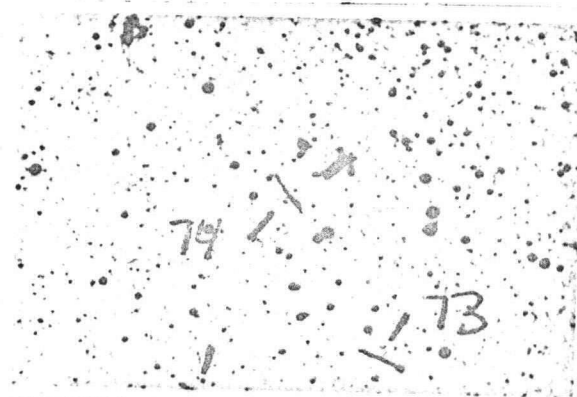
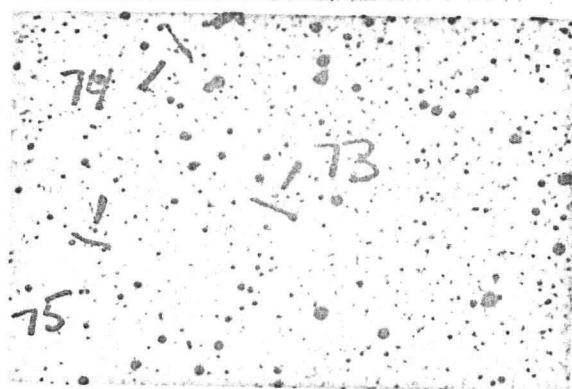
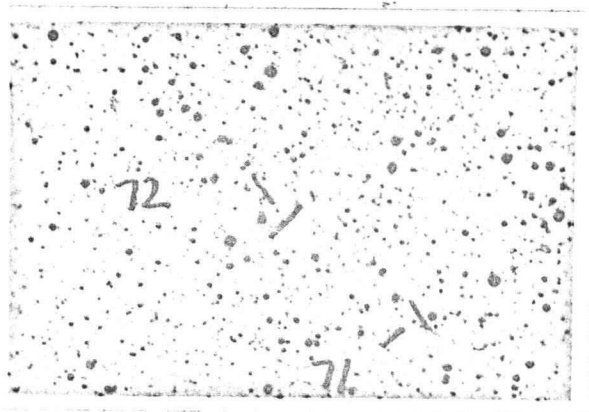


Fig. 1 cont. LMC Field #6

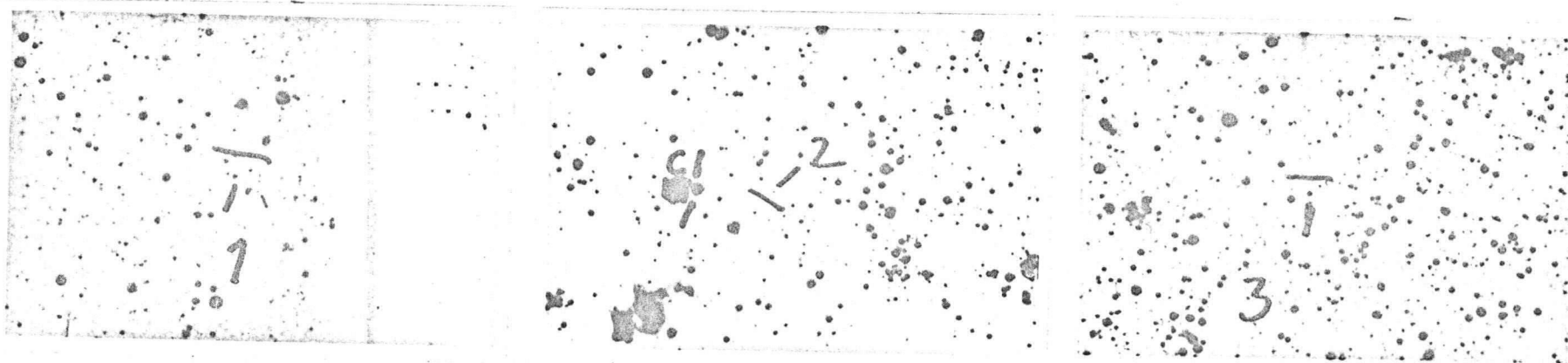


Fig. 1 cont. LMC Field #7

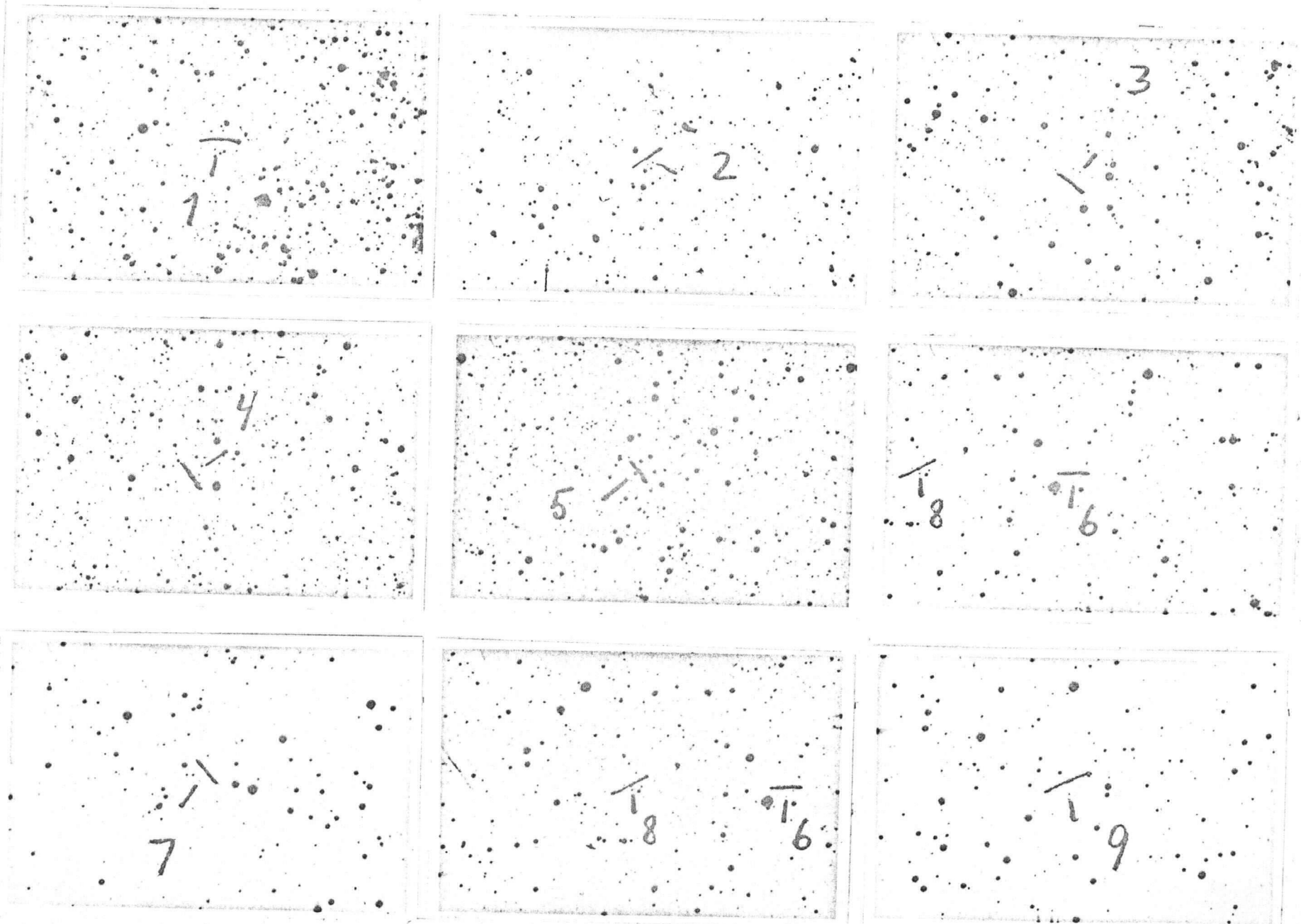


Fig. 1 cont. LMC Field #8

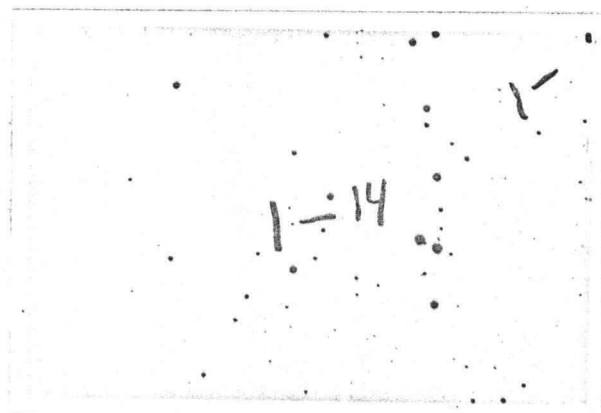
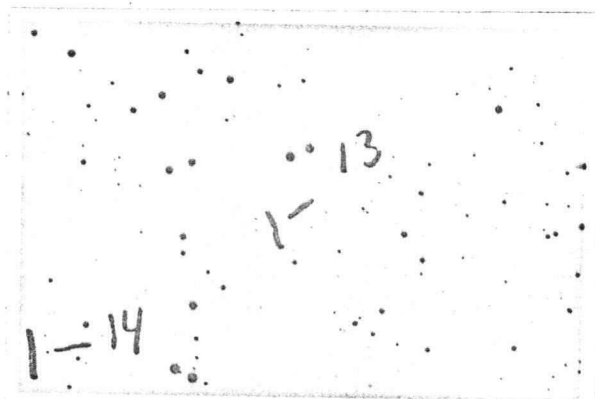
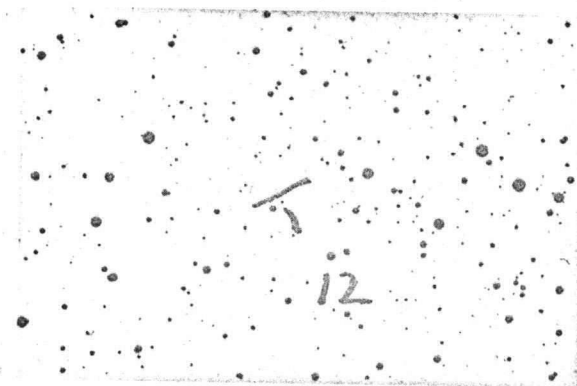
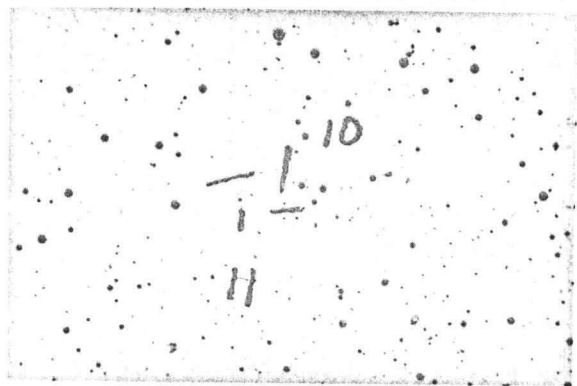


Fig. 1 cont. LMC Field #8

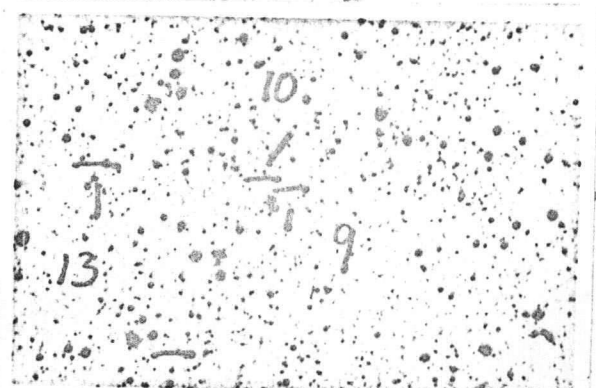
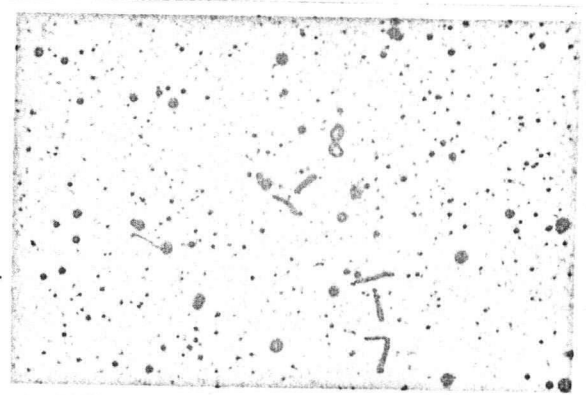
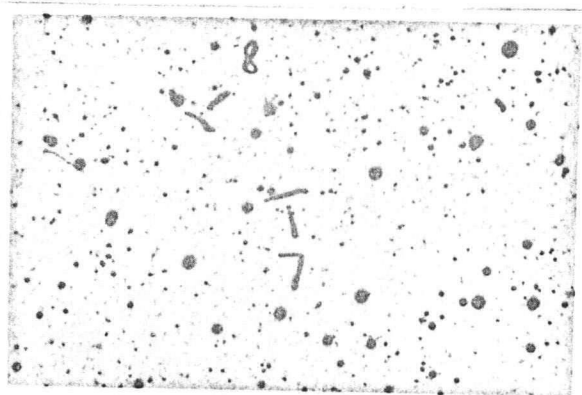
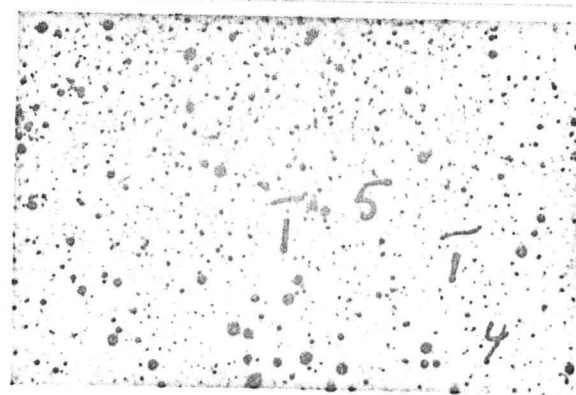
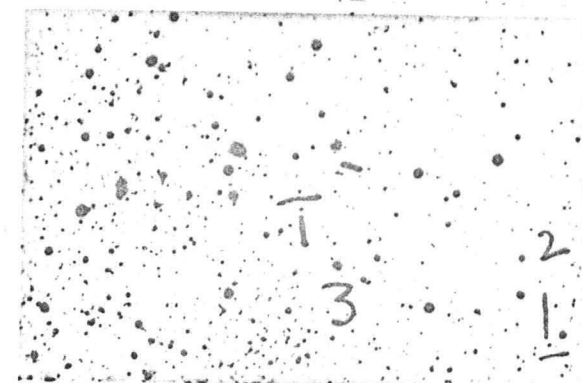
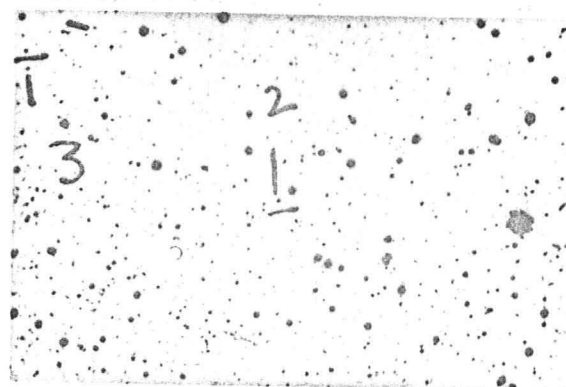
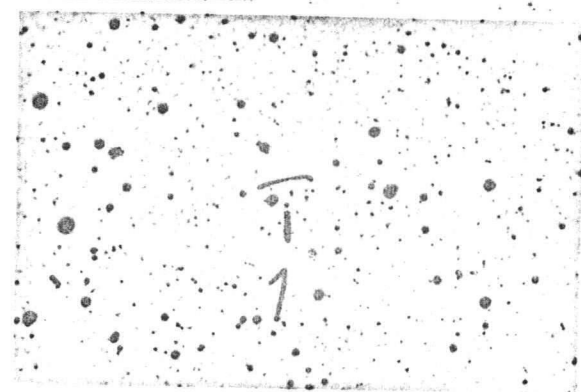


Fig. 1 cont. LMC Field #9

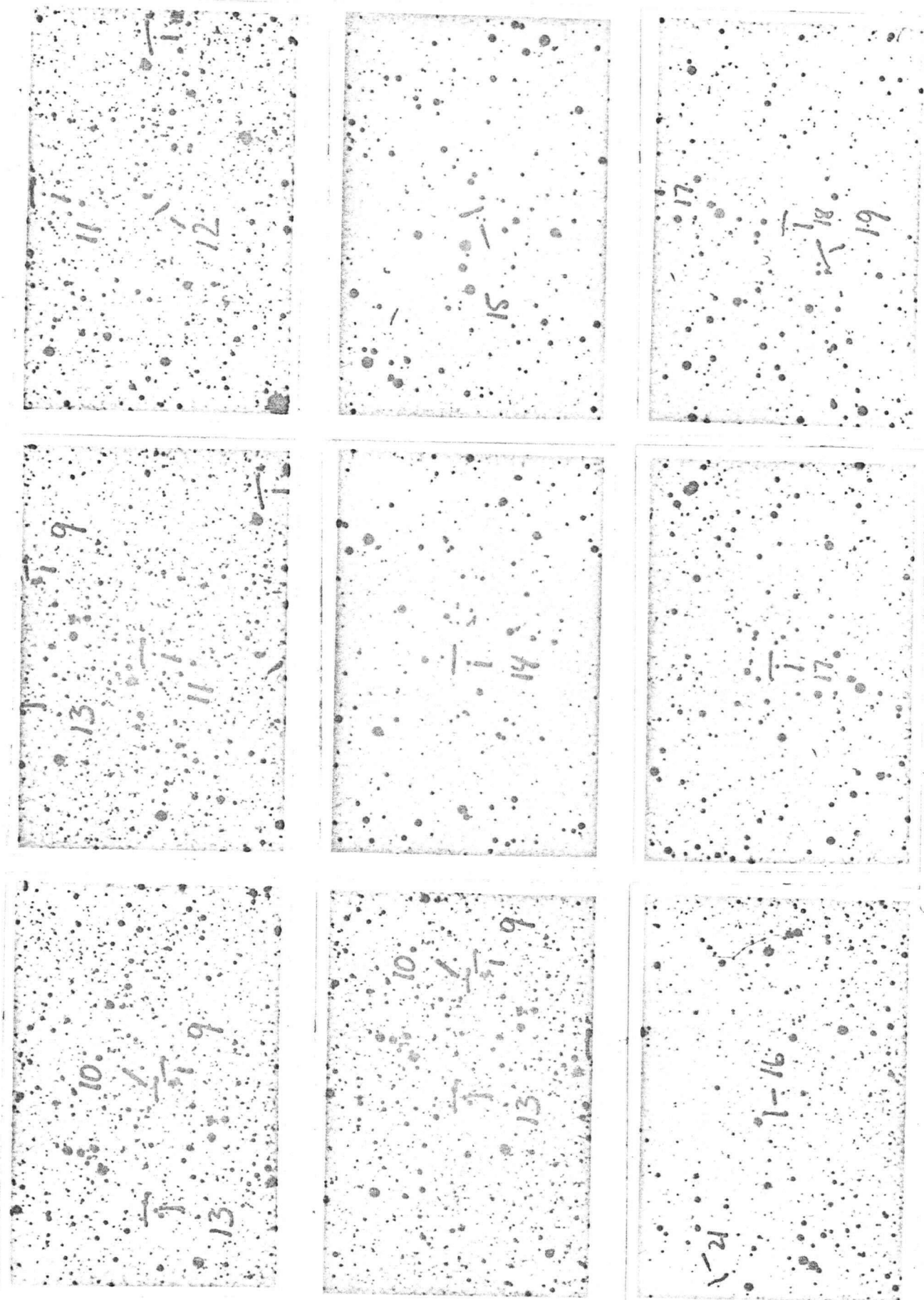


Fig. 1 cont. IMC Field #9

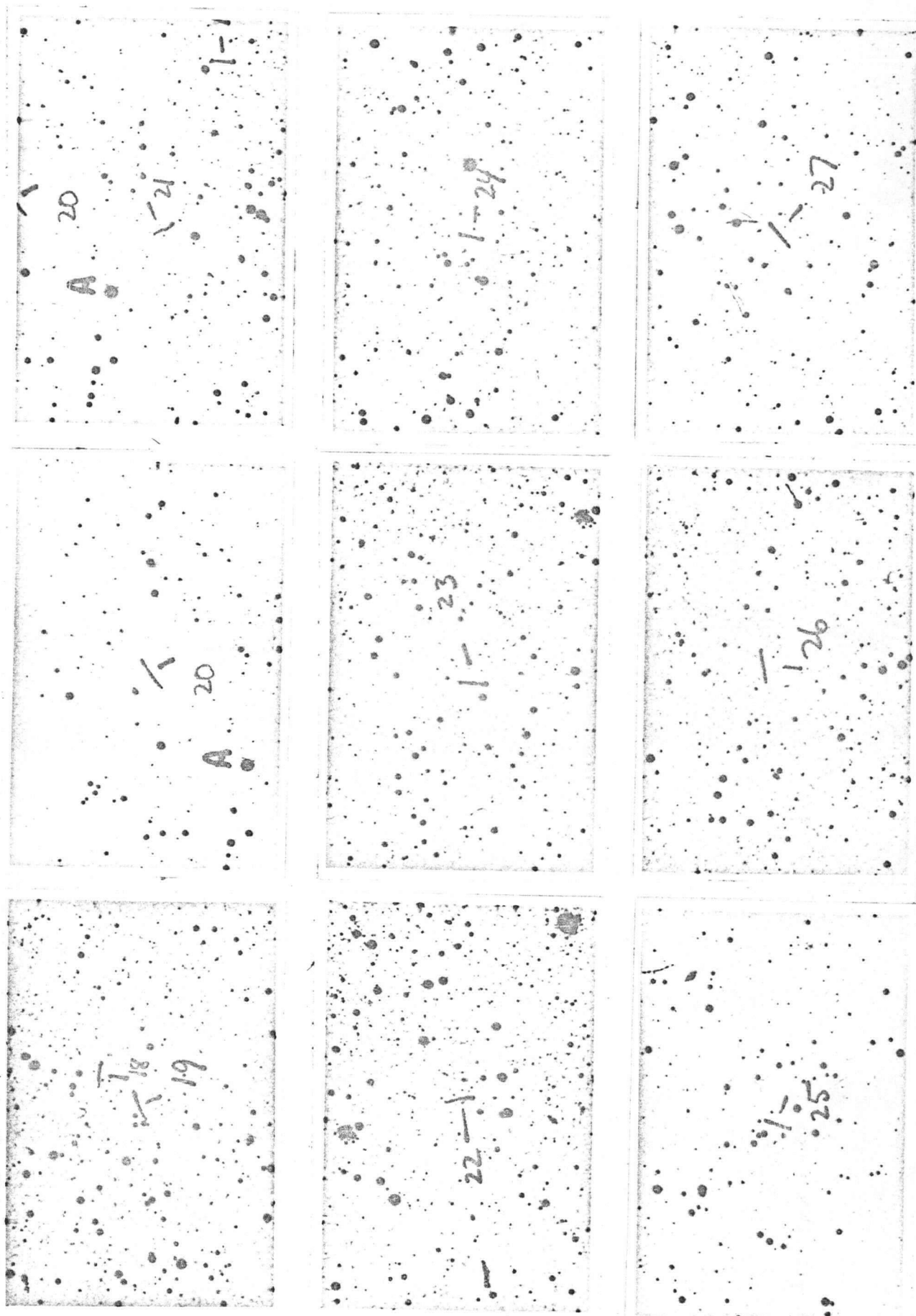


Fig. 1 cont. IMC Field #9

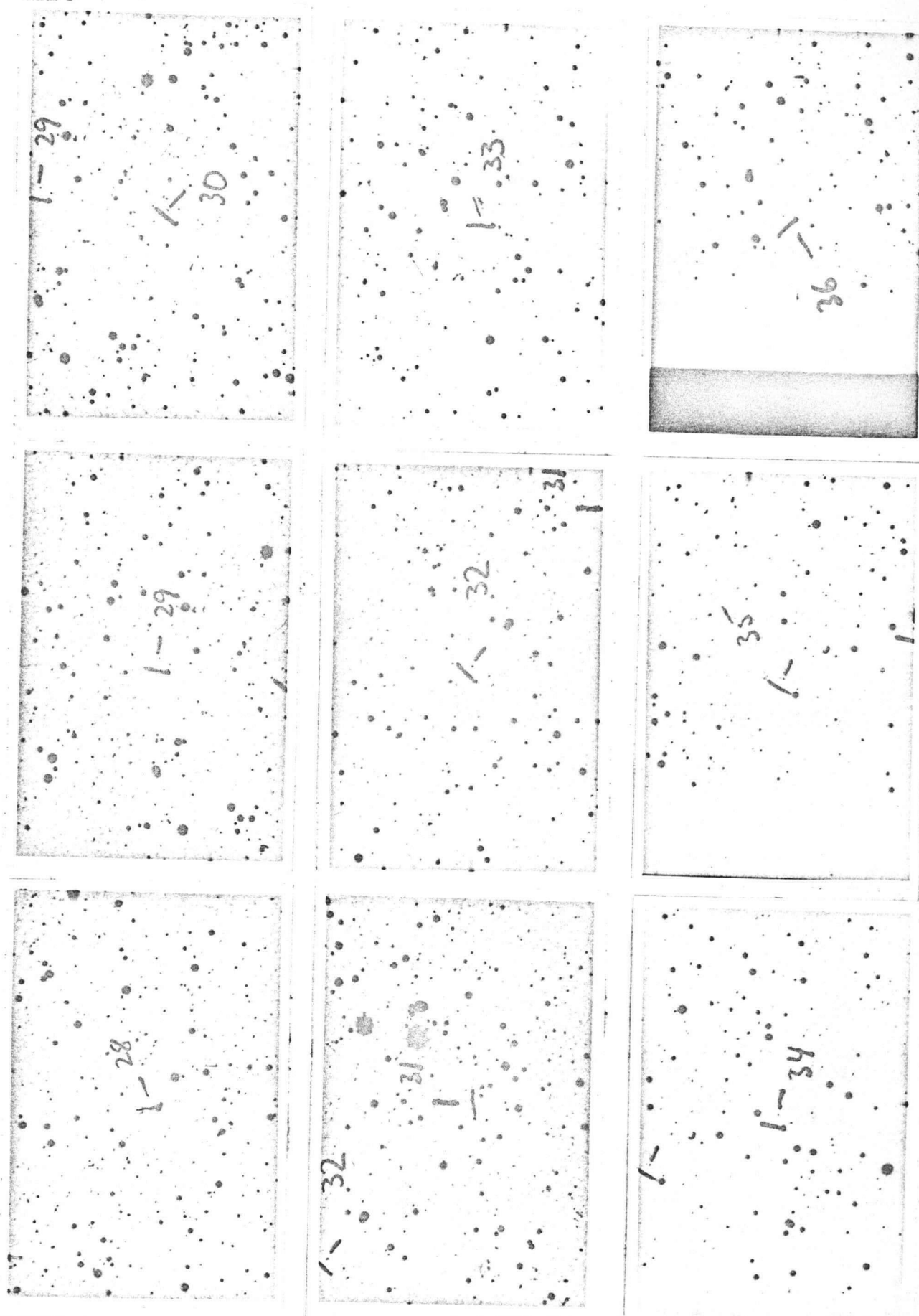


Fig. 1 cont. IMC Field #9

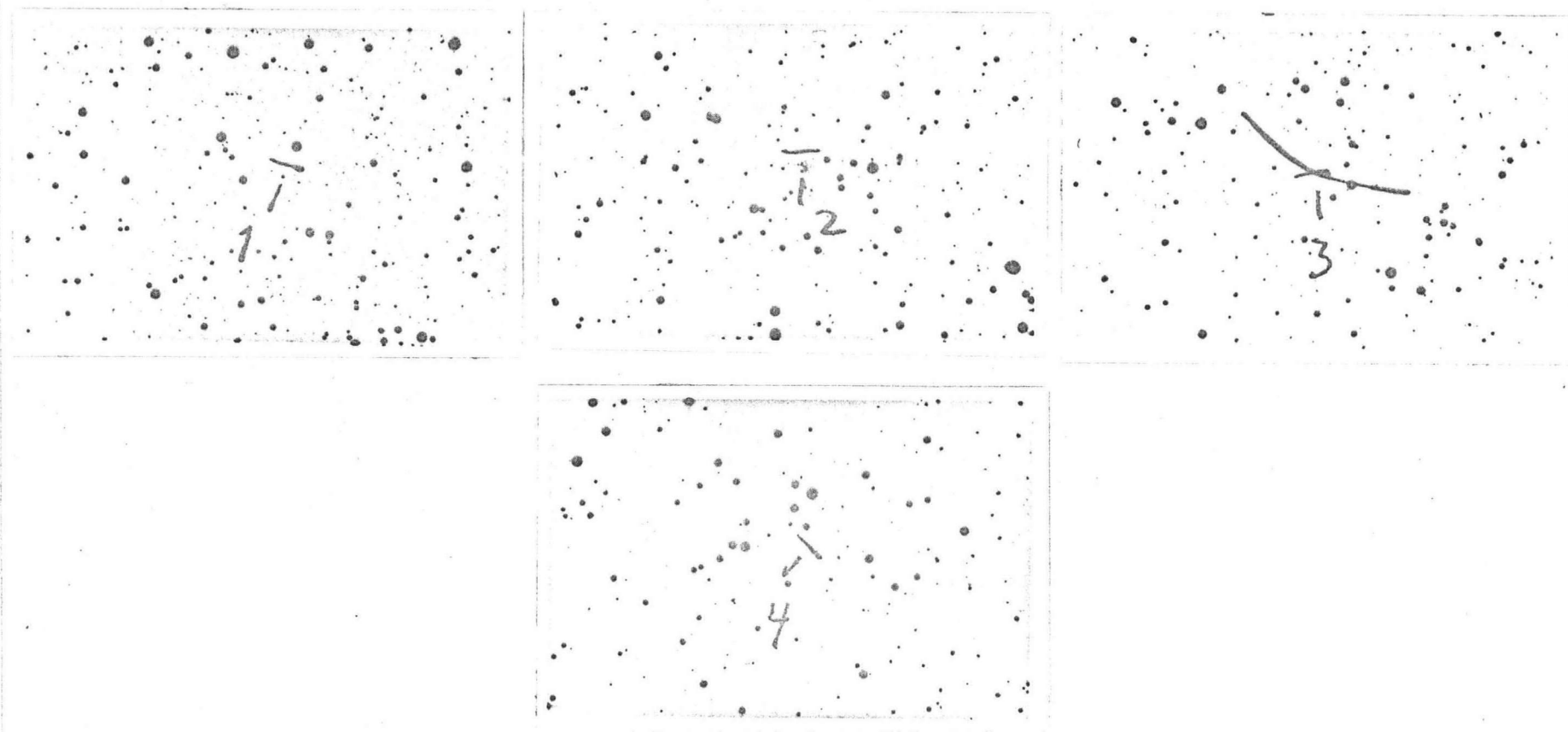


Fig. 1 cont. LMC Field #20

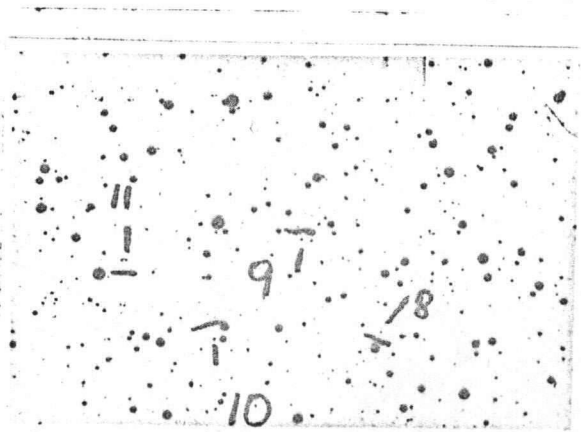
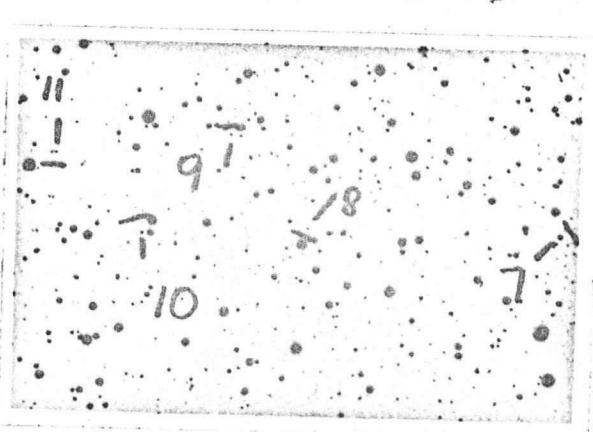
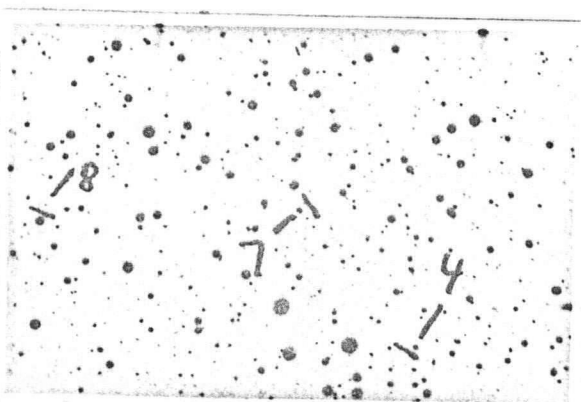
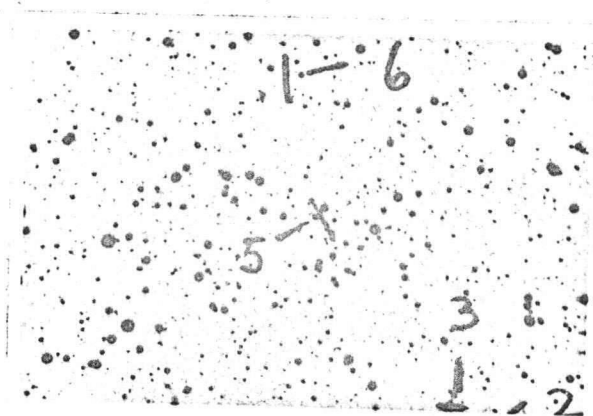
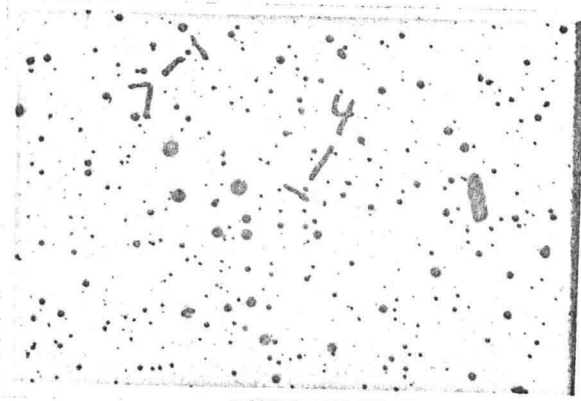
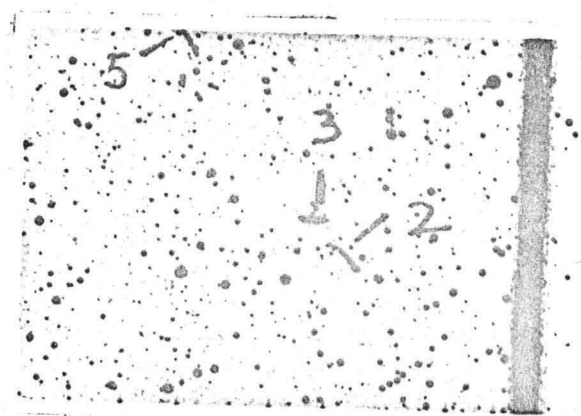
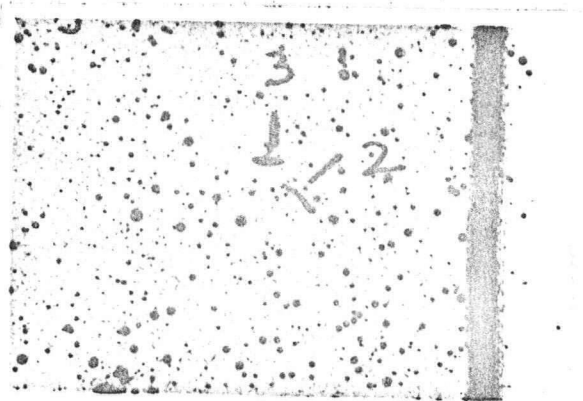
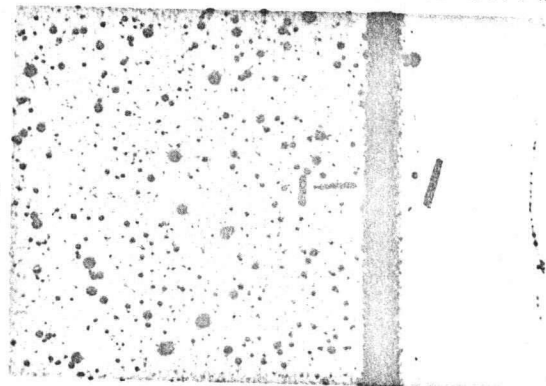


Fig. 1 cont. LMC Field #23

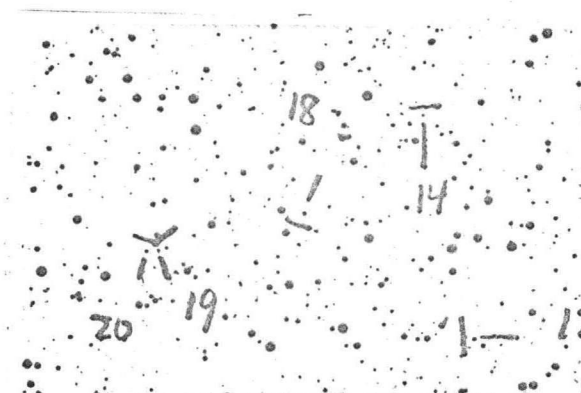
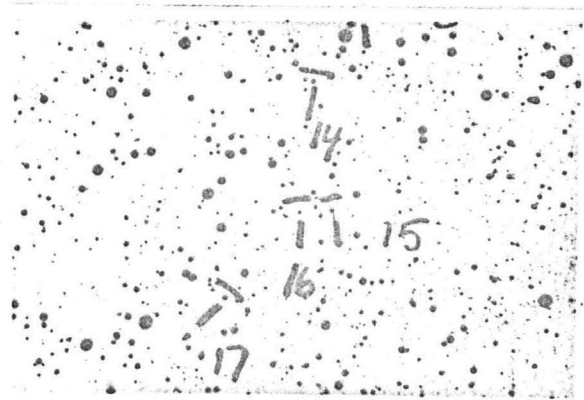
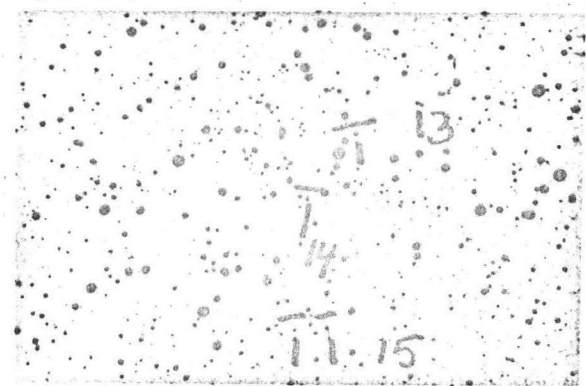
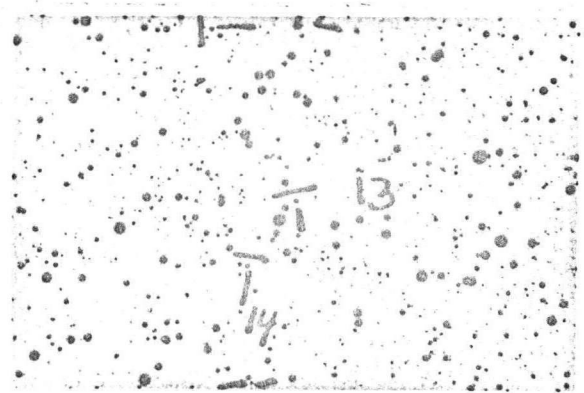
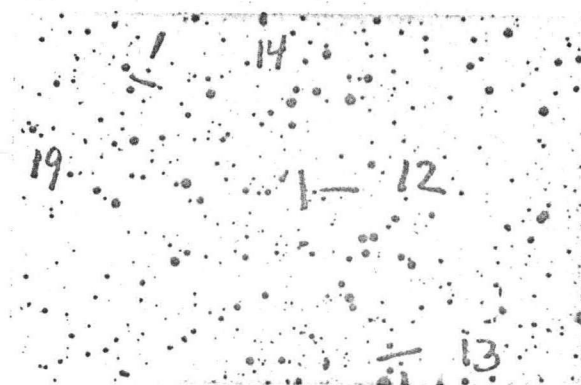
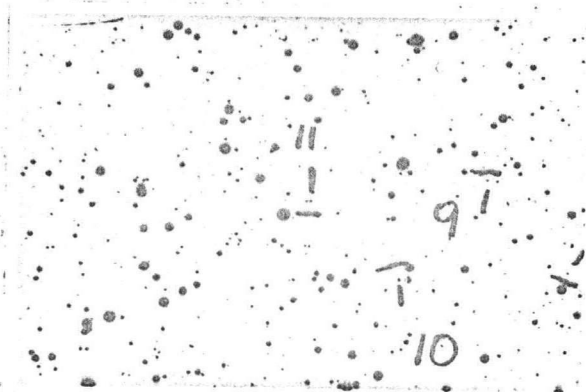
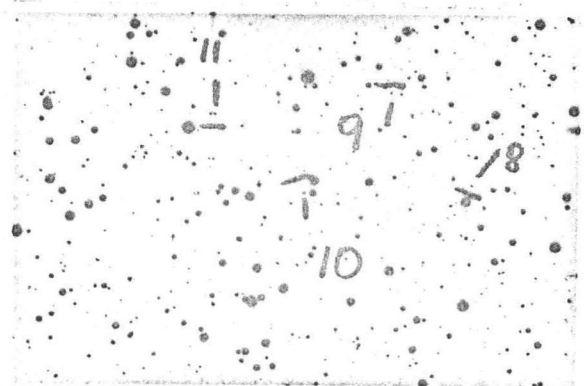


Fig. 1 cont. LMC Field #23

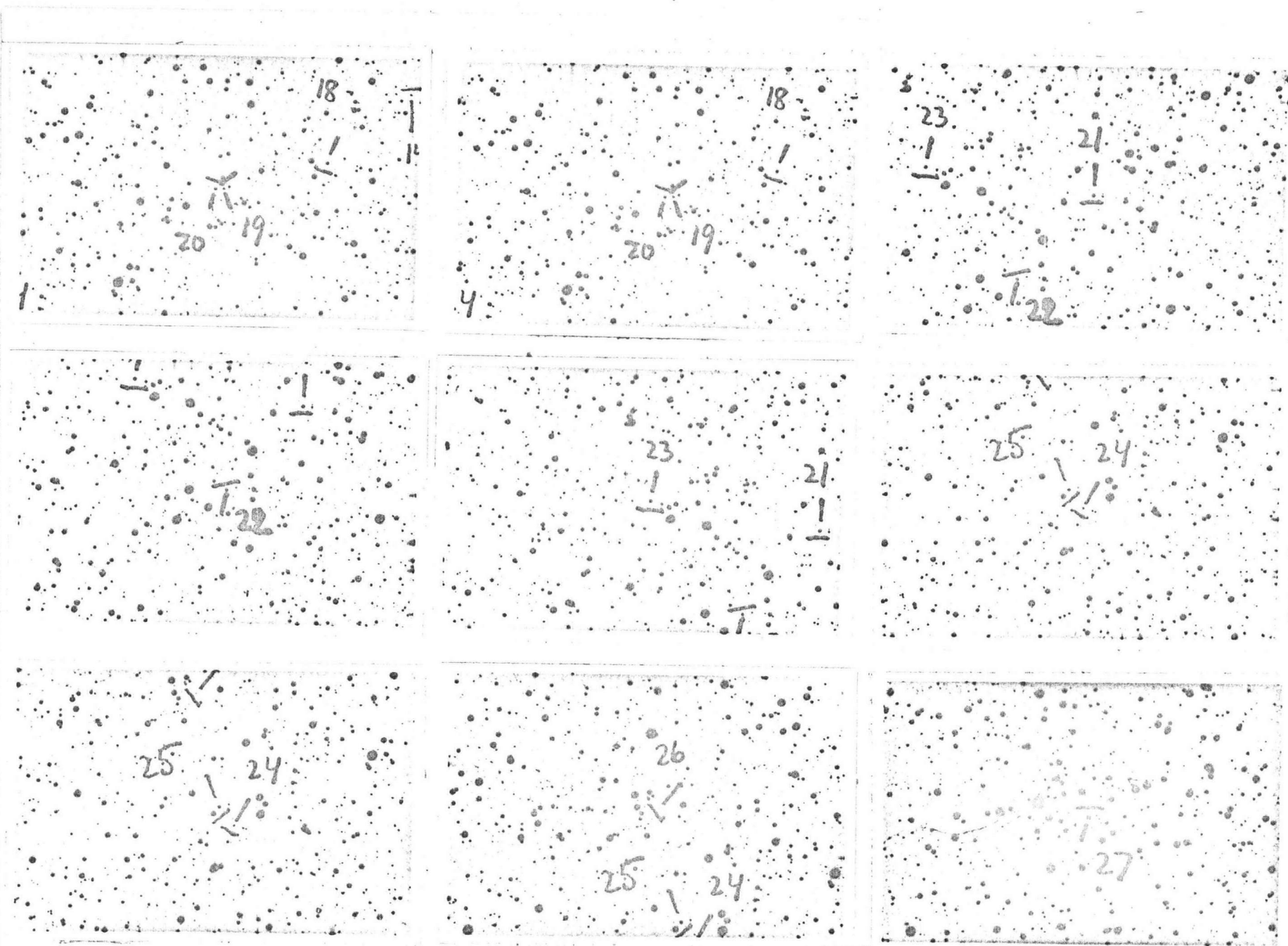


Fig. 1 cont. LMC Field #23

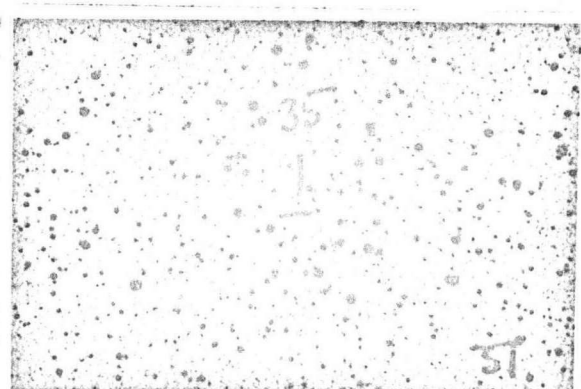
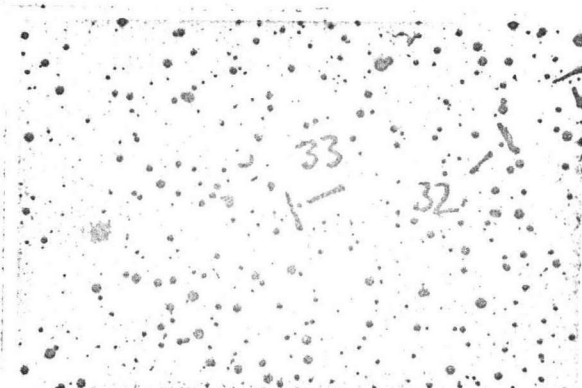
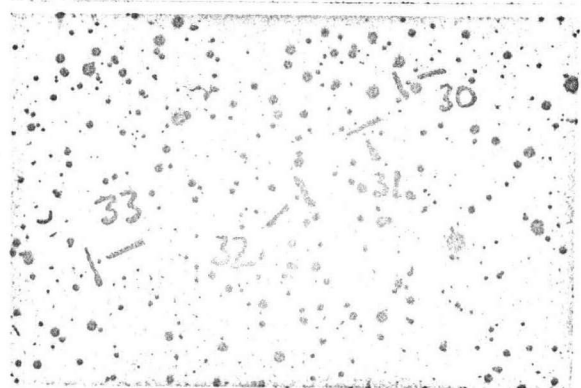
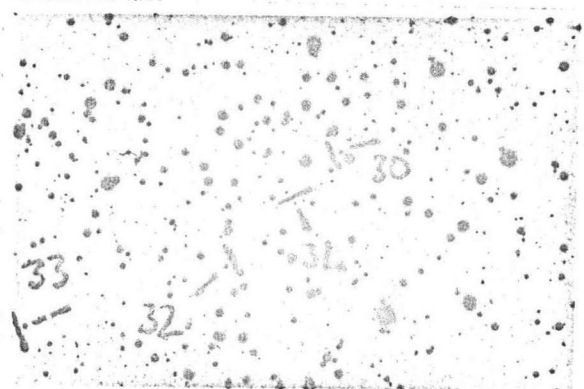
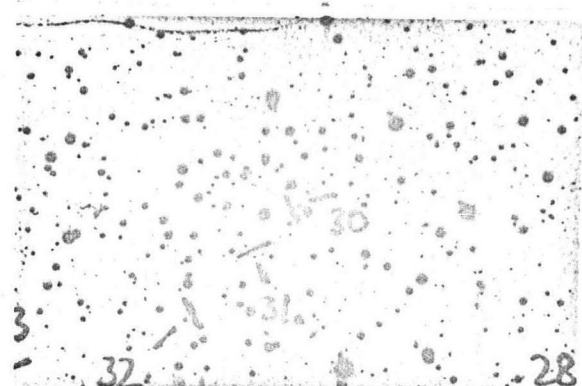
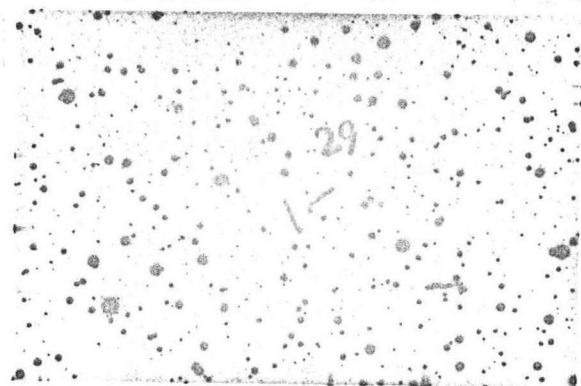
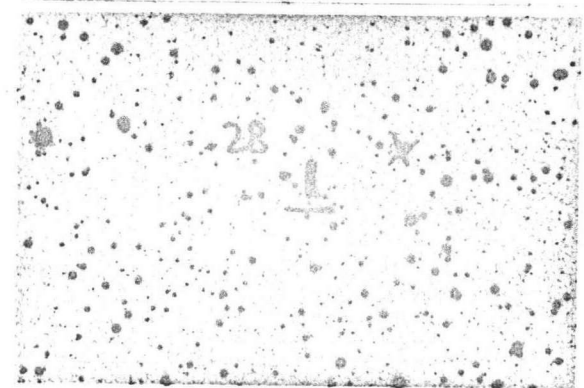


Fig. 1 cont. LMC Field #23

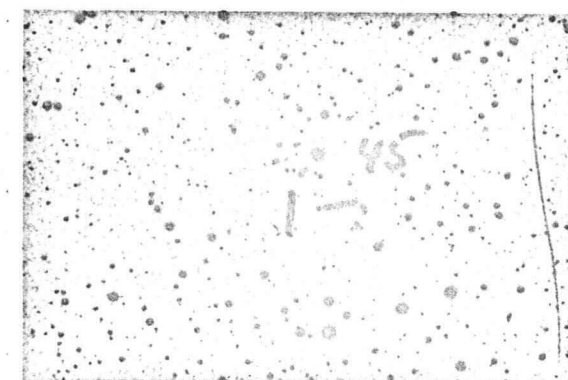
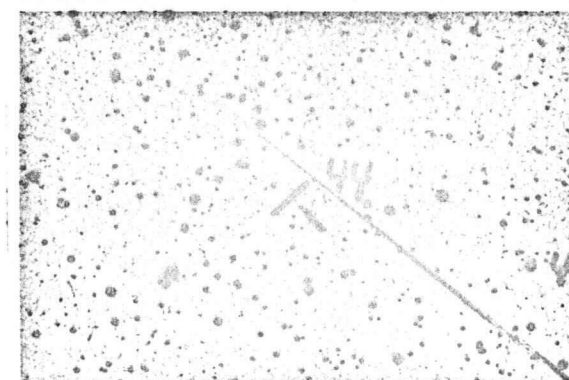
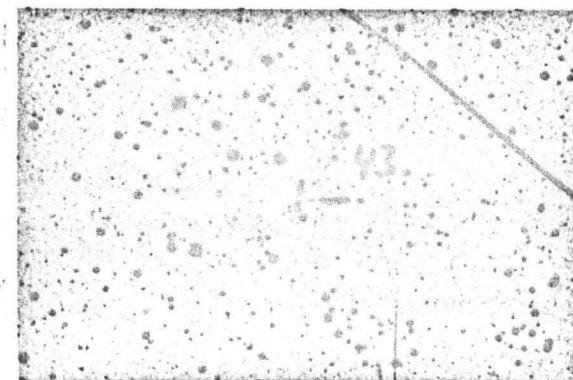
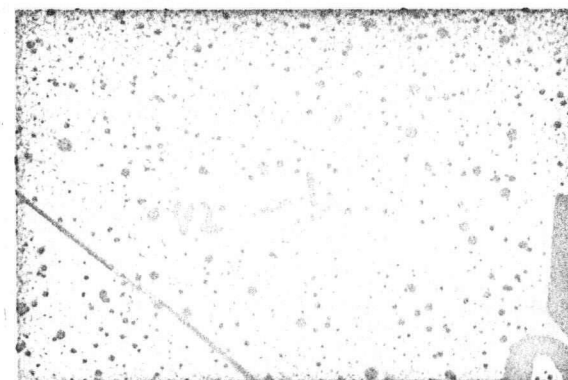
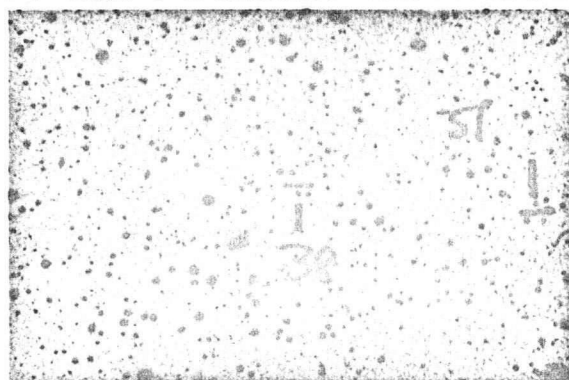
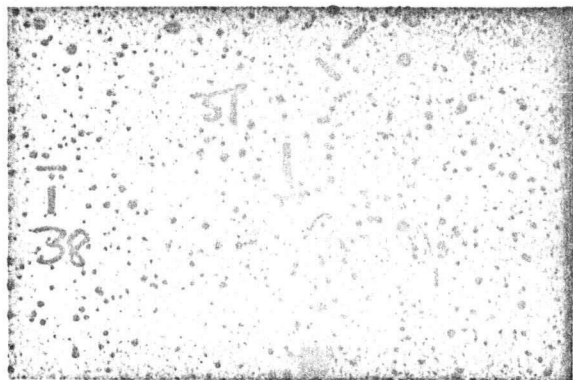


Fig. 1 cont. ILC Field #23

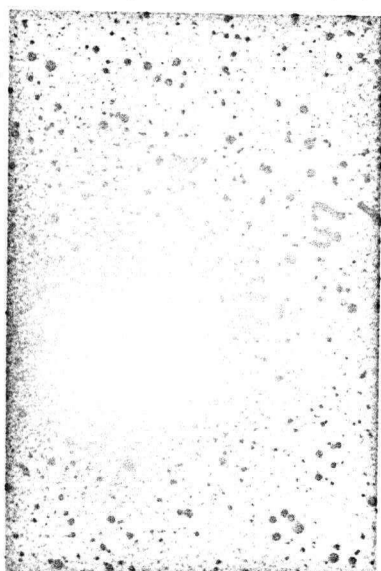
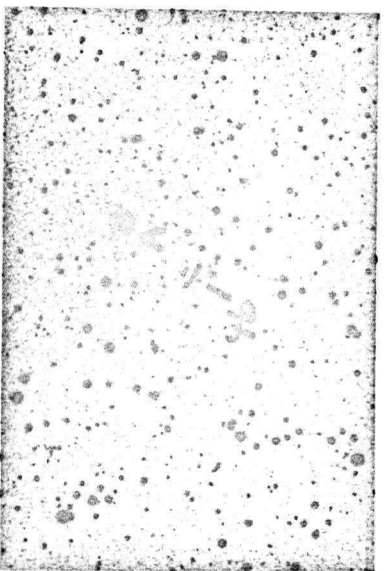
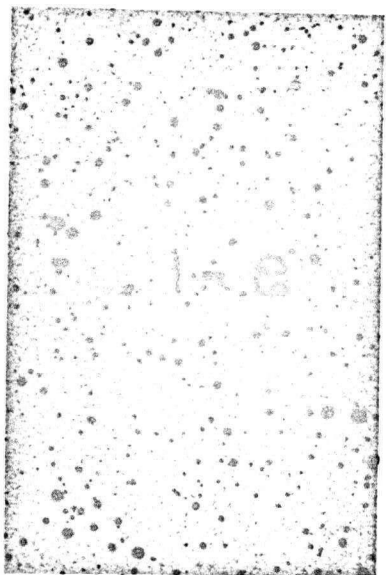
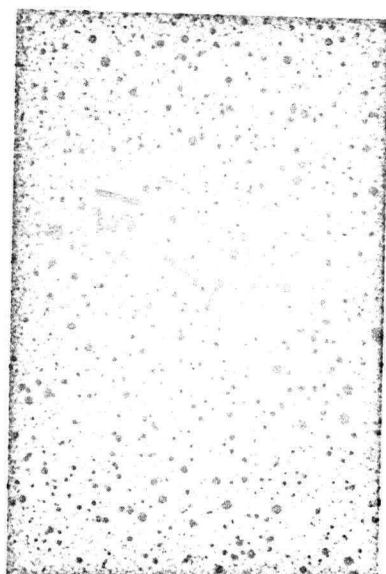


Fig. 1 cont. LMC Field #23

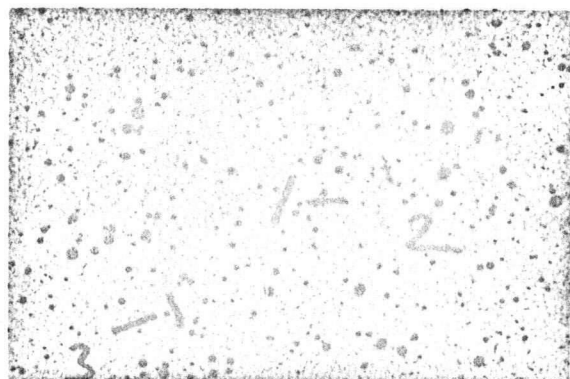
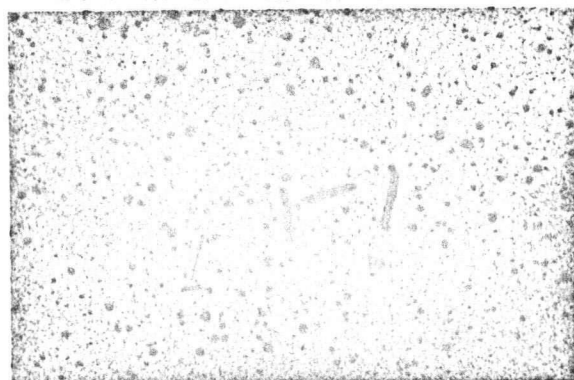


Fig. 1 cont. IMC Field #24

III Photometric Observations

The absolute magnitudes of carbon stars are very poorly known. No carbon star is near enough to have a reliable trigonometric parallax, carbon stars are rarely members of binary systems and they are seldom found in clusters. All the forementioned facts make it difficult to obtain absolute visual magnitudes for these objects. However the Large Magellanic Cloud is near enough and its distance is well enough known so that the absolute magnitudes of carbon stars in the Large Magellanic Cloud can be accurately determined. To this end photoelectric measurements of forty of the stars in the catalogue have been obtained on the VRI system.

The VRI photometry was obtained with the one metre telescope on Cerro Tololo on the nights of Dec. 17-22 1974. Table III contains the photometric data for all the stars which were observed along with comments for some of the stars. For two of the stars only the R-I colour was obtained and for one other star only V and V-R was obtained. The stars for which spectra were taken will be discussed in Section IV. The photometry was calibrated on each night using an average of seven standard stars, and extinction coefficients were calculated for each night. The average extinction coefficients for the three nights were: $K_M=0.111$, $K(V-R)=0.024$, $K(R-I)=0.088$. These average extinction coefficients agree very well with those obtained in previous observing runs (Olson, private communication). The average rms deviation for the standard

Table III Carbon star photometry

STAR	V	V-R	V-I	COMMENTS
1-1	16.34	2.53	3.49	
1-2	16.06	1.87	3.36	
1-4	16.35	2.77	4.16	
1-5	14.20	0.43	1.72	Not a carbon star
1-9	15.68	2.19	3.42	
1-10	15.42	2.15	3.50	
1-11	R-I =	1.25		
1-12	13.87	1.14	2.00	Spectrum obtained
1-13	16.09	1.92	3.16	
1-14	15.71	2.28	3.49	
1-16	14.72	0.28	0.39	Not a carbon star; spectrum obtained
1-18	15.86	1.88	2.71	
1-20	15.57	2.12	3.33	Spectrum obtained
1-21	16.18	2.23	3.68	
1-22	16.17	2.24	3.34	
1-23	16.08	2.42	3.72	
4-1	15.84	1.80	3.05	
4-2	15.74	2.17	3.46	
4-3	16.69	2.74	4.12	
4-5	15.99	2.17	3.53	
4-6	16.80	2.62	4.16	Perhaps in a nebula?
4-9	15.77	2.03	3.49	Spectrum obtained
4-10	16.02	2.31	3.74	
6-1	16.09	2.82	4.24	
6-2	15.70	2.03	3.38	
6-3	R-I =	1.56		
6-4	15.29	2.07	3.29	Spectrum obtained
6-5	15.53	1.78	3.04	
6-6	14.27	1.33	2.32	Spectrum obtained
6-9	15.47	2.17	3.34	

Table III cont'd

STAR	V	V-R	V-I	COMMENTS
6-10	15.69	2.03	3.36	
6-13	15.73	1.86	3.03	
6-14	15.61	1.90	3.14	
6-15	16.30	0.39		Not a carbon star; probably wrong star indicated on chart
6-16	14.94	1.67	2.90	
6-17	15.35	1.91	3.16	Perhaps in a nebula?
6-18	15.91	2.33	3.72	
6-19	15.65	2.37	3.67	
6-20	15.84	3.05	4.37	
6-21	15.48	2.27	3.57	
6-22	15.39	2.06	3.17	Spectrum obtained
6-23	16.45	0.54	2.21	Not a carbon star
6-24	15.49	2.09	3.37	Close companion 6" north
6-25	15.47	1.85	3.10	Spectrum obtained
6-26	15.84	2.34	3.57	
6-27	15.20	0.69	1.88	Not a carbon star
6-28	16.01	1.97	3.27	

stars was 0.04 magnitudes in V and about 0.03 magnitudes for both of the colours.

With this sample of forty carbon stars for which the absolute visual magnitude is known to a fair degree of accuracy, a relationship between absolute magnitude and various parameters can be investigated. However one must remember that we are working with a restricted sample of stars, in the sense that these forty stars are on the average brighter than the average carbon star in the Large Magellanic Cloud. This arises from the fact that only a one metre telescope was used to make the observations. This restricted the observations to the brighter members of the catalogue. The brightest carbon star observed in the visual region has an apparent visual magnitude of 13.87 while the faintest has a magnitude of 16.80. If one assumes a distance modulus to the Large Magellanic Cloud of 18.5 (Westerlund 1972) the absolute visual magnitudes are -4.6 and -1.7 respectively.

Fig. 2 is a plot of apparent visual magnitude versus the photometric colour, $R-I$. It can be seen that in general the fainter stars are also the redder stars, although the scatter around the mean line is quite large. One star, marked by the hourglass symbol seems to be discordant with the rest of the sample. It is possible that this star is not a carbon star but some other type of red giant. The two stars marked by diamonds are separated from the bulk of the stars by about 0.3 magnitudes in $(R-I)$. These two stars are carbon stars as spectra were

Figure 2. V versus R-I

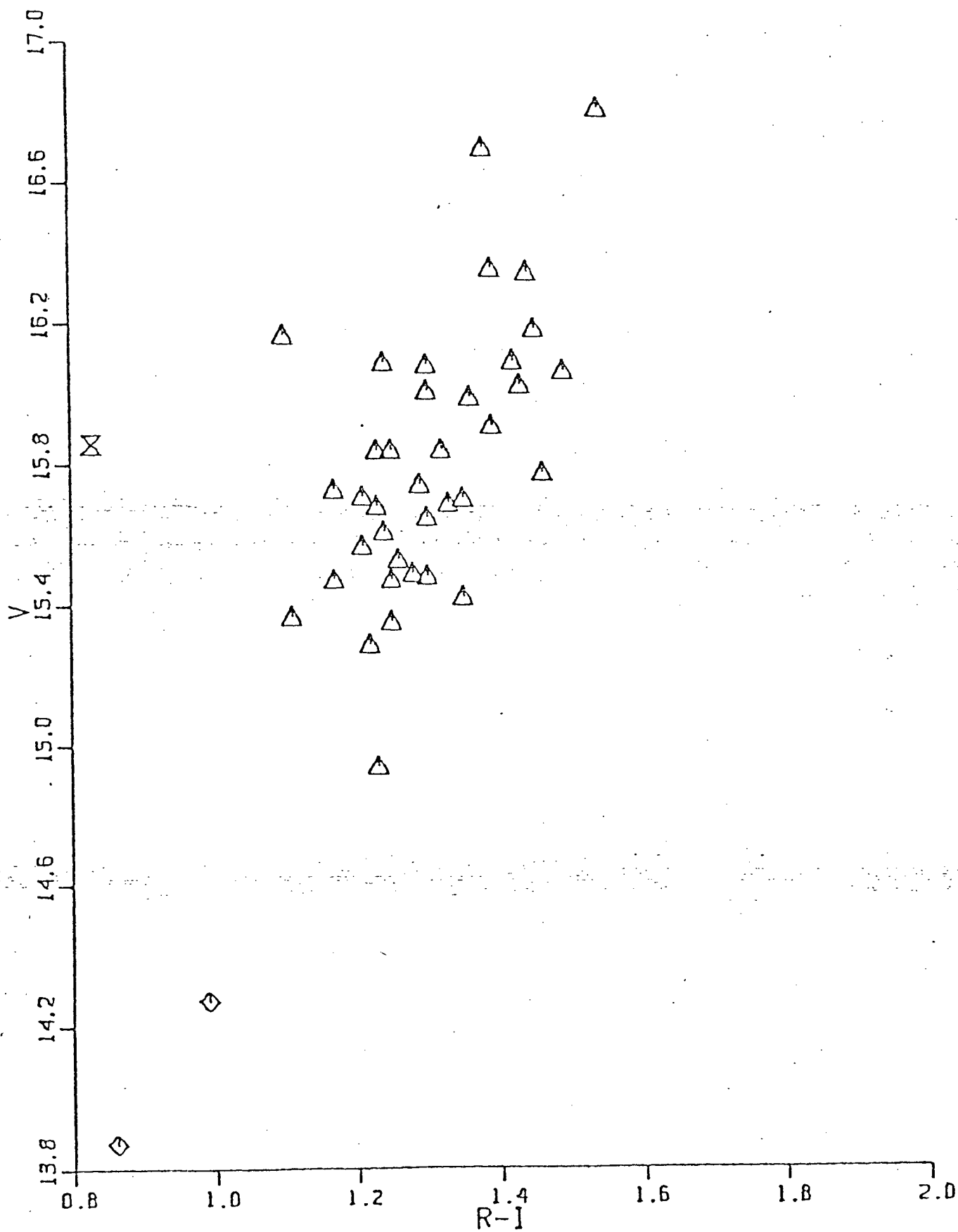


Figure 3. V versus V-I

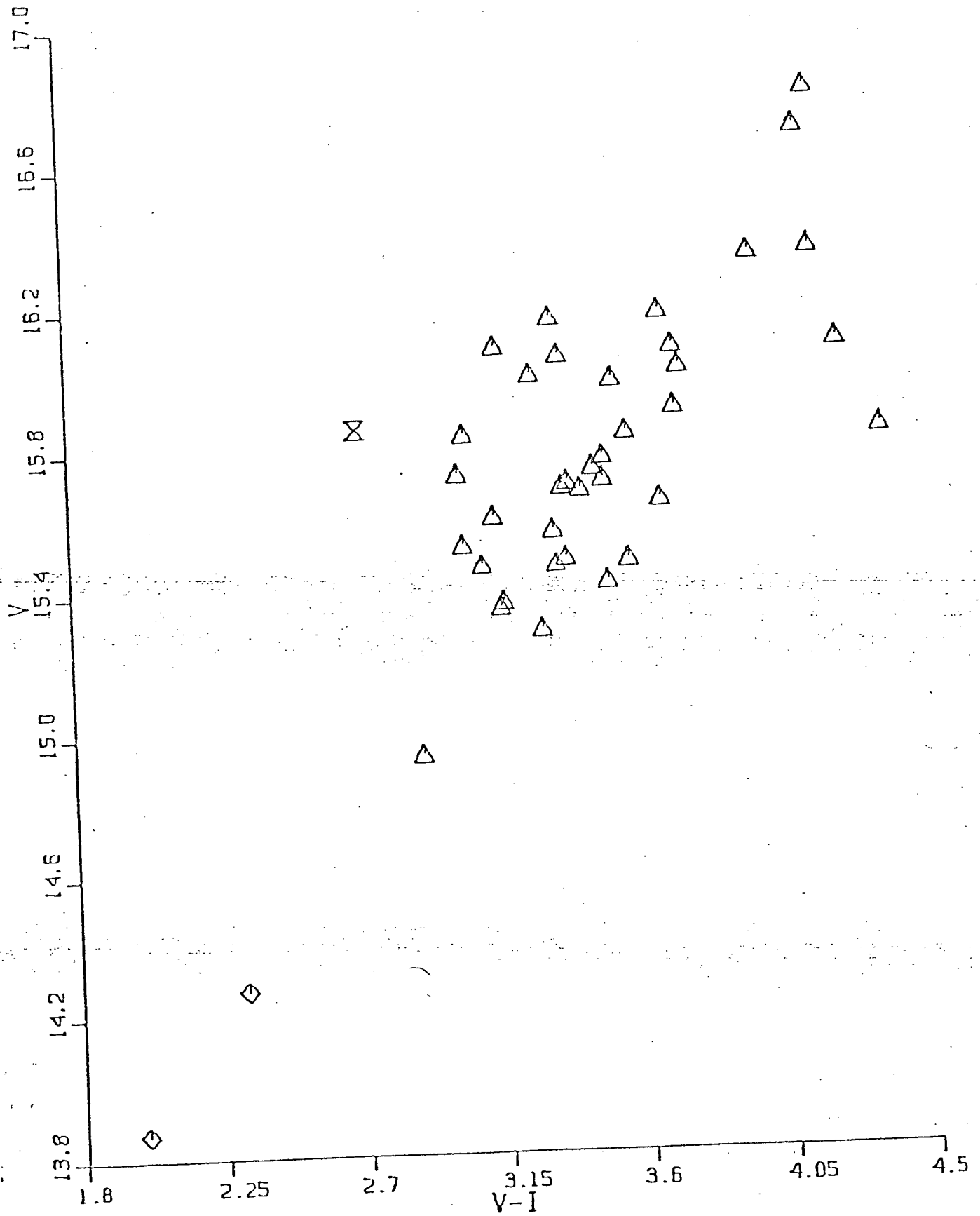
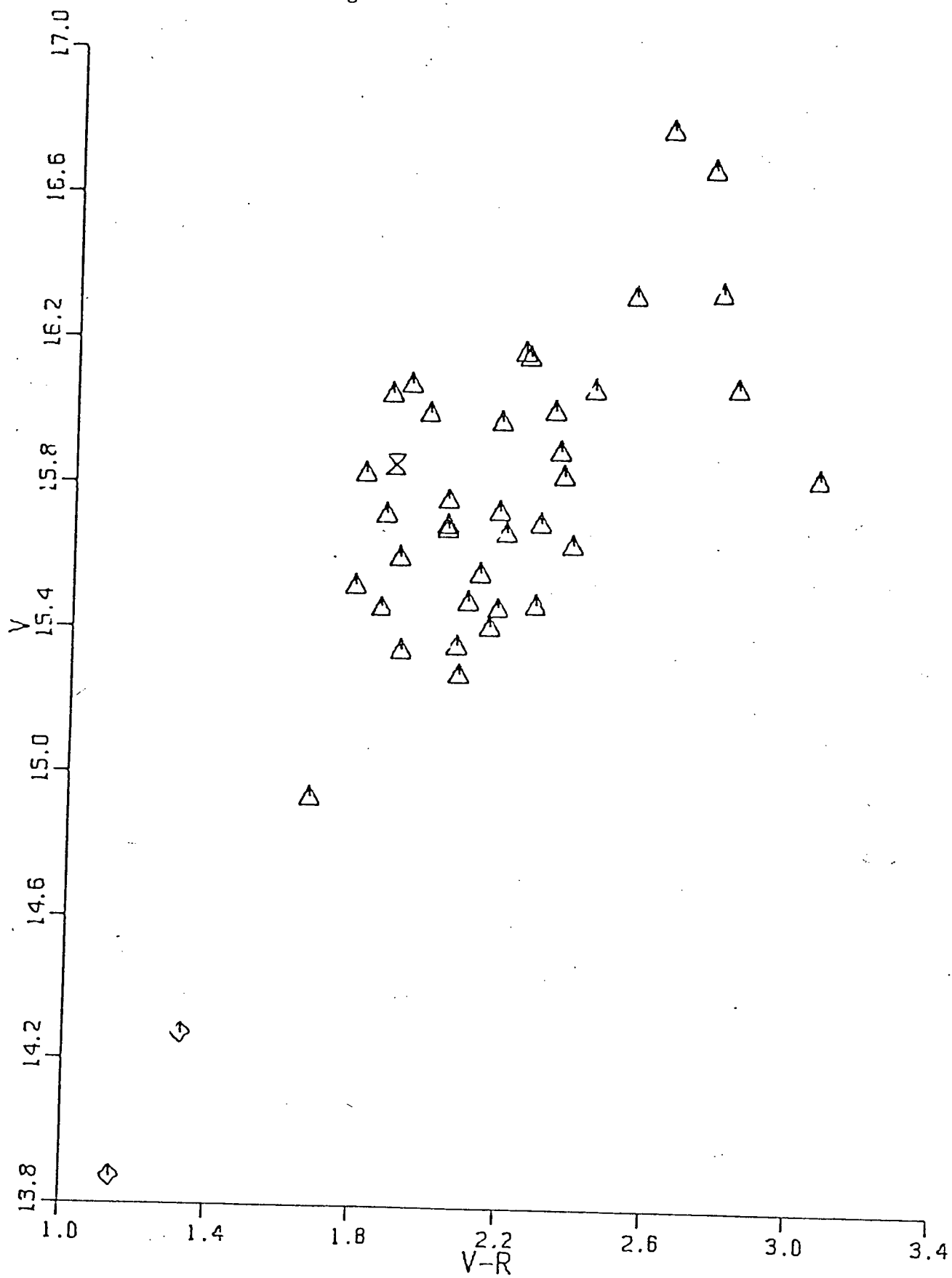
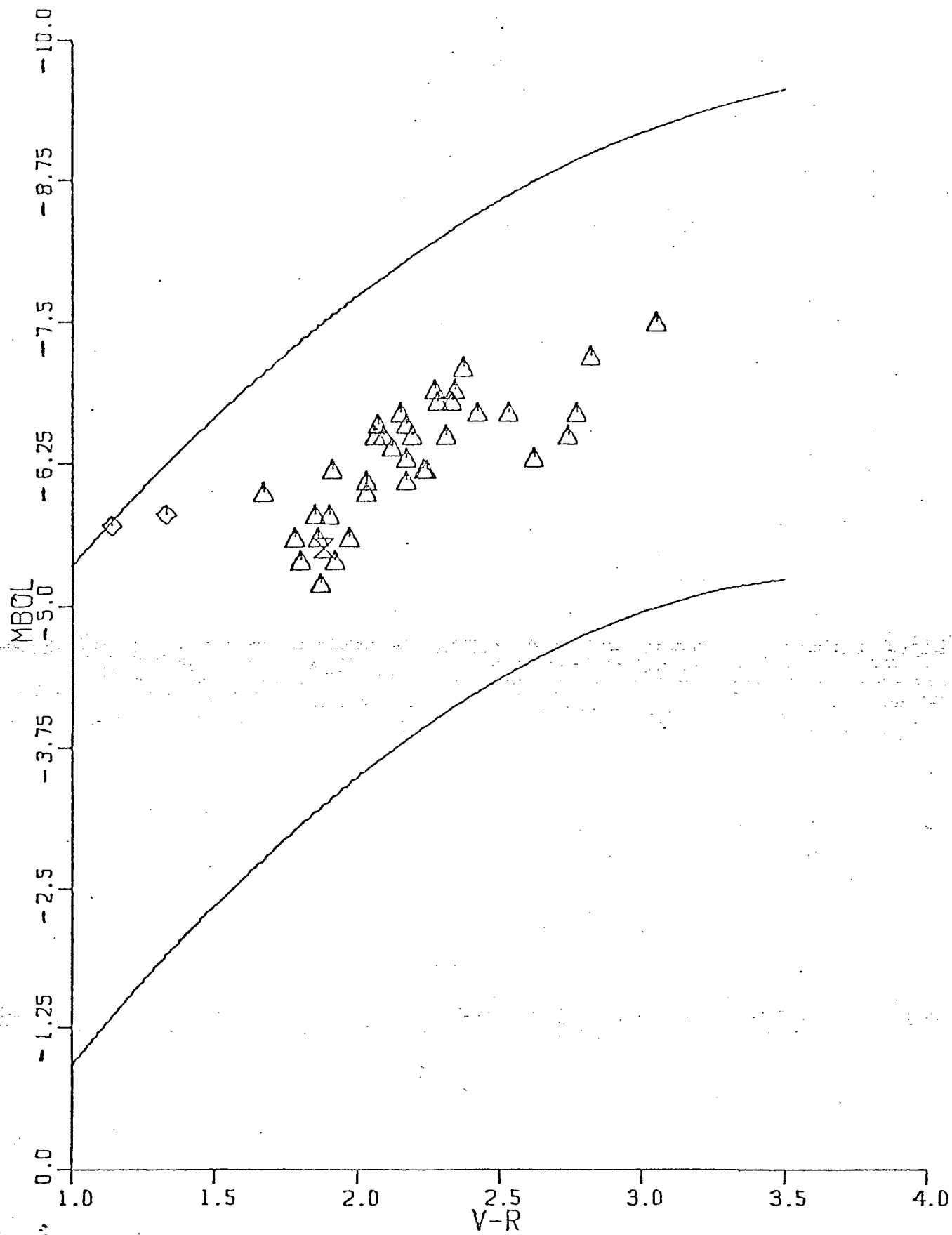


Figure 4. V versus V-R



obtained of both of these. However such warm bright carbon stars are not known in our Galaxy. It is possible that they are high latitude CH-stars although the red spectra available do not allow a distinction to be made between late type carbon stars and CH-stars. In this case blue spectra would be needed to verify this possibility. If these stars were CH-stars then the spectra would be expected to show enhancement of the G-band as well as enhancement of SrII $\lambda 4077$ and BaII $\lambda 4554$. Figures 3 and 4 are the same type of plots as in Fig. 2 only now the independent variable has been changed to (V-I) and (V-R) respectively. The same symbols have been used for the stars mentioned in Fig. 2. In these latter two diagrams the relationship between magnitude and colour is not as tight as in the V versus (R-I) diagram. From these three diagrams it does not appear that any tight correlation can be found between visual magnitude and photometric colour index for the red and near infra-red colours.

Figure 5 shows a plot of absolute bolometric magnitude versus (V-R) for the carbon stars in this sample. The bolometric corrections used were those found by Olson and Richer (1975) in their investigation of the correlation between bolometric correction and photometric colour. The solid lines represent the mean location of the Ib supergiant branch and the class III giant branch. The carbon stars in this sample seem to form quite a definite branch between the Ib supergiants and the normal giants. However this appearance may be somewhat artificial as the sample of carbon stars is somewhat brighter

Figure 5. M_{bol} versus $V-R$ 

than average, as least in the visible region. It would be safe to say that the cool carbon stars seem to cover the range from bright giants to ordinary giants in absolute bolometric magnitude.

IV Spectroscopic Observations

Carbon stars exhibit one of the most complex spectra of any astronomical object in the visible and near infrared regions. This spectral region contains a multitude of atomic lines as well as the absorption bands of such molecules as $^{12}\text{C}^{14}\text{N}$, $^{12}\text{C}^{12}\text{C}$, ^{12}CH and the other isotopes of these species. The complexity of their spectra has always hampered attempts to interpret their spectra in terms of temperature, luminosity and abundance effects.

Any attempts to correlate luminosity and spectral features have been hindered by the lack of good absolute magnitudes for a sufficient number of carbon stars and because of differing abundances. There are just not enough absolute magnitudes of sufficient accuracy known to determine the luminosity from the spectrum of any given carbon star. This of course assumes that it is possible to do this for carbon stars as it is for most other stars. Since the carbon stars in the Large Magellanic Cloud are relatively faint a large telescope is needed to get good slit spectra of a large sample of these stars to investigate luminosity effects. The main purpose of my spectroscopic investigation was to confirm that the objects were indeed carbon stars, by observing molecular $^{12}\text{C}^{12}\text{C}$ bands, and to note some of the grosser features in the spectra.

Slit spectra at a dispersion of 117 \AA/mm were obtained with the image tube spectrograph of the 1.5 meter telescope at Cerro

Figure 6(a) Carbon star spectra, region 1

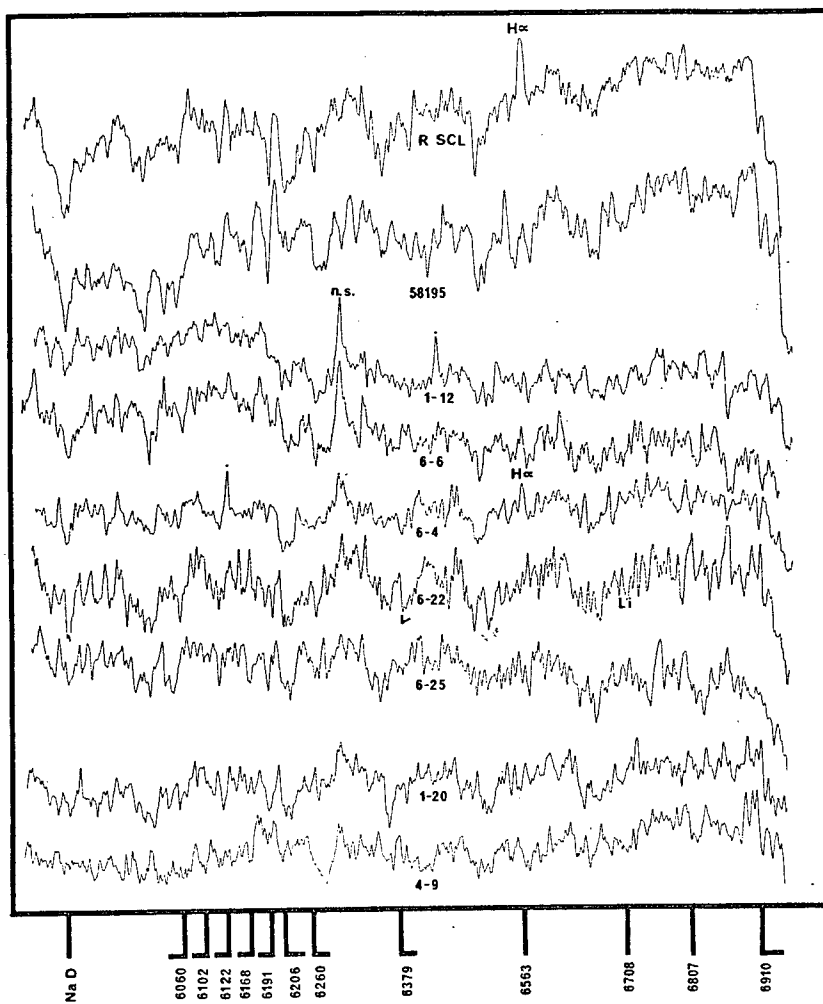
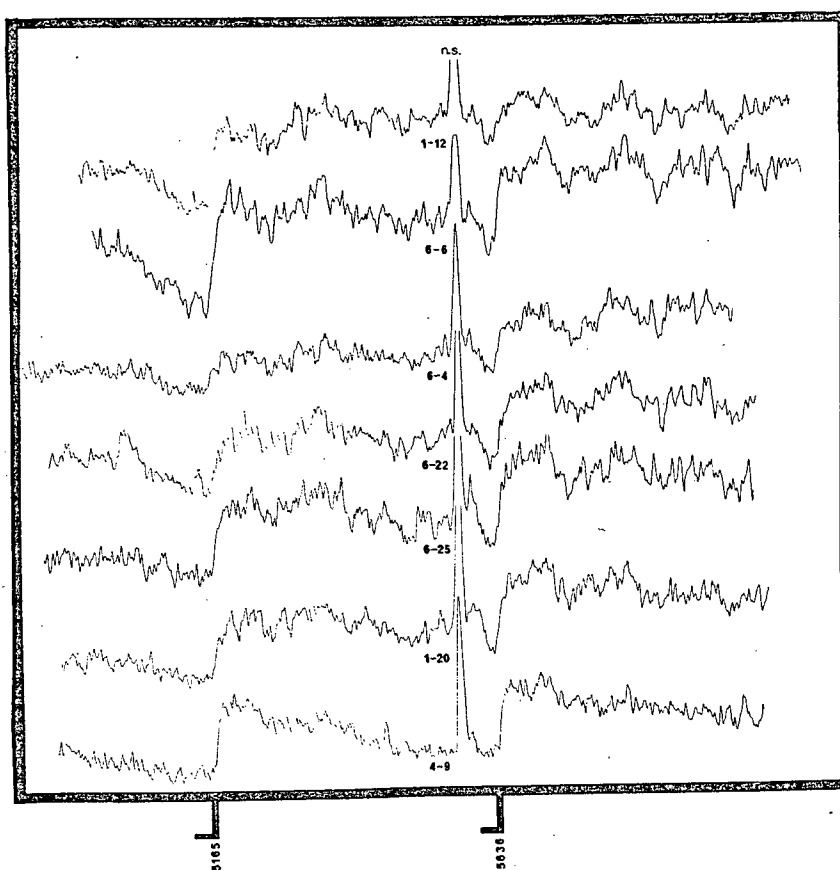


Figure 6(b) Carbon star spectra, region 2



Tololo in December 1974. The phosphor of the image tube allowed the use of baked IIA-0 plates to greatly increase the speed of the system. In general the spectral range covered was from $\lambda 5000\text{\AA}$ -8000 \AA . The faintness of the objects dictated exposures on the order of one hundred minutes. The details of the observations are found in table IV. On such long exposures with an image tube the number of ion events becomes significant and hence the background fog level becomes quite high.

Table IV Spectroscopic Observations

Star	R.A. (1975)	Dec. (1975)	Date (U.T.)	Exp. Time
1-12	5 03 11	-66 02.9	Dec. 14/74	91 min.
6-25	5 39 19	-72 10.4	Dec. 14/74	85 "
1-20	5 00 26	-65 02.5	Dec. 15/74	118 "
6-6	5 05 06	-70 27.6	Dec. 15/74	92 "
6-22	5 38 00	-70 49.1	Dec. 16/74	123 "
4-9	5 17 10	-64 48.5	Dec. 16/74	91 "
6-4	5 02 04	-70 53.3	Dec. 16/74	104 "

Spectra of eight stars were obtained and only one of these (star 1-16) was not a carbon star. The other seven stars showed molecular bands of C_2 as well as bands of CN. The stars showed a great range in the strength of the molecular bands as well as in the strength of the D-lines of sodium. None showed $\text{H}\alpha$ in absorption and only one showed a trace of emission at $\text{H}\alpha$.

Emission at $H\alpha$ is typical of the carbon Long Period Variables. In general the only atomic lines seen were the D-lines and $H\alpha$.

Tracings of the spectra over the wavelength interval $\lambda\lambda 5850-6950\text{\AA}$ are shown in Figure 6(a) while Figure 6(b) shows the interval from $\lambda 5000$ to $\lambda 5900$. These tracings were produced by digitizing the spectra at 5\AA intervals on the Joyce-Loebl Microdensitometer of the Geophysics and Astronomy Department at UBC. The resulting data was smoothed with a nine-point triangular filter to reduce the noise. For comparison, two Galactic carbon stars were also reduced in the same manner.

The Large Magellanic Cloud has a systematic velocity relative to the sun of about 250 kmsec^{-1} . Almost all of this is due to solar motion. This enables one to ascertain whether a star is a probable member of the Cloud or not just by measuring the radial velocity of the star. Several spectra of Galactic carbon stars were obtained each night to serve as radial velocity standards and since the only atomic lines definitely present in the Large Magellanic Cloud stars were the D-lines of sodium, I had to rely on the position of the molecular band heads for radial velocity measurements. This procedure admittedly introduces more error into the velocity measurements but the result should still indicate whether or not the star is a member of the Large Magellanic Cloud. The wavelengths of several band heads in the Galactic carbon stars were measured and after correcting for the motion of the earth a set of standard wavelengths was produced. The positions of the

corresponding band heads in the Large Magellanic Cloud carbon stars were then measured relative to this set of standard wavelengths. The final radial velocity was found after correcting for the earth's motion in the direction of the Large Magellanic Cloud. The results are shown in Table V along with other pertinent quantities for the seven stars. The number in parentheses is the probable error in the radial velocity. The average velocity of 245 kmsec^{-1} is in excellent agreement with the systematic velocity of the Large Magellanic Cloud found by Bok (1966).

Table V Properties of the Seven Carbon Stars

Star	$V_r (\text{kmsec}^{-1})$	V	V-R	V-I	Mv	Mbol
1-12	344 (17)	13.87	1.14	2.00	-4.6	-5.7
6-6	346 (66)	14.27	1.33	2.32	-4.2	-6.0
6-4	198 (50)	15.29	2.07	3.29	-3.2	-6.6
6-22	189 (34)	15.39	2.06	3.17	-3.1	-6.5
6-25	198 (43)	15.47	1.85	3.10	-3.0	-5.8
1-20	190 (38)	15.57	2.12	3.33	-2.9	-6.5
4-9	253 (17)	15.77	2.03	3.49	-2.7	-6.0

The tracings in Figure 6 show the carbon star characteristics of the program stars quite well, particularly Figure 6(b). Prominent features are marked on the tracings. Night sky lines are indicated by n.s. while plate flaws are

marked by a dot. Table VI gives the C-classification as defined by Yamashita (1972) for each star together with an intensity measure for each specific line or band on Yamashita's scale. These intensities were determined by comparing the Large Magellanic Cloud carbon stars with the Galactic ones. (D= Na D-lines; $C_2 = {}^{12}C^{12}C$ bands at $\lambda\lambda 5636, 6191$; $13 = {}^{12}C^{13}C$ band at $\lambda 6168$ and ${}^{13}C^{14}N$ band at $\lambda 6260$; $CN = {}^{12}C^{14}N$ band at $\lambda 5730$ and $\lambda 6206$; Li= Lithium I 6708 ; $H\alpha = \lambda 6563$) A discussion of the spectrum of each individual star follows.

Table VI Classification of Carbon Stars

Star	C-type	D	C_2	13	CN	Li	$H\alpha$
1-12	C4,2J	4+	2	4+	2	0	0
6-6	C4,4J	4	4	4+	3	0	0
6-4	C6,3	6	3+	3+	3+	0	e?
6-22	C6,4	6	4	3	3	0+	0
6-25	C4,4	3+	4	3	3	0	0
1-20	C4,5	3+	5	3	3+	0	0
4-9	C 4,4J	2	4	5+	3	0	0

1-12 - This star was the bluest and brightest (in V) of any of the stars observed. It shows moderate J-star characteristics as defined by Bouigue (1954) and Gordon (1967) with the ${}^{13}C^{14}N$ (4,0) band at $\lambda 6260$

slightly stronger than the corresponding $^{12}\text{C}^{14}\text{N}$ band at $\lambda 6206$. The (0,0) band of $^{12}\text{C}^{12}\text{C}$ is of moderate strength but the (0,1) band is surprisingly weak. The (0,2) band of $^{12}\text{C}^{12}\text{C}$ is barely visible while the (1,3) and (2,4) bands are present but weak. The Sodium D-lines are present with some strength but Li $\lambda 6708$ and $\text{H}\alpha$ are definitely not present at the resolution used.

6-6 - This star was the next bluest one observed as well as being the second brightest visually. The (0,0) and (0,1) bands of $^{12}\text{C}^{12}\text{C}$ are moderately strong and are very well defined. The +2 sequence of $^{12}\text{C}^{12}\text{C}$, (0,2), (1,3), and (2,4), is present but weak. The wavelengths of these features are $\lambda 6191$, $\lambda 6122$, and $\lambda 6060$ respectively. The $^{12}\text{C}^{13}\text{C}$ band at $\lambda 6168$ is present with considerable strength as is the $^{13}\text{C}^{14}\text{N}$ (4,0) band at $\lambda 6260$, implying a relatively high abundance of ^{13}C . Although the spectrum is somewhat weakly exposed shortward of $\lambda 5000 \text{ \AA}$ there is an indication that the Merrill-Sanford band (probably SiC_2) is present at $\lambda 4977$. The sodium D-lines are quite strong but they are not resolved. There is no trace of either H or Li $\lambda 6708$.

6-4 - In the spectrum of this star the $^{12}\text{C}^{12}\text{C}$ (0,1) and (0,0) bands are weak to moderate in strength while the

(1,3) and (2,4) band heads are much stronger. There is a weak trace of $^{12}\text{C}^{13}\text{C}$ at $\lambda 6168$ and the region from $\lambda 6260$ to $\lambda 6285$ seems to be depressed slightly implying a somewhat higher than normal abundance of ^{13}C . The $^{12}\text{C}^{14}\text{N}$ bands are present with moderate strength although the (4,0) and (6,2) band heads appear to be strongly enhanced. Weak emission may be present at $\text{H}\alpha$.

6-22 - The $^{12}\text{C}^{12}\text{C}(0,0)$ and (0,1) bands are of moderate strength and are quite well defined in this star. The $^{12}\text{C}^{14}\text{N}$ bands are well developed and seem to be of average strength. The two Na D-lines are resolved and appear to be of moderate strength. The Li $\lambda 6708$ line appears to be present with considerable strength along with the KI line at $\lambda 7699$. There is also a band, degraded to the red, with the band head at about $\lambda 6380$. This band also appears in the spectrum of WZ Cas, a peculiar Galactic carbon star, but remains unidentified (Catchpole 1975). The $^{12}\text{C}^{12}\text{C}$ bands are stronger in 6-22 than in WZ Cas while the Na D-lines are weaker. The abundance of ^{13}C in this star appears to be normal.

6-25 - The sodium D-lines are present but weak while most of the $^{12}\text{C}^{12}\text{C}$ bands appear to be of moderate strength.

The abundance of ^{13}C seems to be normal as the $^{12}\text{C}^{13}\text{C}$ band is present but very weak and the $^{13}\text{C}^{14}\text{N}$ band at $\lambda 6260$ is not at all visible.. Neither Li $\lambda 6708$ nor $\text{H}\alpha$ are present.

1-20 - All the $^{12}\text{C}^{12}\text{C}$ bands in this star are very well developed. The +2 sequence is especially strong. The abundance of ^{13}C appears to be normal as the $^{13}\text{C}^{14}\text{N}$ band at $\lambda 6260$ is not visible while $\lambda 6168$, $^{12}\text{C}^{13}\text{C}$, is visible but weak. The sodium D-lines are of moderate strength and there is no trace of Li $\lambda 6708$ or $\text{H}\alpha$.

4-9 - This star shows an extremely high abundance of ^{13}C as displayed by the strength of the $^{12}\text{C}^{13}\text{C}$ and $^{13}\text{C}^{14}\text{N}$ bands. The most outstanding feature in the entire spectrum of 4-9 is the (4,0) band of $^{13}\text{C}^{14}\text{N}$ at $\lambda 6260$. The corresponding $^{12}\text{C}^{14}\text{N}$ at $\lambda 6206$ is present but weak. The $^{12}\text{C}^{12}\text{C}$ band at $\lambda 5636$ is very strong but the $^{12}\text{C}^{12}\text{C}$ band at $\lambda 6191$ is actually weaker than the corresponding $^{12}\text{C}^{13}\text{C}$ band at $\lambda 6168$. There may be two $^{13}\text{C}^{13}\text{C}$ bands present, the (1,3) band at $\lambda 6080$ and the (0,2) band at $\lambda 6145$. The Na D-lines are weak but this should be considered in light of the fact that the entire region from $\lambda 5750$ to $\lambda 6150$ is depressed due to absorption from $^{12}\text{C}^{13}\text{C}$ and $^{13}\text{C}^{13}\text{C}$ as is the case for the more extreme Galactic J stars (Yamashita 1972).

It is also possible that this star shows a weak KI line at $\lambda 7699$.

All of the stars above display molecular bands of C_2 . It is perhaps significant that three of the seven show higher than normal abundances of ^{13}C . This is proportionally more stars than for Galactic carbon stars. It is also surprising that none of the stars show definite $H\alpha$ emission, which is characteristic of the Long Period Variables.

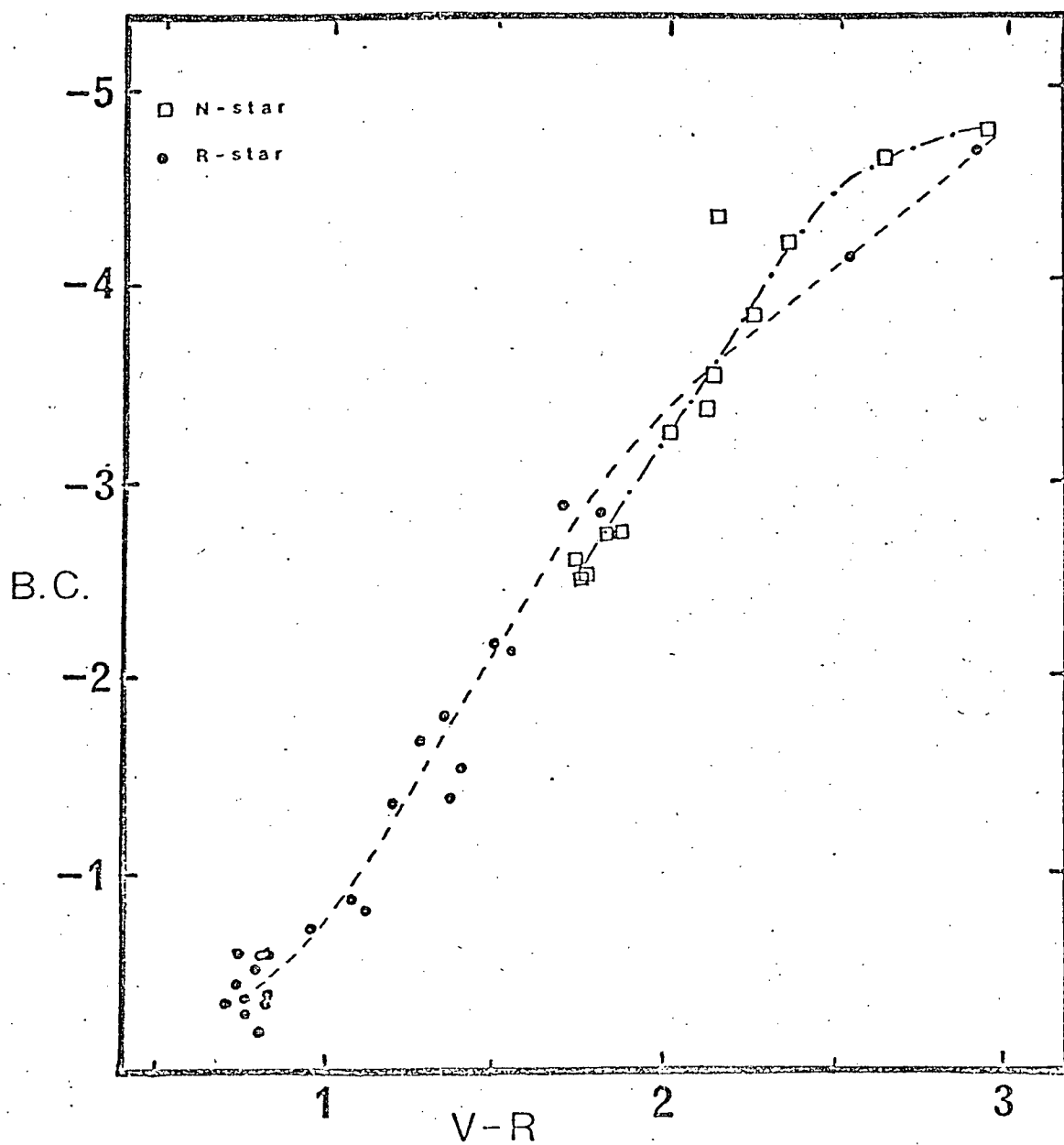
It is possible that the two bluest carbon stars (1-12 and 6-6) are not members of the Large Magellanic Cloud but are actually high latitude CH stars. These stars are mildly peculiar spectroscopically and bear some resemblance to the CH stars found in ω Centauri by Dickens (1972). In the following section I will assume that all seven are members of the Large Magellanic Cloud.

V Carbon Stars in the H-R Diagram

The precise evolutionary phase (or phases) of carbon stars is not presently understood. They are believed to be highly evolved objects which are exhibiting the products of nucleosynthesis in their spectra. Besides determining their evolutionary status from data on masses, ages, spectra, and atmospheric abundances, one would like to know their position in the H-R diagram. The H-R diagram has been very useful for comparing theoretical models with observations in order to determine an object's evolutionary status.

In order to place an object in the theoretical H-R diagram it is necessary to know the absolute bolometric magnitude as well as the effective temperature of the object. First I will address myself to the problem of finding the absolute bolometric magnitude of a cool carbon star. One can find the bolometric magnitude of an object by integrating the observed energy distribution over all frequencies to find the total energy emitted by the object. However this can only be done for the brighter objects. Mendoza and Johnson (1965) have done this for a few dozen Galactic carbon stars, with photometric observations extending far out into the infrared where most of the carbon star's radiation is emitted. It is fortunate that their results show a good correlation between the calculated bolometric correction and the $(V-R)$ colour index for both R and N stars. Olson and Richer (1975) have investigated this correlation and find the relationship shown in Figure 7. There are two

Figure 7. Bolometric corrections



different relations shown; one for the R stars and one for the N stars. Since the R stars are much fainter (absolutely) than the N stars it is expected that all the carbon stars observed in the Large Magellanic Cloud are N-type carbon stars. Therefore the bolometric corrections for N stars were used. In a few cases where the stars were slightly bluer in (V-R) than the bluest Galactic N star used in the calibration the bolometric correction was calculated by simply extending the linear portion of the calibration curve for N stars to find the correct value. It is expected that the bolometric corrections are good to about 0.3 magnitudes. I have neglected interstellar reddening in obtaining the absolute bolometric magnitude for these stars for two reasons. First, there is very little reddening in the direction of the Large Magellanic Cloud (Bok and Bok 1972). Second, any reddening which is present will tend to move the stars along the calibration curves rather than across them. This is because the reddening will cause the star to appear fainter visually but it will also increase the bolometric correction, hence the two effects tend to cancel out.

The problem of assigning effective temperatures to the cool carbon stars is not as easily resolved as the question of bolometric corrections. First, there are only two N stars for which radii have been measured by the method of lunar occultation. Further, no N star is a known member of an eclipsing binary system so that the radius may not be determined by this method. It is not possible to use the calibration based on various photometric colours set up for M giants as the

sources of opacity are quite different for the carbon and M giants. In fact the late type carbon stars radiate more nearly like black bodies than do M stars (Bahng 1966; Barnes 1973; Bessell and Youngbom 1972).

Scalo (1976) has investigated the consistency of using blackbody temperatures for carbon stars as opposed to using temperatures derived from an M star calibration. He has derived blackbody colour temperatures from the $(R-I)$, $((R+I)-(J+K))$, $(I-K)$, and (in most cases) the $(I-L)$ colours for twenty-three stars from the available photometry (Mendoza 1967; Lee 1970; Eggen 1972a). He finds the typical total spread in derived blackbody temperature is only 50-200°K. The requirement that the blackbody temperatures be consistent is a necessary requirement for their use as effective temperatures but it is not sufficient. Thus it is possible to get a blackbody temperature from only one colour measurement, say $(R-I)$, and be reasonably sure that the other colour indices would not give significantly different results.

Bartholdi et al. (1972) have measured an occultation angular diameter for the N star, X Cnc. Using Mendoza's (1967) relation between T_e and bolometric correction to eliminate the bolometric correction, they find a T_e of about 2500°K. However, Mendoza's $(I-L)$ temperatures are probably too small. If one uses the bolometric correction derived from the $(V-R)$ colour index a T_e of about 2640°K is obtained for a fully darkened disk or 2810°K for a uniformly illuminated one. Various authors have measured

occultation diameters for 19 Psc (Lasker et al 1973; De Vegt 1974) and analysed them for effective temperatures. Scalo (1976) adopts a temperature of $3050 \pm 200^\circ\text{K}$ for 19 Psc and $2700 \pm 100^\circ\text{K}$ for X Cnc after considering all the derived values.

Figure 8 shows a plot of colour temperature as a function of $(R-I)$. The filled circles are the calibration of G and M giants by Johnson (1966) while the open circles are the calibration of M giants given by Lee (1970). The open squares are the calibration of M supergiants by Lee (1970) and the crosses represent the calibration of late type Miras by Mendoza (1967). The solid line represents the blackbody relation while the filled triangles are the approximate positions of the two carbon stars for which angular diameters have been measured. Note how the two carbon stars fall closer to the blackbody line than to the M giant calibration. Therefore it seems reasonable to use blackbody temperatures derived from the $(R-I)$ colour index.

In order to help understand the carbon star's place in stellar evolution it is convenient to place them in a theoretical H-R diagram. Figure 9 is such a diagram. The forty stars for which photometry has been obtained are plotted. The effective temperatures used were those derived from a blackbody curve fitted to the $(R-I)$ colour while the bolometric correction used was that of Olson and Richer (1975) from $(V-R)$ photometry. The theoretical evolutionary tracks shown have been adopted from Scalo (1976) and Scalo, Despain and Ulrich (1975) and references

Figure 8. Colour temperature versus R-I

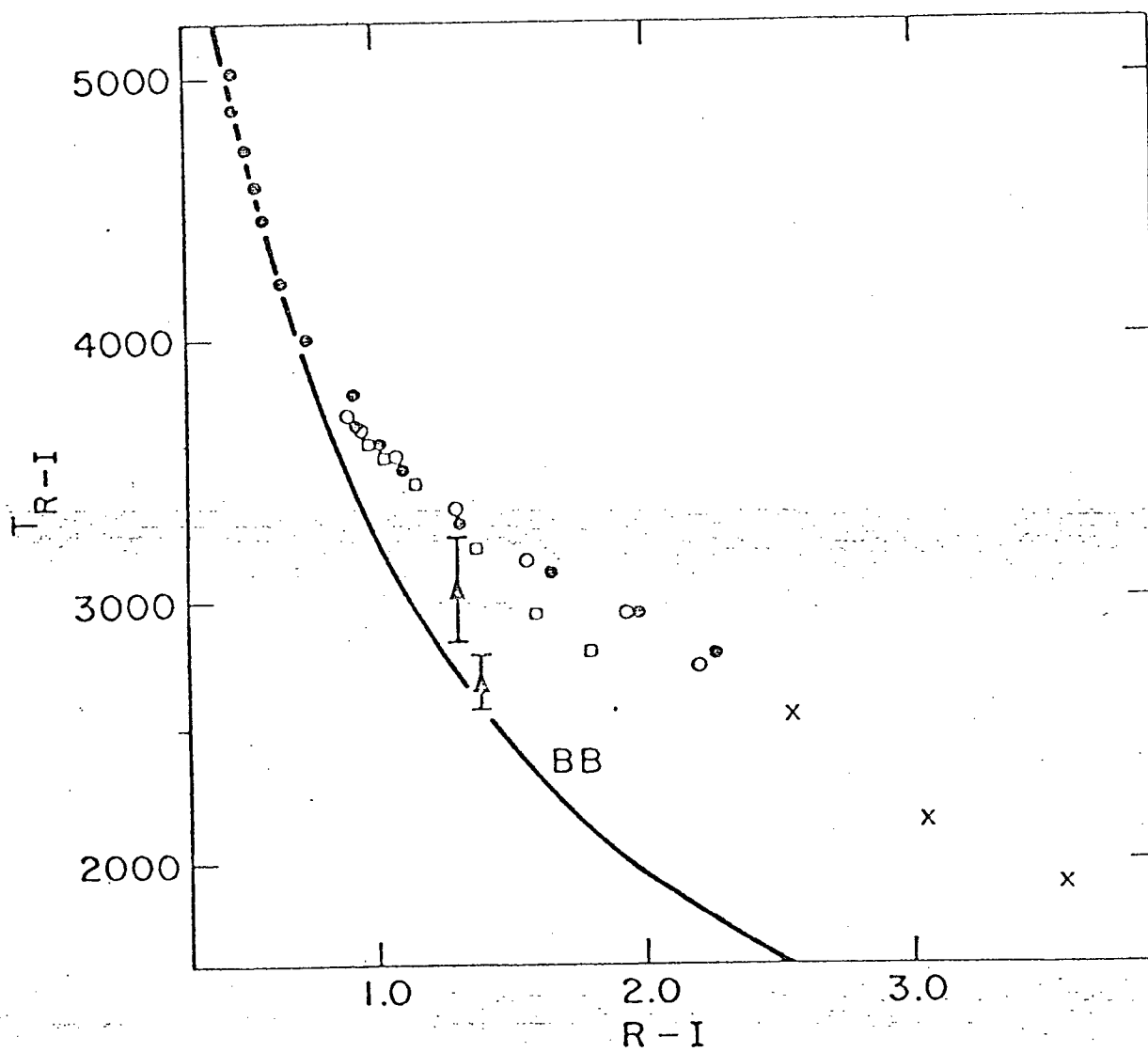
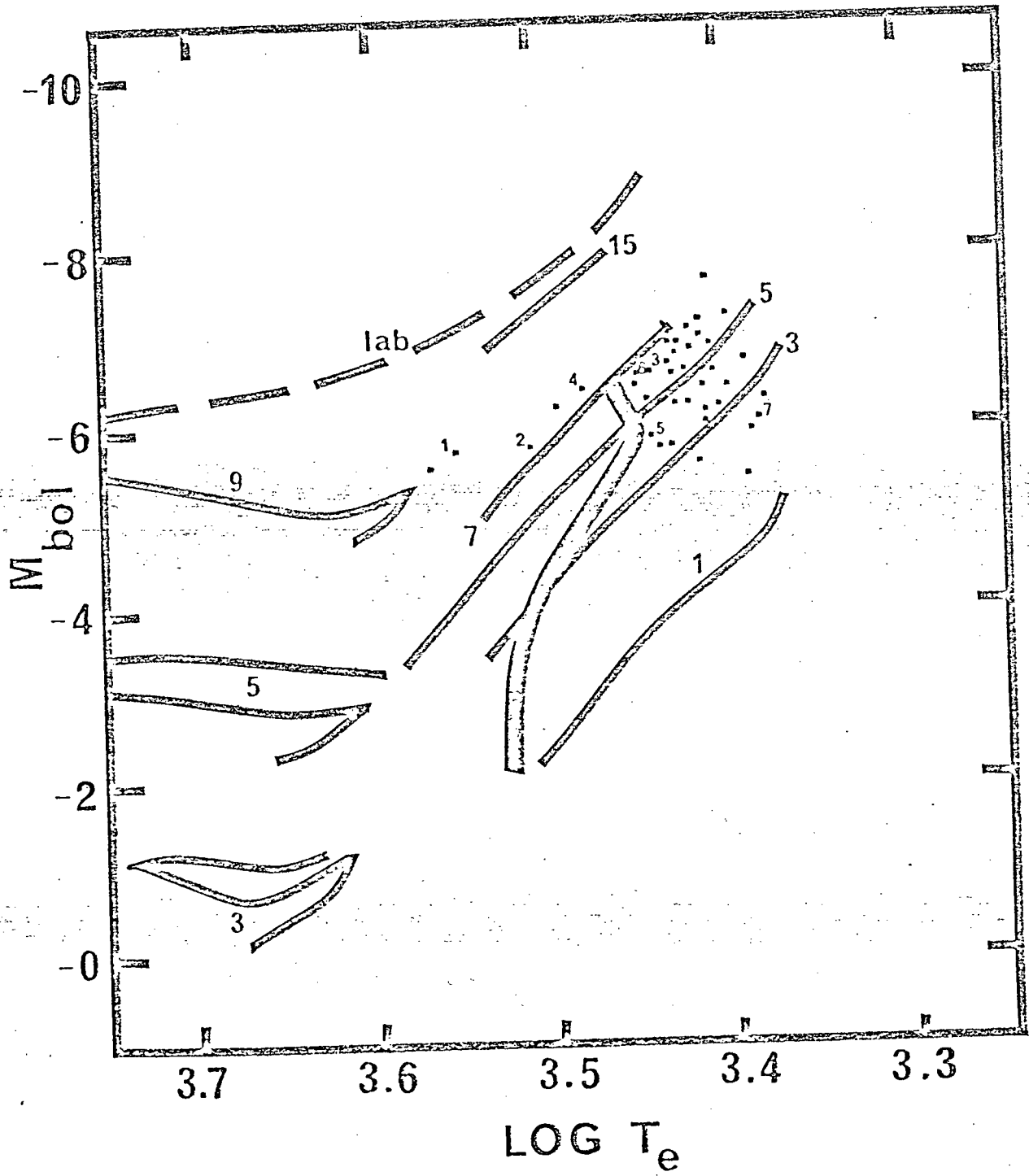


Figure 9. Theoretical Hertzsprung-Russell Diagram



cited therein. All these models represent stars of disk composition. The thinner lines correspond to the first ascent of the giant branch to core helium burning, as well as double shell source models. The double shell source models are the ones lying to the right of the diagram. The thick line represents the locus of points at which the first helium shell flash occurs according to Schwarzschild and Harm (1965) for the $1M_{\odot}$ model and Paczynski (1970) and Iben (1972) for the larger masses. Models to the right of this line have two active burning shells and are undergoing thermal pulses in the helium shell at fairly regular intervals. The broken line corresponds to the mean position of supergiants of luminosity class Iab. The seven stars from Table V for which spectra were obtained are identified by a number beside the corresponding point. This number corresponds to the star's position in Table V. Thus, for example, 1=1-12, 2=6-6, 7=4-9 etc.

Ulrich and Scalo (1976) estimate that the uncertainties in the temperatures of the double shell source tracks due to possible errors in convection theory and in the atmospheric opacities is no more than $\pm 200^{\circ}\text{K}$. Scalo (1976) estimates that the uncertainty in the temperatures adopted from the (R-I) colour to be about 300°K . These uncertainties, along with the effect of composition changes (Scalo and Ulrich 1975) make it dangerous to assign a mass solely from the position in the H-R diagram. Therefore the tracks are labeled mainly for ease of reference although I will be assuming that the stars do have the masses assigned to them.

The first conclusion to be drawn from Figure 9 is that all the stars observed appear to be in the double shell source phase of evolution. This is in disagreement with the suggestion of Eggen (1972b) that the N stars are in the core helium ignition phase. In the double-shell source phase a star consists of a carbon-oxygen core surrounded by a helium burning shell and still further out lies the hydrogen burning shell. Above this lies the outer convective envelope of the star. The two warmest stars in this sample lie fairly close to the tip of the $9 M_{\odot}$ first giant branch so that it is not clear that these are double shell source stars as opposed to core helium ignition stars. However for the remaining discussion I will assume that they are in fact double shell source stars.

The next thing to note from this diagram is the fact that, except for the five stars lying to the left of the $7 M_{\odot}$ track all the stars are bounded on the lower left by the onset of helium shell flashes. No cool carbon star less massive than $7 M_{\odot}$ is found in the pre-helium shell flash phase of evolution. This strongly suggests that stars less massive than $7 M_{\odot}$ become cool carbon stars because of the onset of helium shell flashes. For stars more massive than $7 M_{\odot}$ this fact is uncertain as no models have been constructed which are evolved to the stage of helium shell flashes. These stars could very well be post-helium shell flash objects as well.

The exact mechanism by which the carbon is mixed to the

surface after the onset of the helium shell flashes is uncertain. Several different mechanisms have been suggested (Ulrich and Scalo 1972; Scalo and Ulrich 1973; Ulrich 1973; Smith, Sackmann, and Despain 1973; Sackmann, Smith and Despain 1974; Iben 1975, 1976). The basic idea is to bring hydrogen, carbon and helium into contact at high temperatures. It is possible that the individual mechanisms work more efficiently for certain mass ranges than for others.

There exists an almost unique core mass-luminosity relationship for double shell source red giants (Paczynski 1971; Iben 1976). Knowing the absolute bolometric magnitude of a double shell source star allows one to assign a mass to the core, assuming that the core is non-rotating. It is interesting to calculate the core mass of the most luminous (bolometrically) star in this sample. Using Iben's relationship,

$$L/L_{\odot} = 6 \times 10^4 (M_{\text{core}} - 0.41)$$

one finds a core mass of $1.73 M_{\odot}$. This is well above the Chandrasekhar limiting mass ($1.4 M_{\odot}$) which is the maximum mass for such a carbon-oxygen configuration. The spectra of stars 1-12 and 6-6 indicate that significant mixing has already occurred in these stars. Since they are both above the theoretical upper mass limit for the core flash ($2.3 M_{\odot}$) and if they are pre-helium shell flash objects this implies that the "hot-bottom" convective envelope hypothesis of Scalo, Despain, and Ulrich (1975) may be responsible for the mixing observed in these stars. These stars are well above the critical luminosity for

this effect to occur.

It is also worthwhile to comment on the very interesting star 4-9, number seven in Figure 9. This star exhibits an extremely high abundance of ^{13}C so that it is presumably the most highly evolved object in this sample of seven stars in the sense that shell flashes have been occurring in this object for a significant period of time. As the temperature at the base of the convective envelope increases it becomes easier for ^{12}C to form ^{13}C and ^{14}N by single and double proton captures respectively. If the temperature at the base of the convective envelope keeps rising it is possible that 4-9 could be on its way to destroying its carbon star characteristics.

VI Summary

In this thesis a catalogue of cool carbon stars in the Large Magellanic Cloud has been presented. The catalogue is expected to be complete to an I magnitude of about 13.5, the approximate limiting magnitude of the objective prism survey from which the stars were identified. The stars were kindly identified by Dr. B.E. Westerlund from plates he obtained at the Uppsala Southern Station on Mount Stromlo. Finding charts and equatorial coordinates for the 309 stars which comprise the catalogue have been given. Such a catalogue should prove to be useful now that several large telescopes are operational in the southern hemisphere. The fact that the distance to the Large Magellanic Cloud is well known allows many observations to be made which otherwise would not be possible. It is important to obtain as many accurate absolute magnitudes as possible for carbon stars as the data available now is quite sparse.

Photometric observations on the VRI system of forty carbon stars, selected from the catalogue, were made in order to investigate the photometric properties of carbon stars with known absolute magnitudes. Correlations between absolute visual magnitude and various photometric colours have been searched for but no significant results were found. The bulk of the stars investigated seem to form an empirical bright giant branch on the $M_{bol} - V-R$ diagram. However this could be a selection effect as the photometric observations were restricted to a brighter than average group. Two mildly peculiar stars were

found in this sample of stars. These were stars 1-12 and 6-6 in the catalogue. They are warm luminous stars which exhibit substantial amounts of ^{13}C in their atmospheres. They also appear to lie on the Ib supergiant branch in the Mbol vs (V-R) diagram.

Spectra of seven members of the catalogue have also been obtained at a dispersion of $117\text{\AA}/\text{mm}$. The spectra were obtained mainly to confirm that the stars were indeed carbon stars and to also note some of the grosser features in the spectrum. It was found that three of the seven stars exhibit J star characteristics: a higher than normal abundance of ^{13}C , as defined by Bouigue (1954) and Gordon (1967). This was unexpected as this is proportionally a much larger number of stars than for carbon stars in our Galaxy. One star, 4-9, showed extreme J star characteristics. The most outstanding feature in the spectrum of 4-9 is the $^{13}\text{C}^{14}\text{N}$ band at $\lambda 6260$. In many cases the bands involving ^{13}C are stronger than the corresponding ^{12}C ones.

The evolutionary status of carbon stars is not presently well understood. It is useful to place the stars in a theoretical Hertzsprung-Russell diagram to aid in explaining their evolutionary development. Using the best available data for bolometric corrections and using blackbody temperatures as effective temperatures as argued for by Scalo (1976) the stars were placed in a theoretical H-R diagram. Although the positions of the stars are a bit uncertain due to the effects of

composition changes and uncertainties in the derived temperatures, the cool carbon stars are almost certainly in the double shell source phase of evolution. In this phase the stars have two active burning shells, one of helium and one of hydrogen. It also appears as though they are undergoing thermal pulses in the helium burning shell as described by Schwarzschild and Harm (1965). In fact the stars less massive than seven solar masses seem to be bounded below by the onset of these helium shell flashes. It is quite possible that the helium shell flashes are the mechanism by which intermediate mass stars become carbon stars (Iben 1975). The two mildly peculiar stars, 1-12 and 6-6, appear to be slightly more massive than seven solar masses. These stars may be pre-helium shell flash objects although this point is uncertain as models have not yet been constructed which are detailed enough at this point in the star's evolution.

Now that several large telescopes exist in the southern hemisphere a program of obtaining medium dispersion spectra of as many of these stars as possible should be started. Then it may be possible to devise a classification system in which the temperature, luminosity and abundance effects can be sorted out. Higher dispersion spectra should be obtained of some of the brighter objects to aid in understanding the evolutionary status of the cool carbon stars.

Bibliography

- Bahng, L. 1966, in Colloquium on Late-Type Stars, ed. M. Hack (Trieste: Observatorio di Trieste), p. 255.
- Barnes, T.G. 1973, Ap. J. Suppl. Ser. No. 221, 25, 369.
- Bartholdi, P., Evans, D.S., Mitchell, R.I., Silverberg, E.C., Wells, D.C., and Wiant, J.R. 1972 A.J., 77, 756.
- Bessell, M.S., and Youngbom, L. 1972, Proc. Astr. Soc. Australia, 2, 154.
- Bok, B.J., and Bok, P.F. 1962, M.N.R.A.S., 124, 435.
- Bouigue, R. 1954, Ann. d'Ap., 17, 104.
- Catchpole, R.M. 1975, Pub. A.S.P., 87, 397.
- De Vaucouleurs, G. 1955, A.J., 60, 40.
- De Vegt, C. 1974, Astr. and Ap., 34, 457.
- Dickens, R.J. 1972, M.N.R.A.S., 159, 7P.
- Eggen, O.J. 1972a, Ap. J., 174, 45.
- Eggen, O.J. 1972b, M.N.R.A.S., 159, 403.
- Gordon, P.C. 1967, dissertation, University of Michigan.
- Gordon, P.C. 1968, Pub. A.S.P., 80, 597.
- Iben, I. 1972, Ap. J., 178, 433.
- Iben, I. 1975, Ap. J., 196, 525.
- Iben, I. 1976, Ap. J., to be published.
- Johnson, H.L. 1966, Ann. Rev. Astr. and Ap., 4, 193.
- Keenan, P.C., and Morgan, W.W. 1941, Ap. J., 94, 501.
- Lasker, B.M., Bracker, S.B., and Kunkel, W.E. 1973, Pub. A.S.P., 85, 109.
- Lee, T.A. 1970, Ap. J., 162, 217.
- Mavridis, L.N. 1967, in Colloquium on Late-Type Stars, ed. M. Hack (Trieste: Observatorio di Trieste), p. 420.
- Mendoza, E.E. 1967, Bull. Tonantzintla y Tacubaya Obs., 3, 305.
- Mendoza, E.E., and Johnson, H.L. 1965, Ap. J., 141, 161.

- Olsen, B.I., and Richer, H.B. 1975, Ap. J., 200 , 88.
- Paczynski, B. 1970, Acta Astr., 20 , 47.
- Richer, H.B. 1971, Ap. J., 167 , 521.
- Richer, H.B. 1972, Ap. J. (Letters), 172 , L63.
- Richer, H.B. 1975, Ap. J., 197 , 611.
- Sackmann, I.J., Smith, R.L., and Despain, K.H. 1974, Ap. J., 187 , 555.
- Scalo, J.M. 1973, Ap. J., 186 , 967.
- Scalo, J.M. 1976, Ap. J., 206 , 474.
- Scalo, J.M., Despain, K.H., and Ulrich, R.K. 1975, Ap. J., 196 , 805.
- Scalo, J.M., and Ulrich, R.K. 1975, Ap. J., 200 , 682.
- Schwarzschild, M., and Harm, R. 1965, Ap. J., 145 , 496.
- Shane, C.D. 1928, Lick Obs. Bull., 13 , 123.
- Smart, W.M. 1971, Textbook on Spherical Astronomy (5th ed.; Cambridge: Cambridge University Press), p. 278.
- Smith, R.L., Sackmann, I.J., and Despain, K.H. 1973, in Explosive Nucleosynthesis, ed. D.N. Schramm and W.D. Arnett (Austin: University of Texas Press), p. 168.
- Ulrich, R.K. 1973, in Explosive Nucleosynthesis, ed. D.N. Schramm and W.D. Arnett (Austin: University of Texas Press), p. 139.
- Ulrich, R.K., and Scalo, J.M. 1972, Ap. J. (Letters), 176 , L37.
- Ulrich, R.K., and Scalo, J.M. 1976, in preparation.
- Wallerstein, G. 1973, Ann. Rev. Astr. and Ap., 11 , 115.
- Westerlund, B.E. 1964, in IAU Symposium 20, The Galaxy and the Magellanic Clouds, ed. F.J. Kerr and A.W. Rodgers (Canberra: Australian Academy of Science), p. 239.
- Westerlund, B.E. 1972, Proc. 1st European Astronomical Meeting, ed. L.N. Mavridis.
- Wing, R.F. 1967, Ph.D. Dissertation, University of California, Berkely.

Yamashita, Y. 1972, Ann. Tokyo Astr. Obs., 2d Ser., Vol. 13, No. 3.